1949

Vibration damping of stranded cable, Ph.D. Dissertation, Lehigh University, 1949

A. T. Yu

VIBRATION DAMPING OF STRANDED CABLE

by

Ai-ting Yu

A DISSERTATION

Presented to the Graduate Faculty

of Lehigh University

in Candidacy for the Degree of

Doctor of Philosophy

Lehigh University
1949

Approved and recommended for acceptance as a dissertation in partial fulfillment of the requirements for the degree of Doctor of Philosophy

Sept 16, 1949 (Date)

Bruce Johnston (Professor in Charge)

Accepted, Sept 16, 1949 (Date)

Special Committee directing the doctoral work of Ai-ting Yu

H. L. Sutherland Chairman

Wm. J. Eney

C. A. Shook

Bruce Johnston

B. E. Raynor

CONTENTS

PREFACE

(A) SYNOPSIS

The basic nature of internal damping of stranded cable was investigated by first considering a segment of stranded cable vibrated under pure bending load and then analyzing the effect of tension. The deformation and energy relationships were analyzed and again determined by experimental methods. From these investigations, the predominant dry friction nature of internal damping in stranded cable was established. The basic properties of damping capacity, frictional force function, and the influencing factors were revealed. The agreement between the static and the dynamic test results was very satisfactory.

Based on the knowledge of internal damping, an analytic solution was obtained for damped vibrations of stranded cable strung under tension. Three different cases of damping were discussed. The experimental results checked very well with the theory.

(B) ACKNOWLEDGEMENT

The author wishes to express his deep appreciation to Professor Bruce G. Johnston and Professor Clarence A. Shook for their invaluable advice and help. He is indebted to Professor J. P. Den Hartog of Massachusetts Institute of Technology for his continued interest and guidance.

The author also wishes to express his gratitude to Mr. Robert F. Joy, Engineer, Bethlehem Steel Company, for his cooperation and help in different phases of the work.

The author is particularly indebted to Mr. C. Harry Yang, Research Fellow, Fritz Laboratory, for his unfailing encouragements and valuable suggestions.

Many thanks are due Messrs. R. L. Stiles and Donald Derr for the preparation of test results, and Mr. John Karshner for checking the manuscript.

(C) INTRODUCTION

The vibration of stranded conductors and structural cables has induced a great many fatigue failures which could not be forseen from the prior knowledge and experience governed by the conventional design theories.

In the past three decades, a considerable number of investigations have been carried out largely in the field and in laboratories simulating field conditions (see Bibliography in the Appendix); external causes were analyzed, cables were compared in their fatigue properties, empirical formulae were derived and vibration absorbers were developed (Reference 1 provides a very comprehensive review of these investigations). Little work, however, has been done on the analytic and fundamental aspects of the problem. On the problem of damping of cable, Bate (Reference 2) derived an empirical formula expressing energy dissipation as a function of wind velocity, and conducted tests for large spans simulating field conditions. Sturm (Reference 3) treated "damper cable" in the Stockbridge Damper by making use of its static hysteresis properties. As to the complete analysis and thorough study of the basic nature of the problem of internal damping and its influence on vibration of stranded cable, there appear to be no published work.

Since a knowledge of the basic nature of the internal damping of stranded cable is a necessary prerequisite for a solution of the problem of cable vibration, and since

it is also indispensable as a theoretical basis and a guide for further developments of effective preventive measures for vibration fatigue failure of cables, it is the purpose of this paper to attempt an investigation in order to throw some light on this basic problem.

Work in this paper consists of two parts, the first part aims at an investigation of the basic nature of internal damping of stranded cables whereas the second part deals with the analysis of the vibration characteristics of a stranded cable based on the knowledge of its internal damping obtained from the first part of work.

Due to the limitation of time, work presented in this paper is far from completion. However, it is the belief of the author that in this paper a rational approach towards the complete solution of the problem has been outlined and further work may follow in logical sequence.

(D) SYMBOLS

a, a_n	parameters defined in Appendix C
a_{f_1}, a_{f_2}	parameters defined on p. 69
a_i	maximum amplitude in the i-th half-cycle
$a_{r,s}, a_{u,v}$	parameters defined in Part II and in Appendix C
$2A_i$	area of hysteresis loop due to ideal dry friction
$2A_t$	reduction of area of hysteresis loop due to initial slipping in transition stage
b,B	arbitrary constants
c,C	arbitrary constants
EI	equivalent flexural rigidity of cable
f	unit inter-strand dry friction force
f′	constant, a function of the coefficient of friction of the wire surface
f(x)	unit interstrand friction force function
F_0, F_1	coefficients of the damping function (p. 54)
F(x)	function of constant damping
g, h	parameters in De Moivre's equation (Appendix C)
H	parameter defined in Appendix C
i	subscript denoting the number of half-cycle; or square root of -1
I_c	solid moment of inertia of cylinder about its axis of symmetry
k	spring coefficient ($= \frac{2EI}{L}$)
k'	modified spring coefficient (Part II)
K	a constant

KE	kinetic energy
L	span of cable specimen
m_f	unit frictional resisting moment (p. 11)
M	applied bending moment at ends of specimen
M_1	maximum end moment in the i-th half-cycle
M_f	frictional resisting moment (p. 12)
n	number of wires in cable
N	normal pressure
P(f)	input force function
p	circular frequency (radians per second) = $2\pi q$
q	frequency (cycles per second)
Q	ratio of frequencies (p. 71)
r	any integer
R	radius of curvature
S	tension
t	time
T	function of time; or period of vibration of a full cycle ($= \frac{2\pi}{p}$)
$\ddot{T}$	$\frac{d^2T}{dt^2}$
u	relative displacement of the contacting elements of the two wires
W_1	maximum potential energy at the peak of the i-th half-cycle
ΔW_1	energy dissipation in the i-th half-cycle
x	horizontal coördinate axis
X	function of x
X"	$\frac{d^2X}{dx^2}$

From (1) we get

$$y_m^2 - 2\,y_m R = \frac{L^2}{4}$$

Divide through by R^2

$$\left(\frac{y_m}{R}\right)^2 - 2\frac{y_m}{R} = -\left(\frac{L}{2R}\right)^2 \qquad (2)$$

Now since

$$y_m \ll R$$

hence the first term on the left side is of second order of magnitude compared with the rest and (2) becomes

$$\frac{y_m}{R} = \frac{1}{8}\left(\frac{L}{R}\right)^2$$

or

$$y_m = \frac{L^2}{8}\left(\frac{1}{R}\right) = \frac{L^2}{8}\,y'' \qquad (3)$$

Since the arc length on a circle equals its angle multiplied by the radius of the circle, from the diagrams, we obtain,

$$L\ (\text{arc}) = 2\phi \cdot R \qquad (4)$$

When y_m is small, one may take

$$L\ (\text{arc}) = L$$

hence

$$L = 2\phi \cdot R \qquad (4a)$$

or

$$\phi = \frac{L}{2}\left(\frac{1}{R}\right)$$

or

$$y'_o = \frac{L}{2} \cdot y'' \qquad (5)$$

The results of (3) and (5) may be tabulated as follows:

	y_m	y'_o (=ø)	y'' (=$\frac{1}{R}$)
y_m	1	$L/4$	$L^2/8$
y'_o (=ø)	$4/L$	1	$L/2$
y'' (=$\frac{1}{R}$)	$8/L^2$	$2/L$	1

APPENDIX B

EQUIVALENT FLEXURAL RIGIDITY OF STRANDED CABLE

The equivalent "EI" values of stranded cable specimen 771 obtained from static bending tests using two different types of loading are listed in the following table:

Mid-span Deflection (in.)	Equivalent EI ($\times 10^6$ lb.-in.^{2})	
	Pure Bending Load at Ends	Concentrated Load at Mid-span
0.367	2.25	2.26
0.292	2.23	2.32
0.230	2.28	2.40

The ends of the cable specimen were free when concentrated loads at mid-span were applied.

APPENDIX C

PARTICULAR SOLUTION $y_f(x)$

The differential equation to be satisfied is

$$EI \frac{d^4y}{dx^4} - S \frac{d^2y}{dx^2} \mp F_1 Sy \mp F(x) = 0 \qquad (1)$$

The solution of (1) is a combination of the solution of the homogeneous equation with $F(x)=0$ and a particular solution as a function of $F(x)$, namely

$$y_f = y_{f_1}(x) \pm BF(x) \qquad (2)$$

Since the sign in front of F_1 plays a vital roll in the solution $y_1(x)$, the two cases for different signs for F_1 should be treated separately. We shall begin by first studying the homogeneous equations:--

(A) Equation $EI\, y^{iv} - S\, y'' - F_1 Sy = 0 \qquad (1a)$

The solution is straight forward

$$y_{10}(x) = c_{11} \cos a_u x + c_{12} \sin a_u x + c_{13} \cosh a_v x + c_{14} \sinh a_v x \qquad \ldots\ldots(3)$$

where $$a_u^2 = -\left(\frac{S}{2EI} - \sqrt{\left(\frac{S}{2EI}\right)^2 + \frac{F_1 S}{EI}}\right)$$

$$a_v^2 = +\left(\frac{S}{2EI} + \sqrt{\left(\frac{S}{2EI}\right)^2 + \frac{F_1 S}{EI}}\right)$$

(B) Equation $EI\, y^{iv} - Sy'' + F_1 Sy = 0 \qquad (1b)$

The "auxiliary equation" obtained by substituting y by e^{ax} is

$$EI\, a^4 - S\, a^2 + P_1 S = 0 \qquad (4)$$

the solution of which being

$$a = \pm\sqrt{\frac{S}{2EI} \pm \sqrt{\frac{S}{2EI})^2 - \frac{P_1 S}{EI}}} \qquad (5)$$

$$= \pm\sqrt{\frac{S}{2EI} \pm \sqrt{H}}$$

Three cases ought to be investigated separately:

(i) $P_1 < \frac{S}{4EI}$

$$\therefore\ H > 0 \quad \frac{S}{2EI} > \sqrt{H} > 0$$

$$a_1^2 = \frac{S}{2EI} - \sqrt{\frac{S}{2EI})^2 - \frac{P_1 S}{EI}} > 0$$

$$a_2^2 = \frac{S}{2EI} + \sqrt{(\frac{S}{2EI})^2 - \frac{P_1 S}{EI}} > 0$$

$$y_{11}(x) = c_1' e^{a_1 x} + c_2' e^{-a_1 x} + c_3' e^{a_2 x} + c_4' e^{-a_2 x}$$

$$= c_{21} \cosh a_1 x + c_{22} \sinh a_1 x + c_{23} \cosh a_2 x + c_{24} \sinh a_2 x$$

(6)

(ii) $P_1 = \frac{S}{4EI}$

$$\therefore\ H = 0,\ a_3^2 = \frac{S}{2EI} > 0$$

$$\therefore\ y_{12}(x) = (c_1'' + c_2'' x)\, e^{a_3 x} + (c_3'' + c_4'' x)\, e^{-a_3 x}$$

$$= (c_{21} + c_{22} x) \cosh a_3 x + (c_{23} + c_{24} x) \sinh a_3 x$$

(7)

(iii) $P_1 > \frac{S}{4EI}$

$$\therefore \quad H < 0, \sqrt{H} = ih$$

where $$h^2 = \frac{P_1 S}{EI} - \left(\frac{S}{2EI}\right)^2 > 0$$

call $$g = \frac{S}{2EI}$$

we have $$g^2 + h^2 = \frac{P_1 S}{EI}$$

Eq. (5) becomes

$$a = \pm\sqrt{g \pm ih} \tag{5a}$$

By de Moivre's theorem (Ref. 13) for complex roots, (5a) becomes

$$a = \pm\frac{1}{\sqrt{2}}\left(\sqrt{\sqrt{g^2+h^2} + g} \pm i\sqrt{\sqrt{g^2+h^2} - g}\right)$$

$$= \pm\frac{1}{\sqrt{2}}\left(\sqrt{\sqrt{\frac{P_1 S}{EI}} + \frac{S}{2EI}} + i\sqrt{\sqrt{\frac{P_1 S}{EI}} - \frac{S}{2EI}}\right)$$

$$= \pm (a_4 \pm i\, a_5)$$

$$y_{13}(x) = (c'_{41} e^{a_4 x} + c'_{42} e^{-a_4 x}) \cos a_5 x + (c'_{43} e^{a_4 x} + c'_{44} e^{-a_4 x}) \sin a_5 x$$

$$= (c_{41} \cosh a_4 x + c_{42} \sinh a_4 x) \cos a_5 x + (c_{43} \cosh a_4 x + c_{44} \sinh a_4 x) \sin a_5 x \tag{8}$$

Condition of Symmetry

Since physical set-up requires the cable to be symmetrical with respect to the line $x = \frac{L}{2}$, after transforming all the x's into $(x-\frac{L}{2})$, in general, all the unsymmetrical terms should drop out, hence

$$c_{12}, c_{14}, c_{22}, c_{24}, c_{31}, c_{32}, c_{33}, c_{34},$$
$$c_{42}, c_{43}, c_{44}, = 0 \qquad (9)$$

Eq. (3), (6), (7), and (8) become

$$y_{10}(x) = c_{11} \cos a_u (x - \tfrac{L}{2}) + c_{13} \cosh a_v (x - \tfrac{L}{2}) \qquad (3a)$$

$$y_{11}(x) = c_{22} \cosh a_1 (x - \tfrac{L}{2}) + c_{23} \cosh a_2 (x - \tfrac{L}{2}) \qquad (6a)$$

$$y_{12}(x) = 0 \qquad (7a)$$

$$y_{13}(x) = c_{41} \cosh a_4 (x - \tfrac{L}{2}) \cdot \cos a_5 (x - \tfrac{L}{2}) \qquad (8a)$$

Boundary Conditions

For simply-supported ends, assume

$$y_f(o) = y_f(L) = 0$$
$$y_f''(o) = y_f''(L) = 0 \qquad (a)$$

For the case

$$F(x) = F_o \sin \frac{\pi x}{L}$$
$$B_1 = \frac{F_o}{k' \frac{\pi}{L} S} = a_f \qquad (10)$$

where $k' = EI \frac{\pi^4}{L^4} + S \frac{\pi^2}{L^2}$

From boundary conditions (a), we obtain

$$c_{11} = c_{12} = c_{21} = c_{22} = C_{41} = 0 \qquad (11)$$

consequently,

$$y_f(x) = \pm a_f \sin \frac{\pi x}{L} \qquad (12)$$

where "a_f" is defined by Eq. (10)

APPENDIX D

BIBLIOGRAPHY ON VIBRATIONS OF CABLES

1. Bate, Ernest — "The Vibration of Transmission Line Conductors" Institute of Engineers, Australia Trans. VII, 1930, pp. 277-290

2. Bechtold, K. & Folkerts, H. — "Resistance of Cable to Transverse Vibration Especially Hollow Overhead Cable" - Elektrotechnik und Maschinenbau v. 47, 1929, p. 593-604

3. Bonnerville Power Admin., U. S. Dept of Interior — "Conductor Vibration Manual" Nov., 1947

4. Buchanan, W. B. — "Vibration Analysis-- Transmission Line Conductors" Trans AIEE Vol. 53 p. 1478 1934.

5. Carroll, J. S. — "Laboratory Studies of Conductor Vibration" Trans. AIEE Vol. 55 1936, p. 543.

6. Davison, A. E. — "Dancing Conductors" AIEE Summer Convention (see AIEE Journal) 1930

7. Davison, A. E. & Ingles, J. A. & Martinoff, V. M. "Vibration and Fatigue in Electrical Conductors" Trans AIEE p. 1076 Dec., 1932

8. DenHartog, J. P. "Transmission Line Vibration Due to Sleet" Trans AIEE Vol. 51, p. 1074, 1932

9. Levey, H. C. Prett, P. H. "The Vibration of Telephone Line Wires" Symposium on the Failure of Metals by Fatigue pp. 447-499, Melbourne Univ. Press, 1946

10. Monroe, M. A. & Templin, R.L. "Vibration of Overhead Transmission Lines" AIEE Quarterly Trans. Dec. 1932 Vol. 51, pg. 1059

11. Ontario Hydro-Electric Power Commission, Canada "Bibliography of Vibration in Electrical Conductors including Allied Researches" May 1946 and April 1947

12. Preston, G. W. "Conductor Vibration-Experience on Overhead Lines in North America" The Electrician, Oct., 15, 1937 pp. 431-32

13. Relf, E. F. & Ower, E. "The Singing of Circular

x^{iv}	$\frac{d^4X}{dx^4}$
y	deflection of cable
$y_f(x)$	particular solution induced by the constant dry friction damping term $F(x)$
y_m	deflection at mid-span
$(y')_o$	$(\frac{dy}{dx})_o$, or slope of cable at the ends
$(y'')_m$	$(\frac{d^2y}{dx^2})$ at mid-span
	lay length of cable
μ	mass of cable per unit length
ϕ	angular displacement at ends of cable specimen
ϕ_c	critical amplitude
ϕ_i	peak angular displacement in the i-th half-cycle
$\dot{\phi}_{ci}$	width of hysteresis loop - or residual angular displacement of the i-th half-cycle ($= \frac{M_f}{k}$)
$\dot{\phi}_i$	maximum angular speed of motion in the i-th half-cycle
$\ddot{\phi}$	angular acceleration
$\Delta\phi_i$	decay of angular amplitude from the i-th to the (i+1) - th half cycle
$\delta\varphi_i$	modification of amplitude due to the deviation from ideal friction
θ	angle of twist of the stranding wires

and Streamline Wires"
Aeronautical Research Comm.
No. 825 (Ae. 76) March, 1921

14. Speight, James W. "Conductor Vibration--Theory of Torsional Dampers Trans. AIEE, Vol. 60 p. 907, 1941

15. Stickley, G. W. "Stress-Strain Studies of Transmissions of Line Conductors" AIEE Trans Vol. 51, Dec. 1932 page 1052-73

16. Stockbridge, G. H. "Overcoming Vibration in Transmission Cables" Elec. Wld., 1925, p. 1304 Vol 86, No. 26

17. Sturm, R. G. "Vibration of Cables and Dampers" Trans. AIEE, Vol. 55, 1936, pp. 455 and 673

18. Tebo, Gordon, B. "Measurement and Control of Conductor Vibration" Trans AIEE Vol. 60 p. 1380, 1941

19. Varney, Theodore "Notes on the Vibration of Transmissions-Line Conductors" Trans AIEE, Vol. 45 pg. 791 1926

20. Wright, E. M. & Mini, J. Jr "Field Tests on Conductor Vibration" Elec. Eng. Vol. 83, July 1954, pp. 1123-7

21. Yu, Ai-Ting & Johnston, B. G. "A Method for Vibration Fatigue Tests of Stranded Conductors" Proc., Society for Experimental Stress Analysis, No. II, Vol. VI, 1948

PART I

INVESTIGATION OF THE NATURE OF INTERNAL DAMPING

(A)

PRELIMINARY ANALYSIS OF THE DEFORMATION AND ENERGY RELATIONSHIPS

(1) STATEMENT OF THE PROBLEM

In the vibrations of a stranded cable strung under tension, many external sources of energy dissipation often enter into the picture; among them, air resistance, dissipation in the frame structures, loss in the end connections, loss in the drive motor (in laboratories), etc. In order to isolate the system from these external effects so that the basic nature of internal damping of stranded cable alone may be uncovered, a short segment of cable vibrated under pure bending load will first be considered. The effect of tension will then be analyzed independently as a separate problem.

With damping existing in the cable, the system is non-conservative. One of the most outstanding characteristics of a non-conservative system is the fact that the variation of energy relationships from one configuration to another is not independent of path (Ref. 4). Furthermore, whenever dissipation takes place, the path between two configurations is in general many-valued (depending on the initial conditions, the direction of travel, etc.). Therefore, in order to study the energy relationships in the cable, in particular,

the energy dissipation and the dissipation functions, one must first define the path between the configurations.

The configuration of the cable under pure bending load at a particular instant is completely defined by three variables, namely, time, moment and deformation. Therefore, the paths for the system to pass from one configuration to another may be conceived as the space curves connecting two points in the three-dimensional space of time-moment-displacement.

The nature of these three-dimensional space curves may best be analyzed by projecting them into the two coördinate planes, namely the moment-displacement coördinate plane and the displacement-time coördinate plane. Thereby the path which we shall investigate are reduced to two individual plane-curves.

Now, if we define the "path in the moment-displacement plane" by the projection of the path between configurations in the moment-displacement coördinate plane, and at the same time, define the "path in the displacement-time plane" by the projection of the same in the displacement-time coördinate plane, we may then formulate our first problem as follows:

THE PROBLEM

"To determine, for a stranded cable subjected to cyclically varying pure bending loads, the following:

(a) Its path between any two configurations in

the moment-displacement plane and also in the displacement-time plane, and

(b) The energy relationships, in particular energy dissipation, along these paths."

Limiting our case to small deformations, we assume the shape of the deformed axis of the cable under consideration to be a circular arc. Thus the curvature, angular displacement at the ends and the mid-span deflection of the cable become linearly proportional to each other (see Appendix A). If the angular displacement at the ends of the hypothetical circular arc is considered as our only generalized coordinate, the system is reduced to one of a single degree of freedom (having the angular displacement at the ends of the cable as the only independent variable).

(2) PATH AND ENERGY RELATIONSHIPS IN THE FORCE-DISPLACEMENT PLANE

Path in the M-ϕ Plane

Consider a segment of stranded cable of length L simply supported at both ends and subjected to pure bending load M. Assume the equivalent flexural rigidity "EI" of the cable to be constant. The angular displacement at the ends which corresponds to the bending moment M is ϕ, and the maximum deflection at the center-span is y_m.

If there were no internal damping, the well-known Bernoulli-Euler's law for bending of beams may be applied (Ref. 5), in brief:

$$M = EIy'' \qquad (1)$$

where EIy'' is the elastic resisting moment developed in the cable due to the flexural rigidity of the cable.

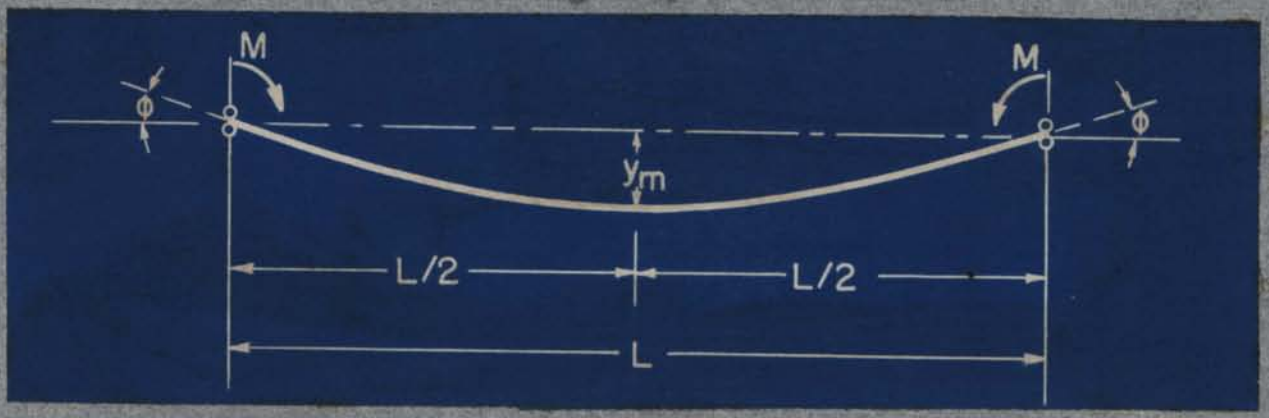

Figure 1

In actual cases, when a segment of cable is deformed by M, in addition to the elastic resisting forces, resistance to the deformation is also built up by the dissipative forces — predominantly the dry friction in between strands and the internal solid friction of wire materials. The nature of these dissipative resisting forces is basically different from that of the elastic resisting forces in that the work done by the former is not recoverable.

Assume the cable to be uniform throughout its length; on each section along the span, a unit moment due to friction "m_f" acting opposed to the effect of the external load M may

be thought to have developed upon deformation.* m_f is here defined as the "unit damping force function", its magnitude being equal to the frictional bending resisting moment per unit length of span and its unit being the same as that of force. If the bending deformation is uniform throughout the span L, m_f is constant along L, and the total frictional resisting moment M_f developed in the span becomes

$$M_f = m_f.L$$

The frictional resisting moment M_f varies from cable to cable and is a function of the geometrical and elastic properties of a particular cable. Although their relationships may be analyzed by studying these properties, they are not discussed in this paper.

Owing to the existance of these additional resisting forces in the cable, the Bernoulli-Euler's law should be modified by adding the integrated effect of these dissipative resisting forces M_f to the elastic resisting force EIy'' as follows:

$$M = EIy'' + M_f \qquad (2)$$

Since M_f acts in opposite directions during processes of loading and unloading and since the sign in front of it

*When a stranded cable is bent by pure bending loads, shear is developed in all directions except those parallel and perpendicular to the neutral axis. The shearing force parallel to the bending wires is taken up by the inter-strand dry friction.

is not self-adjustable (as y") during these changes; for both loading and unloading, Equation (2) should be written as

$$M = EIy'' \pm M_f \tag{2a}$$

When the deformation is small, the centerline of the deformed cable may be taken as a plane circular arc and the following relations may be obtained (see Appendix A),

$$y'' = (y'')_m = \frac{2}{L}(\phi) \tag{3a}$$

$$\phi = (y')_o = \frac{4}{L}y_m \tag{3b}$$

Substituting (3a) into (2a), we get

$$M = \frac{2EI}{L}\phi \pm M_f$$

or

$$M = k\phi \pm M_f \tag{4}$$

where M = applied bending moment

$k = \frac{2EI}{L}$

ϕ = angular displacement at the end of the cable

M_f = frictional resisting moment

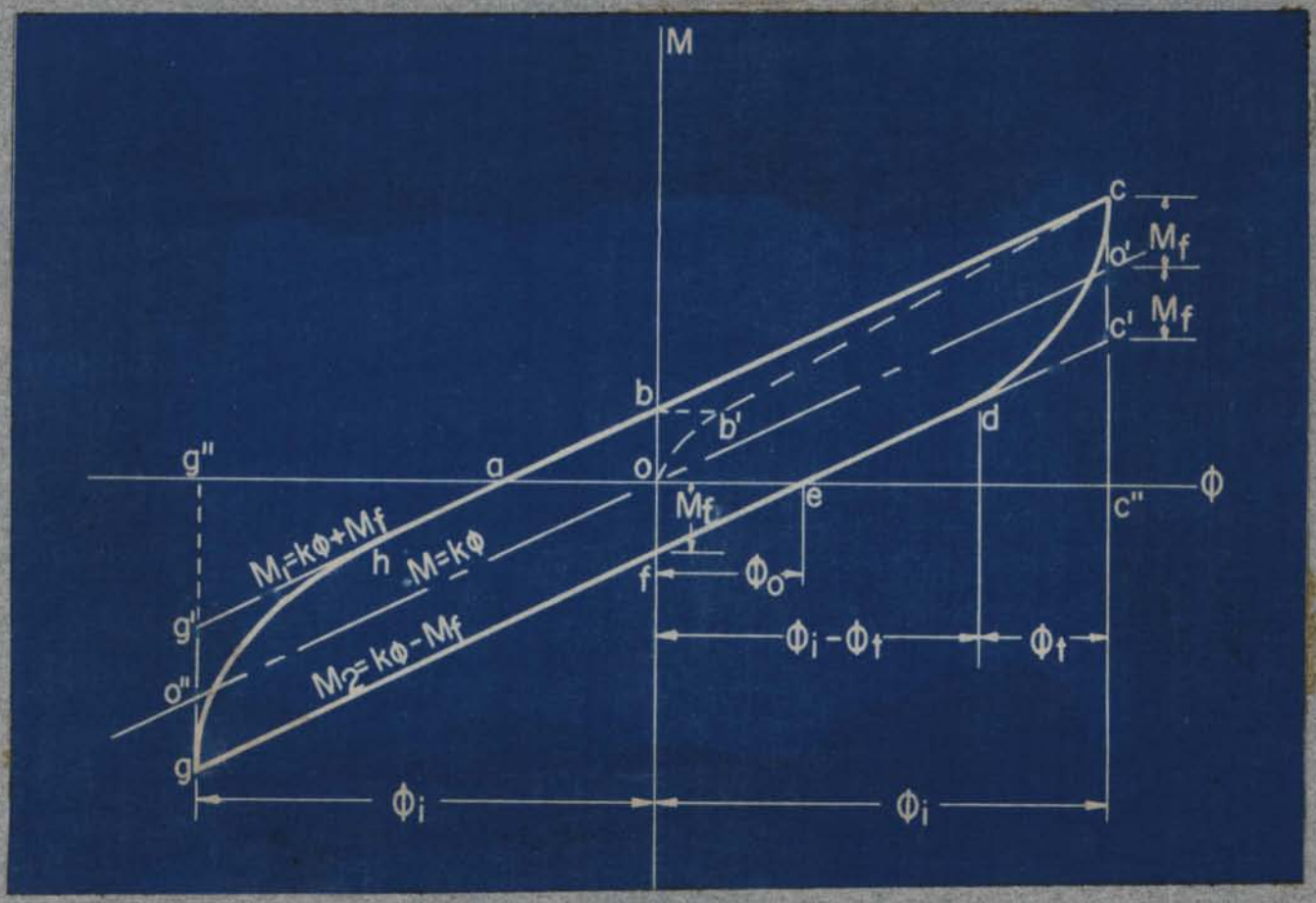

Figure 2

Equation (4) is represented by lines g'c and gc' in Figure 2. o"oo' represents the case where there is no friction ($M_f = o$). When a segment of cable is bent by cyclic bending loads of identical maximum positive and negative magnitudes $\pm M_1$, after a few initial transient cycles (Ref. 6), g'c (or $M = k\phi + M_f$) becomes the steady sustained path in the M-ϕ plane which the cable will follow when its motion is toward $+\phi$; whereas c'g (or $M = k\phi - M_f$) is the path for motion in the reversed direction. Due to the abrupt change of sign of M_f at the peak of loadings (c or g) in either direction, the steady cyclic path is discontinuous at these points. Furthermore, at these points of discontinuity, "transition paths"

must be followed for the cable to pass from one state of motion governed by "$M = k\phi + M_f$" (g'c) to another governed by "$M = k\phi - M_f$" (cg') or vice versa. In ideal cases, where the frictional resisting moment in the cable is a constant regardless of load-displacement conditions, no movement of the cable will commence upon release of load at c until the load reduction has surpassed twice the value of limiting dry friction moment M_f. Hence the transition path is cc' from c to $M = k\phi - M_f$ and similarly gg' from g to $M = k\phi + M_f$. Consequently, in the ideal case, the steady sustained path in the M-ϕ plane for the cable of Figure 4 is the parallelogram cc'gg'c.

In actual cases, upon the release of load at c, stranded wires in the cable will tend to readjust themselves in order to resist the abrupt change of direction of bending load. Under normal circumstances some initial slipping between wires will take place at this stage of readjustment, and hence ϕ_1 will not remain constant until the bending load drops to $M_1 - 2M_f$, the passing-over from c to $M = k\phi - M_f$ is therefore relatively gradual. cd and gh in Figure 2 represents qualitatively the transition paths in actual cases and the steady sustained path becomes cdghc.

Since dry friction is independent of the time rate of loading, in the ideal case, the system will follow the cyclic path cc'gg'c (or cdghc in actual cases) regardless how fast

the load M is applied. Therefore, this path pattern represents both the cases of sustained steady-state vibrations in vacuum and the static cyclic loadings (where speed approaches zero). In the latter case, the path is commonly known as the static hysteresis loop of damping on account of its similarity in shape with the hysteresis in magnetism.

Energy Relationships

Refer to the M-ϕ plane shown on Figure 2, p. 14, the potential energy stored into the system during the process of loading from zero load to maximum moment M_i by external forces is represented by the area acc". For a complete cycle, when the system is symmetrical with respect to the neutral axis, the energy input is the system is

$$W_i = 2 \times \int_0^{\phi_i} \phi_i M d\phi$$

= area $\overline{acc}$" + area $\overline{egg}$"

= 2 x (area $\overline{acc}$")

$$= k (\phi_i - \phi_o)^2 \qquad (5)$$

The energy released by the system during the process of unloading is represented by the area c'ec" in the ideal case and the area cdec" in actual cases. The "Damping Capacity" of a system is defined as the energy dissipated per cycle; it is the difference in between the energy input and the energy released, and therefore equals twice the area

bounded by the ϕ-axis and the loading path abc and the unloading path cc'de in the ideal case or cde in actual cases. Over a complete cycle, the energy dissipation is represented by the closed area cc'gg'c in the ideal case or the area cdghc in case where there is initial slipping. This bounded area is commonly known as the hysteresis loop area, and its value may be obtained as the line integral of the area evaluated along the loading and unloading paths.

Let $2A_i$ = area of the parallelogram cc'gg'c and

A_t = area cc'dc or area gg'hg (induced by initial slipping)

In general, we may equate the energy dissipation over a complete cycle as

$$\Delta W_i = \oint M d\phi$$

$$= 2 (A_i - A_t)$$

$$= 4 M_r \cdot \phi_i - 2A_t \qquad (6)$$

In ideal cases where there is no initial slipping, $A_t = 0$, and

$$\Delta W_i = 4 M_r \cdot \phi_i \qquad (6a)$$

A non-dimensional quantity commonly known as the "specific damping capacity" (Ref. 7) which expresses the damping capacity per unit amount of potential energy stored up in the same cycle is obtained by dividing ΔW_i with $2W_i$. Hence from (5) and (6)

$$\frac{\Delta W_1}{2W_1} = \frac{2M_f \cdot \phi_1 - 2A_t}{k(\phi_1 + \phi_o)^2} \qquad (7)$$

If A_t is independent of ϕ_1, Equation (7) is essentially a diagonal hyperbolic function of ϕ_1 which is characteristic of dry friction damping (Ref.8).

When $M_f = o$, ΔW_1 vanishes, the system is conservative; and the energy stored up in the system during the process of loading equals the energy released in the unloading process which are both represented by the area oo'c"o or area oo"g"o, which equals $\frac{1}{2}k\phi_1^2$.

(3) PATH AND ENERGY RELATIONSHIPS IN THE DISPLACEMENT-TIME PLANE

Mechanically Equivalent System

To analyze the behavior of a piece of cable under pure bending load in the ϕ-t plane, the system shown in Figure 1, p. 11, is replaced by a mechanically equivalent system shown in Figure 3.

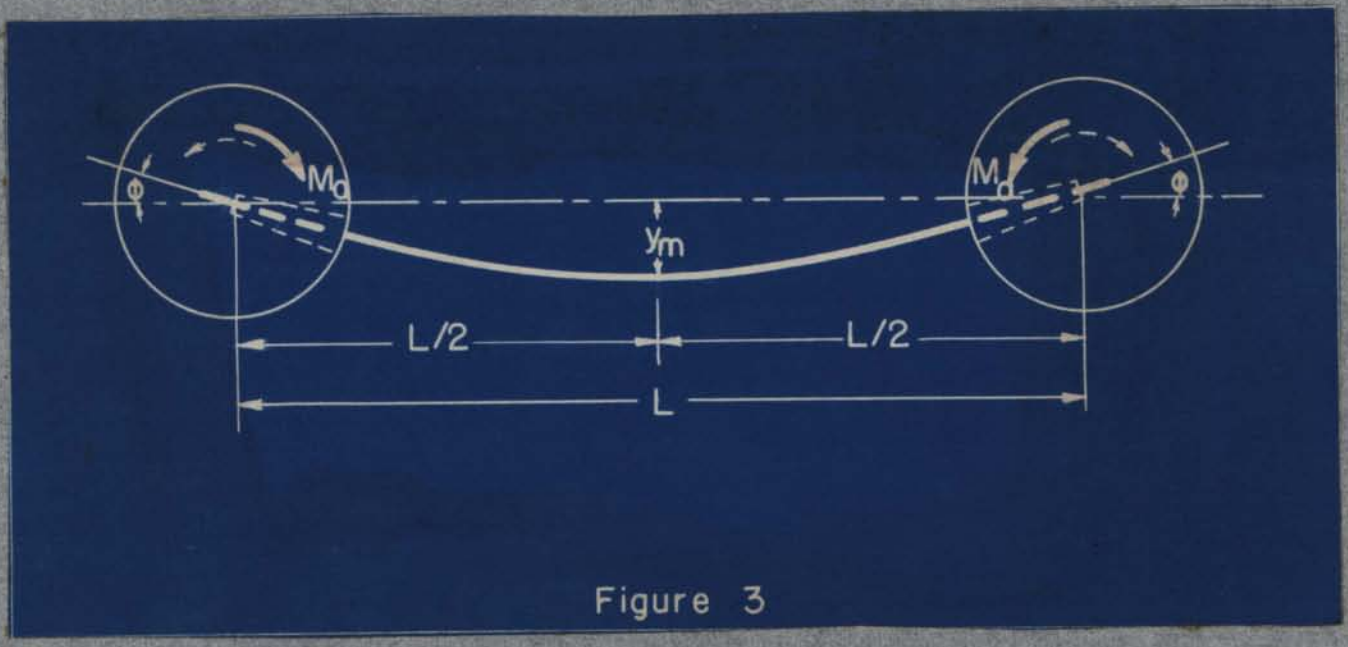

Figure 3

The ends of the cable are fastened to the center of a pair of identical round cylinders. The cylinders are rested on frictionless bearings or suspended by flexible wires so that they may oscillate freely about their individual axis of symmetry through center. If the deflection of the cable is small, relative displacement of the two cylinders in the x- direction may be neglected. Figure 3 is a plane view of the system.

If symmetrical external moments are applied on the cylinders, after being transmitted to the ends of the cable, the moments will cause it to bend in the plane of the cross-section of the cylinders as shown on Figure 5. If this external load is applied periodically, an additional moment due to the inertia of the system is induced in the direction opposed to the motion (and also to the periodical external load P). Since the mass of the cable is small compared with the cylinders, one may neglect the inertia effect of the cable and express the total value of the moment "acting on" the ends of the cable at a certain instant "t" by using D'Alembert's principle (Ref. 4) as

$$M(a) = P(f) - Ic\ddot{\phi} \qquad (8)$$

where $Ic\ddot{\phi}$ = torque induced by the inertia of the oscillating cylinder at the instant "t" where the end angular displacement is ϕ

$P(f)$ = external load

The total resisting moment induced in the cable at the same instant "t", where the end angular displacement is ϕ, from (4), p. 13, is

$$M(\phi) = k\phi \pm M_f \tag{9}$$

where M_f is the frictional resisting moment in the cable.

At any instant, the applied moment M(a) should always be in equilibrium with the resisting moment $M(\phi)$, hence

$$M(a) = M(\phi) \tag{10}$$

and it follows

$$P(f) = Ic\ddot{\phi} = k\phi \pm M_f \tag{10a}$$

Equation (10a) is essentially the same as (4), p 13, except for the terms on the left hand side of (10a) which are governed by the dynamic characteristics of the complete system and therefore are subjected to further restrictions for continuous motion (Ref. 9).

If the motion starts from a preset amplitude without applying any external load, hence P(f) = 0 and a free decay vibration is resulted;

$$-Ic\ddot{\phi} = k\phi \pm M_f \tag{11}$$

Here the only force "acting on" the ends of the cable at instant t is the inertia force "$-Ic\ddot{\phi}$" exerted by the cylinders in the direction against the displacement and its magnitude is "$k\phi \pm M_f$".

- Equation (11) may be made identical with (4), p. 13, if we equate the left hand side of both, which yields

$$M = -Ic\ddot{\phi} \tag{11a}$$

Therefore the path of (11) in the M-ϕ plane is obtained by merely taking $-I_c\ddot{\phi}$ as the applied moment M.

The solution of (11) gives the decay path of the system shown on Figure 3 in the ϕ-t plane. At every instant "t", there is a corresponding value of ϕ on the ϕ-t path, for this value of ϕ there is again a corresponding value of M on the M-ϕ path. These three variables determine a point on the path between any two configurations in the M-ϕ-t space. Since in general M is a many-valued function of ϕ characterized by the dissipative system, the energy relationships of the system can only be determined by a detailed study of the corresponding paths in both the ϕ-t and M-ϕ plane simultaneously.

Determination of the ϕ-t Paths

The equation of motion of forced vibrations of the system shown on Fig. 3 is (10a), or, by transposing terms,

$$I_c\ddot{\phi} + k\phi \pm M_f = P(f) \qquad (10b)$$

where I_c = Moment of inertia of cylinder about its axis of symmetry.

ϕ = Angular displacement.

k = Spring coefficient (assumed constant throughout each half cycle.)

M_f = Friction resisting moment.

P(f) = Driving force function

Eq. (10b) is nothing but the equation of forced

vibration of a system with one degree of freedom having dry friction damping, the only coordinate being the end angular displacement ϕ of the cable. Its general solution was given by Den Hartog for sinusoidal driving force functions (Ref. 9).

If the external driving force on the cylinders P(f) is dropped out, the equation of motion of free vibration (11) may be written as

$$I_c\ddot{\phi} + k\phi \pm M_f = o \qquad (11b)$$

The free decay path of the end angular displacement of the cable in the ϕ-t plane is given by the solution of this equation. When M_f is independent of ϕ, the solution of (11b) is well known (Ref. 10).

$$\phi = (\phi_i + \phi o) \cos pt \qquad (12)$$

where ϕ_i = Maximum angular displacement of the cylinder (or the ends of the cable) in the i-th half cycle.

$\phi o = \frac{M_f}{k}$ = Residual displacement (half of the width of hysteresis loop).

p = frequency of vibration.

Equation (12) represents the decay ϕ-t path in the i-th half cycle started from $\phi = \phi_i$ and ended at $\phi = \phi_{i+1}$. The sign in front of ϕo changes at the end of each half cycle; hence the curvature of the path is also discontinuous at the

ends of each half cycle.

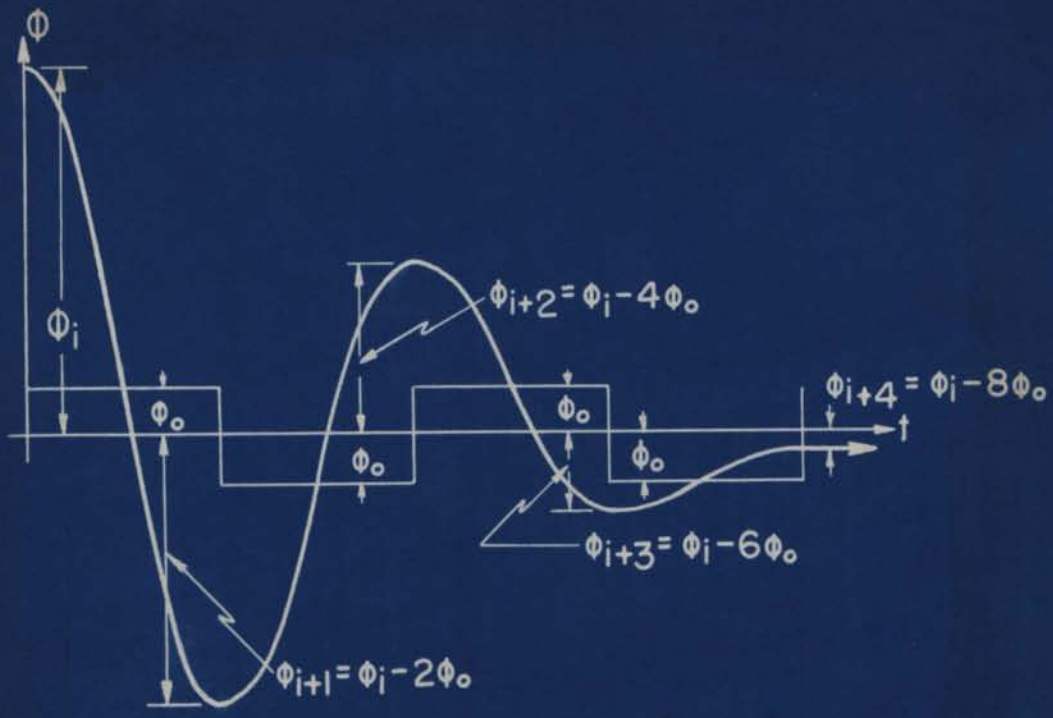

Fig. 4 Typical Free Φ-t Path

Figure 4 is an example of a typical decay path in the ϕ-t plane for the case of ideal internal dry friction damping where the frictional resisting moment in the cable $M_f(=k\phi_o)$ remains constant through-out the passage.

From both Equation (12) and Figure 4, it is easily seen that the motion of each half-cycle is simple harmonic about a mid-position distant ϕ_o from the position corresponding to zero inertia force. The mid-position changes from + ϕ_o to -ϕ_o and then to ϕ_o at the end of each half

cycle while the frequency remains constant.

The maximum amplitude ϕ_i at the end of each half-cycle, measured from neutral position, is $2\phi_o$ less than at the end of the preceding half-cycle. Hence we can equate the decay of the end angular displacement of the cable in each half-cycle for the case of ideal dry friction damping as

$$\Delta\phi_i = \phi_i - \phi_{i+1} = 2\phi_o \tag{13}$$

The spring coefficient "k" may be determined from the decay path by the following:

$$k = I_c \left(\frac{2\pi}{T}\right) \tag{14}$$

where T is the period of vibration and I_c is the solid moment of inertia of the cylinder with respect to its axis of rotation.

Path and Energy Relationships

During steady sustained vibrations, energy dissipated per cycle in the cable is equal to the work done against the frictional resisting moment M_f along the path of vibration in the ϕ-t plane, hence, for ideal dry friction, if the motion is harmonic,

$$\Delta W_i = \int_o M_f d\phi$$

$$= M_f \int_o d(\phi_i \cos pt)$$

$$= 4M_f \cdot \phi_i \tag{15}$$

Equation (15), obtained from path in the ϕ-t plane,

is essentially the same expression for ΔW_i in Equation (6a), p. 17, obtained in the M-ϕ plane.

Without external energy supply, since a part of the potential energy in the deflected cable is being dissipated along the ϕ-t path into the universe, the vibration amplitude of the cable will gradually die down.

In Figure 5a, the dotted lines represent the cases of ideal dry friction whereas the solid lines represent actual cases where initial slipping occurs at the transition stages. Figure 5b shows the corresponding path of decay in the M-ϕ plane.

In ideal cases, ϕ_o remains constant and the M-ϕ paths follow along clearly the square edges of a parallelogram. During the progress of decay, when c of the i-th cycle at amplitude ϕ_i is reached, the system has stored up potential energy to the amount of (Equation 5)

$$W_i = \tfrac{1}{2}k\,(\phi_i + \phi_o)^2$$

As motion changes direction at c, the direction of the frictional resisting moment M_f changes instantly to remain opposing to it. At this instant, point c drops to c' on the M-ϕ path. As the system moves from c' along c'de, the stored potential energy gradually releases itself along the path, and at the same time the potential energy released is transformed into kinetic energy as evidenced by the increase of speed along the ϕ-t path until it reaches its maximum value at the point e. Point e is the end of

FIGURE 5 IDEAL AND ACTUAL PATHS

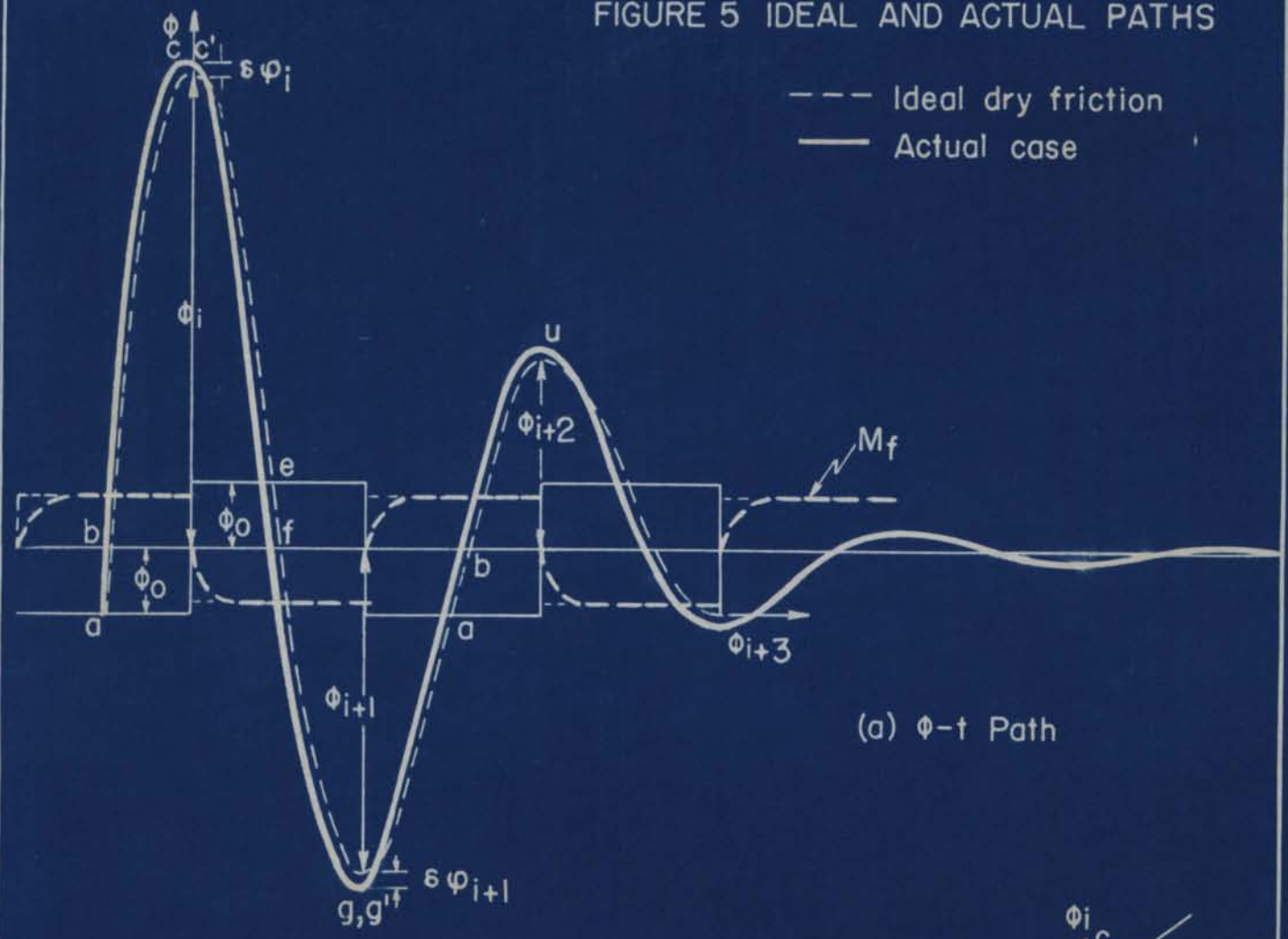

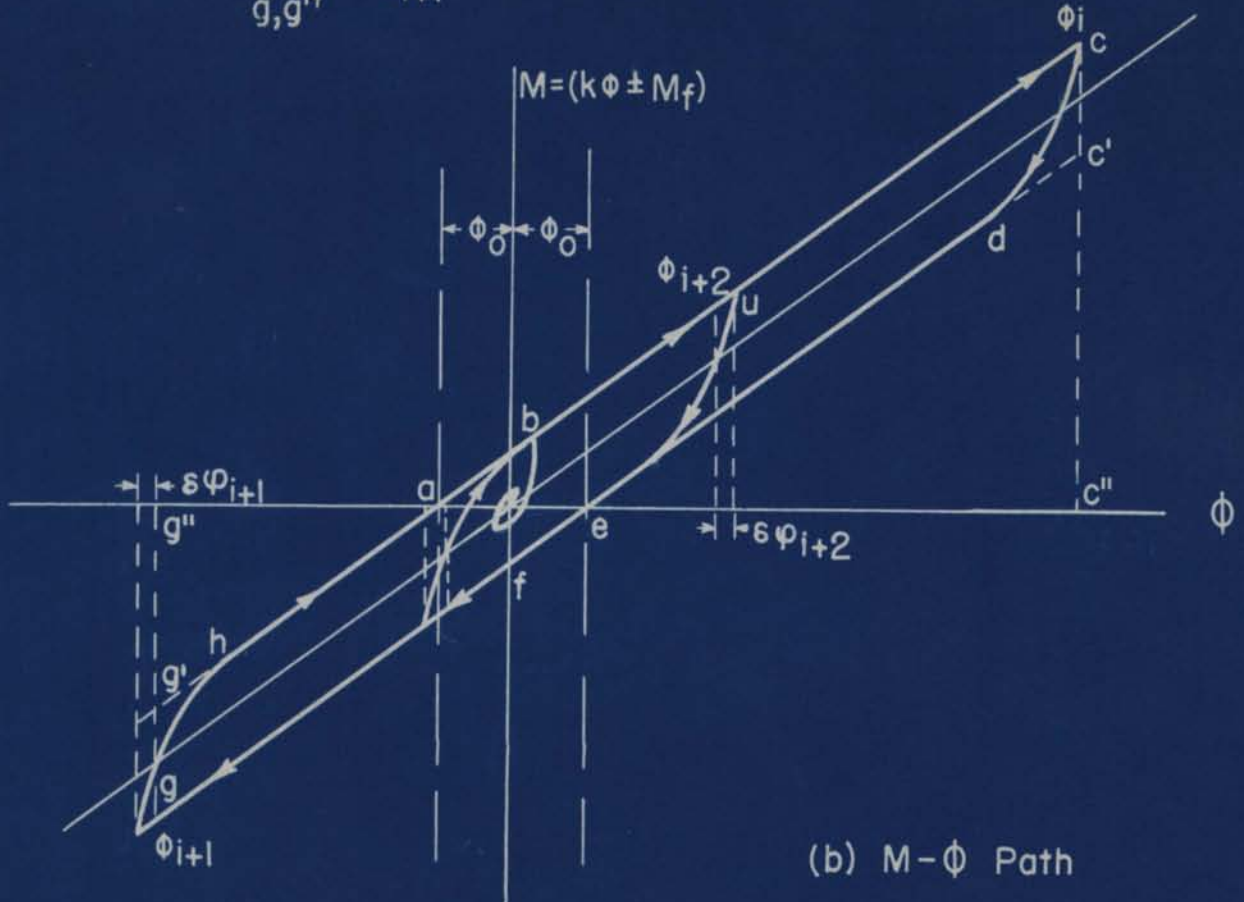

the half cycle ac-c'-e, through which the potential energy W_i (= area acc"a) is partly dissipated (ΔW_i = area acc'ea) and partly transformed into kinetic energy (KE_i = area ec'c"e), hence

$$W_i - (KE)_i = \Delta W_i \tag{16}$$

The kinetic energy $(KE)_i$ will now force the motion to proceed to point g at amplitude ϕ_{i+1} by transforming $(KE)_i$ along the path $\overline{cg}$ into the potential energy. The potential energy will reach its maximum at point g where

$$W_g \equiv W_{i+1} = KE_i \tag{17}$$

$$\text{area } c'ec"c' = \text{area } g'eg"g \tag{17a}$$

(17a) may be written as

$$\tfrac{1}{2}k\,(\phi_i - \phi_o)^2 = \tfrac{1}{2}k\,(\phi_{i+1} + \phi_o)^2$$

From which, for constant ϕ_o and constant k, we obtain

$$\phi_i - \phi_o = \phi_{i+1} + \phi_o \tag{17b}$$

$$\therefore \Delta\phi_i \equiv \phi_i - \phi_{i+1} = 2\phi_o \tag{17c}$$

which is exactly the same as expression (13) obtained by considering relations of force and displacement only (p. 22).

In actual cases, at least two factors often enter into the picture and hence necessitate the modification of the ideal relationships described above; they are (a) initial slipping between wires during the transition stages (see p. 15) and (b) the fact that k and ϕ_o vary with the amplitude ϕ_i.

The effect of initial slipping at the beginning of each half-cycle is indicated in Figure 5a. The heavy broken lines show the frictional resisting moment as plotted against time axis. In ideal cases, where there is no initial slipping, frictional resisting moment changes direction abruptly at the end of each half-cycle, and remains constant throughout each half-cycle. In practical cases, where some amount of initial slipping in between wires usually takes place at the beginning of each half-cycle, the building-up of friction force in the opposite direction is somewhat gradual; as a result, the first part of each half-cycle of the frictional resisting moment tends to be rounded off.

As the system takes the transition path $\overline{cd}$ upon decay from amplitude ϕ_i of the i-th cycle, an additional amount of energy represented by the transition area A_{ti} (cc'dc) in the M-ϕ plane is released and transformed into kinetic energy. This additional energy will tend to increase the peak amplitude ϕ_{i+1} of the following cycle by the amount of $\delta\phi_{i+1}$. The value of $\delta\phi_{i+1}$ is obtained by modifying (17a) as follows,

$$\text{area } c'ec''c' + A_{ti} \cong \text{area } geg''g + k(\phi_{i+1} + \phi_o)\delta\phi_{i+1}$$

$$\cong \text{area } geg''g + k(\phi_i - \phi_o)\delta\phi_{i+1}$$

Now subtract (17a) from above and transpose terms, we obtain

$$\delta\phi_{i+1} = \frac{A_{ti}}{k(\phi_i - \phi_o)} \qquad (18)$$

where ϕ_i = amplitude of i-th half-cycle

A_{ti} = Increase of kinetic energy due to initial slipping in the i-th half-cycle.

ϕ_o = Residual displacement (width of hysteresis loop)

$= \frac{M_f}{k}$

k = Spring coefficient

The existance of initial slipping during the transition stages also tends to distort the sinusoidal shape of the ϕ-t path produced in ideal cases. As the system moves down from the peak point c, higher kinetic energy produced by the additional transition area A_t (=cc'dc) induces higher speed of motion throughout the quarter cycle along path cdo. This higher speed of motion will tend to make the slope of the ϕ-t decay path steeper at every point than that of the corresponding path in the case of ideal dry friction.

The modified ϕ-t path due to the influence of initial slipping at transition stages is represented qualitatively by the solid line in Figure 5a.

Since the mid-position of each half-cycle is determined by the magnitude of ϕ_o (Equation 12, p. 22), the variation of ϕ_o will shift the mid-positions of the half cycles and consequently vary the maximum amplitudes. In cases where ϕ_o is a vanishing function of ϕ_i, the decay path will tend to terminate at the neutral position where the vibration moment (due to inertia) is zero.

Except for the cases of ideal friction, any half-cycle along the free decay path as mapped into the M-ϕ plane is basically different from the paths of sustained steady vibrations at the same amplitude, because the latter is a limit curve approached by many consecutive transient cycles near a certain constant amplitude (Ref. 6). The free decay path, however, in a sense may be looked upon as nothing but many continuous transition paths for the vibrations at one amplitude to reach some other.

Based on this concept, in a strict sense, the energy dissipation in each half cycle obtained from the decay path is basically different from the same value obtained from the sustained steady path at the same amplitude. The difference tends to become more and more noticeable as the magnitude of damping increases.

Energy Evaluation from Decay Path

For cases of ideal dry friction, the potential energy at the peak of the i-th half-cycle where the amplitude is ϕ_i is (Equation 5, p. 16)

$$W_i = \tfrac{1}{2}k\,(\phi_i + \phi_o)^2$$

Energy dissipated at the end of the i-th half-cycle is the difference between W_i and the maximum kinetic energy at the end released through this half-cycle, which is again equal to the maximum potential energy to be stored up in the next half-cycle (i+1). Therefore, the amount of energy

dissipation in the i-th half-cycle is

$$\Delta W_i = W_i - W_{i+1} \tag{19}$$

or $$\Delta W_i = \tfrac{1}{2}k(\phi_i+\phi_o)^2 - \tfrac{1}{2}k(\phi_{i+1} + \phi_o)^2 \tag{19a}$$

From (17b) and (17c), p. 26, we obtain,

$$\Delta W_i = \tfrac{1}{2}k\left[(\phi_i + \phi_o)^2 - (\phi_i - \phi_o)^2\right]$$

$$= 2k\phi_i\Delta\phi_o$$

$$= k\phi_i\Delta\phi_i \tag{19b}$$

where ϕ_i = amplitude of the i-th half cycle

$\Delta\phi_i = \phi_i - \phi_{i+1}$

= Decay of amplitude from i-th half-cycle to (i+1) th half-cycle

k = Spring coefficient of the cable.

Since $\Delta\phi_i = 2\phi_o = 2(\frac{M_f}{k})$ is a constant for ideal dry friction damping with constant spring, equation (19b) indicates the fact that the energy dissipation per cycle of the system is a linear function of the amplitude along the decay path.

The percentage energy dissipation or "specific damping capacity" in the cycle is

$$\frac{\Delta W_i}{2W_i} = \frac{k\phi_i\Delta\phi_i}{k(\phi_i+\phi_o)^2}$$

$$= \frac{\frac{\Delta\phi_1}{\phi_1}}{(1+\frac{1}{2}\frac{\Delta\phi_1}{\phi_1})^2} \qquad (20)$$

For small damping,

$$\Delta\phi_1/\phi_1 < 1, \text{ hence}$$

$$\frac{\Delta W_1}{2W_1} \simeq \frac{\Delta\phi_1}{\phi_1} \qquad (20a)$$

which indicates that specific damping capacity is equal to percentage decay, the latter is a close approximation of which is commonly known as "logarithmic damping coefficient" (Ref. 8). For ideal dry friction, where $\Delta\phi_1$ remains constant, equation (20a) gives the specific damping capacity as an equilateral hyperbolic function of decay amplitude ϕ_1.

In actual cases where initial slipping in between wires takes place and / or ϕ_0 varies as a function of ϕ_1, the situation is not so simple. Exact evaluation of energy from ϕ-t decay path may only be obtained by evaluating the kinetic energy and potential energy at every point along the decay path. The corresponding M-ϕ diagram may then be constructed and the final energy relationships evaluated therefrom.

In many instances, very close approximations may be obtained by more simplified procedures. When the amount of damping is comparatively small, the errors resulting from these procedures often become insignificant.

Among various approximate methods, one which deals with

potential energy alone proves to be most simple. In this method, k is assumed to be the same for two consecutive half cycles along the path, the corresponding decay paths of the two half-cycles in the M-ϕ plane are assumed to be similar in shape, and both the variations of $\delta\varphi_i$ (Equation 18, p. 27) and of ϕ_o in the same interval are assumed to be small. Equation (19), p.30, then goes into the form

$$\begin{aligned}\Delta W_i &= W_i - W_{i+1} \\ &= 2k\,(\phi_i + \delta\varphi_i)\,\phi_o \\ &= k\,(\phi_i + \delta\varphi_i)\,\Delta\phi_i \qquad (21)\end{aligned}$$

where $\delta\varphi_i$ is obtained by Eq. (18)

When damping is small, $\delta\varphi_i$ is very small compared with ϕ_i, and damping capacity of the cable per half cycle becomes,

$$\Delta W_i \cong k\phi_i\,\Delta\phi_i \qquad (21a)$$

which is the same expression for ideal dry friction as given by (19b) for ideal dry friction, p. 30.

A closer approximation may be obtained by considering the maximum kinetic energy instead of W_i's. From (17), p. 26, we may generalize

$$W_{i+1} = (KE)_i \qquad W_i = (KE)_{i+1}$$

Therefore,

$$\begin{aligned}\Delta W_i &= W_i - W_{i+1} \\ &= (KE)_{i-1} - (KE)_i \qquad (22)\end{aligned}$$

The value of (KE)'s are obtained from the slopes at the mid-position of each half-cycle along the ϕ-t path, hence (23) may also be written as

$$\Delta W_i = \tfrac{1}{2} I_o (\dot{\phi}_{i-1}) - \tfrac{1}{2} I_o \dot{\phi}_i$$

$$= \tfrac{1}{2} I_o (\dot{\phi}_{i-1}^2 - \dot{\phi}_i^2) \qquad (22a)$$

If the location and magnitude of maximum slopes could be accurately determined, (22a) becomes an exact form where ϕ_i now represents the maximum slope of the ϕ-t path in the i-th half-cycle.

(B)

DETERMINATION OF THE DEFORMATION AND ENERGY RELATIONSHIPS BY EXPERIMENTAL METHODS

(1) EXPERIMENTAL TECHNIQUE

To study the deformation and energy relationships of a segment of cable vibrated under uniform bending, two individual test set-ups were developed; one for the determination by static methods of both the sustained and decay paths in the M-ϕ plane and the other as a mechanically equivalent system (see Section A, Figure 3) for the determination of ϕ-t paths of free decay vibrations. Since the M-ϕ paths obtained are similar to the magnetic hysteresis curves, the test scheme is commonly termed as "static hysteresis test".

The speed of vibration in the dynamic test set-up was designed to be very low in order to reduce the effect of air resistance to insignificance thus providing a basis for the comparison with the results obtained in the static tests.

Both the sustained and the decay vibrations were simulated in the static M-ϕ test. The sustained tests were based on the criterion of identical positive and negative bending loads. The decay amplitudes were determined by energy relationships and the results compared with those obtained in the dynamic tests.

The basic idea of the dynamic test set-up is due to Searle (Ref. 11), who devised a very ingenious oscillation system for the determination of Young's Modulus of a solid bar. The set-up is modified by using a pair of round cylinders the air resistance around which being negligible during oscillations about their individual axis of symmetry.

(2) DETAILS OF TEST SET-UP

Static Hysteresis test

Figure T-1 is a complete view of the static hysteresis test set-up. The cable specimen rests at both ends on roller supports, the details of which are shown on Figure T-2. The short cable ends beyond the span are inserted in tight sockets and fastened by set-screws. Round steel rods used as loading arms are screwed in the extreme ends of the sockets. Pure bending moment is applied by hanging dead weights at the extreme ends of the loading arms. Bending in the reverse direction is achieved by a pulley arrangement (see Figure T-1).

The deflection at mid-span is measured by an Ames dial gage. The spring in the dial gage was taken away to avoid possible errors induced by the additional load exerted on the cable specimen by the spring force.

The moment arm (distance from the point of application of dead weight to the roller support) is fixed at 10" to facilitate the evaluation of test results. The base beam

and roller supports may be adjusted for any desired length of span. The roller end supports may be easily adjusted for different sizes of specimen (see Figure T-2).

Free Decay Test

The decay test set-up consists of a vibration unit and a recording system, the complete view being shown on Figure T-3. Figure T-4 is a schematic diagram of the same set-up.

The vibration unit is built to produce the motion of the system described in Figure 3, p. 14. A pair of round cylinders are each suspended upright at the center of its top surface by thin wires to the roof structure. The distance from center to center of the cylinders may be selected by moving the attachments on the ceiling structure. The cable specimen is clamped at both ends in the middle portion of the cylinders by grooved half-cylinders (see Figure T-5) and held in position by set-screws (Figures T-3 and T-4). For specimens of smaller overall diameter, tightly fitted bushings were inserted (Figure T-5). The weight of the cylinders may be varied for the selection of varied frequencies of vibration. The highest speed was designed not to exceed 2 cps. in order to minimize the influence of air resistance. Thin thread is used to tilt the cylinders and thus bend the cable specimen into the initial amplitude desired. Dampers are provided at the bottom of the cylinders to reduce the system to stand-still before each test.

The recording system consists of a motion picture camera (Figure T-6 and T-7), a semi-transparent screen scale and a timing mechanism. The camera contains two 35mm. 100 ft. reels, one loaded and one serving as a winding wheel. The film slides behind a thin slot (less than 0.01" wide and parallel to the axes of the reels) on the rear of the light chamber and around a roller which keeps it focused on the object to be photographed through the lens (See Figure T-7). If the film were standing still, the picture photographed on the film would be only a thin strip exactly the size of the narrow opening behind the light chamber. When the camera is positioned as shown in Figure T-3 where the axis of the cable specimen at neutral position is parallel to the direction of the travel of the film (or, in other words, perpendicular to the long side of the thin slot), if the cable were replaced by a very thin wire, only a small point of the thin wire will appear on the "slice" photograph. As the film moves along and the lens remains open, the stationary image of this tiny point on the thin wire will trace a continuous straight line on the film parallel to the direction of its travel. The width of the thin straight line is the thickness of the wire. Now, if the thin wire starts to vibrate at the same time that the film is travelling, the image of the tiny point will record a motion curve of this vibration, and the latter is the displacement-time record of this tiny point. When the motion of a cable specimen instead of a thin wire is photographed, the motion curve becomes a wide band the width

of which equals the thickness of the cable.

A small motor and rheostat together with a transmission gear mechanism are used in order that the travelling speed of the film may be adjusted at will. The speed range of the film travel is 0.1 in/sec. to 100 in/sec.

Flood light and reflector are provided above the cable specimen facing the camera lens; thereby a black band for the cable vibration is obtained. A semi-transparent screen marked with a scale is provided underneath the reflector and it is thus projected on the film as reference lines. The distance of the specimen from the lens is so focused and calibrated that the ratio between the object and the photographed picture is a constant.

A timing gear is built making use of the mechanism of a standard metronome. A wing is attached to the tip of the needle that it may swing freely in front of the lens and hence cast a crossing line image superimposed on the vibration image at a constant time interval to provide a scale for the time axis (see Figures T-3 and T-4). At high speeds of vibration, the timing mechanism is replaced by a small motor carrying a propeller which swings in front of the lens and the speed of which is calbrated by a stroboscope. (see Figure T-10)

(3) TEST SPECIMENS

Four types of high strength carbon steel stranded cables and their constituent wires with the following specifications

were tested:-

Designation	771	771-P	772	331
Nominal Dia. (in.)	3/8		3/8	0.297
Number of Wires	7		7	3
Dia. of Wire (in.)	0.120		0.120	0.138
Designation of Wire	701		701	301
Lay Length (in.)	5.5		8.4	5.0
Weight (lb./ft.)	0.273		0.280	0.156
Breaking Strength (lb.)	10,800		11,000	5,620

The 7-wire specimens have the form of six wires stranded around one core wire, while the three wires twist around each other to form the 3-wire strand. All the constituent wires are zinc-coated and are of similar chemical composition.

Specimen 771-P has the same properties as 771 except for the process of manufacturing; the former being constructed by the "preform" process during which the desired twist in the wires was formed before they were stranded together.

Prestressing up to 30%, 50%, 70%, and 90% breaking strength was applied on several 3-strand specimens (331) for the investigation of effect of prestress.

Single wire specimens were obtained by releasing the wires from the corresponding cables after the tests on strands were completed.

All specimens were straightened by hand before tests.

(4) TEST PROCEDURES

Each specimen was tested for free decay to obtain the ϕ-t path and then had its ends trimmed to fit the end sockets for the static hysteresis tests to get the M-ϕ path.

Span of tests (L) was chosen at 40" in all the tests in order to provide for a simple relation between the angular displacement ϕ and the deflection at midspan y_m the latter being the quantity directly recorded in all the tests. From Equation (3b), p. 13

$$\phi = \frac{4}{L} y_m$$

$$= 0.1 \, y_m \qquad (23)$$

Static Hysteresis Tests

Sustained steady vibrations were simulated by cycles of bending in positive and reversed directions at a constant amplitude. Readings were taken after at least one complete cycle of loading and unloading. Only the readings for a half cycle were recorded on account of the symmetrical behavior of the cables evidenced in all tests.

Decay tests were performed by the consideration of energy relationships of each half cycle (see Section A, pp. 22-50) as follows:

(1) Load the specimen to amplitude ϕ_1.

(2) Unload to zero load and plot the M-ϕ path of unloading.

(3) Compute the remaining energy $W_i - \Delta W_i$ at the end of the half-cycle by measuring the area underneath the unloading path.

(4) Assume the slope of the loading path for the next half-cycle to be the same as that of the previous half-cycle and compute ϕ_{i+1} from $(W_i - \Delta W_i)$

(5) Load the specimen in reversed direction to amplitude ϕ_{i+1} and repeat the above process to obtain ϕ_{i+2}.

Gentle tapping was applied on the base beam until the reading on the dial gage became stabilized before each reading was taken. This procedure helps to minimize the possible frictional resistance exerted by the roller end supports.

4. Free Decay Test

Three different speeds of vibrations may be obtained by removing from or adding disk weights to the moment cylinders (Figure T-3).

The cable specimen was bent into a desired maximum amplitude by tieing a thin thread on one point in the middle of each of the pair of cylinders and drawing them slightly together (see Figures T-3 and T-4). The system was brought to rest by applying dampers at the bottom of the cylinders. Decay vibration was started by burning the thread in the middle.

The motion picture camera was focused at the mid-span of the cable specimen.

The speed of the film travel was selected to best suit various purposes of tests by merely adjusting the calibrated rheostat.

The 35mm picture obtained was enlarged to eight times the original size and the results were analyzed by using one edge of the thick motion band.

(5) DISCUSSIONS OF TEST RESULTS

Results of the bending free decay tests of wire and strands as represented by five typical sample pictures of the amplitude decay at mid-span are shown in Figures R-1, R-1a, R-2, R-3 and R-4 inclusively. It is of interest to note that the amplitudes of the stranded cables damped out very rapidly in a few cycles, while the amplitude decay of the single wire is hardly noticeable. Figure R-1a shows the vibrations 800 cycles behind the first cycle of Figure R-1.

Hysteresis loops for Specimens 771, 331, and 772 obtained from static bending tests at identical positive and reverse cyclic loadings are shown in Figures R-5, R-6 and R-7 respectively. Only half of the loops are presented because the other halves obtained during reversed loadings were identical in shape due to the symmetrical nature of the load-deformation relationships. The validity of the

modified Bernoulli-Euler's law (Eq. 4, p. 13) namely

$$M = k\phi \pm M_f$$

is evidence by the straight-line boundaries of all the loops. Slipping during the transition stages is revealed by the curved portions of the loops at the beginning of unloading.

Static bending tests were also carried out at cyclic diminishing loadings to simulate the dynamic free decay tests. The results obtained for Specimen 331 are shown in Figure B-8. Amplitudes of each half-cycle as computed from the remaining strain energy at the end of the previous half-cycle "$W_i - \Delta W_i$" (which is equivalent to the kinetic energy in the dynamic free decay test, see Eq. 16, p. 26) are compared with results obtained from dynamic free decay test (Figure B-4) as follows:

ϕ_i (radians x 10)		
Static	Dynamic	% Difference from Dynamic Test
0.783	0.768	-1.95
0.535	0.538	0.56
0.331	0.345	4.05
0.143	0.178	19.71

The close agreement between the dynamic and static decay tests indicates the fact that the internal damping of stranded cable is independent of the speed of vibration in the range observed and the validity of the procedures of investigation by studying separately the paths in M-ϕ

and ϕ-t planes.

The increase of % difference at low amplitudes is due to the increasing deviation from constant of slope of loading M-ϕ paths.

The damping capacity ΔW_i due to internal solid friction of material (energy dissipation per cycle) and specific damping capacity $\Delta W/2W$ of single wire Specimens 301 and 701 were obtained from free decay test results by the use of Eq. (20a) and (21a) and are shown in Figure R-9. The curves for both Specimens 301 and 701 appear to indicate the following relation

$$\Delta W = C\phi^{2.5} \qquad (21b)$$

where C is an arbitrary constant.

The energy relationships for cable Specimens 771 and 331 are shown in Figures R-10 and R-11 respectively. Dissipation is evaluated for each half-cycle instead of the full cycles to assure more exact values. Investigation of the two graphs reveals the following:--

(1) The dynamic decay test results agreed very well with the static hysteresis tests (despite the differences in basic principles underlying the two methods).

(2) Damping capacity ΔW_i is a linear function of maximum amplitude ϕ_i.

(3) A "critical amplitude" seems to exist for both specimens around ϕ_i = 0.02 radians, above which the curve of specific damping capacity begins to assume the shape of a diagonal hyperbola as given by Eq. (20a). The value

of specific damping capacity increases steadily with amplitude before it reaches its critical value.

The existance of the critical amplitude is probably due to the unavoidable non-uniformity of contact of wire surfaces in a cable specimen. As the segment of cable is bent from its neutral position, the cable becomes tightened and the contact surface between wires increases. The critical amplitude appears to be the amplitude at which relatively uniform contact of wires in the strand has arrived.

Damping capacities of both Specimens 771 and 331 are again plotted on Figure R-12 together with damping capacities of their constituent wires multiplied by the corresponding number of wires in strand. Comparison of the curves indicates that not more than 5% of energy dissipation was due to the internal solid friction of material in 3-stranded cable (No. 331) while 3% is the maximum of the same in the case of 7-stranded cable (No. 771).

Comparison of damping capacity of Specimens 771 (5.5" lay), 772 (8.4" lay) and 701 x 7 (equivalent to ∞" lay) as given by Figure R-13 indicates the increase of damping capacity with the reduction of lay length of stranded cable.

Approximately 30% increase of speed of vibration over 94.7 cpm for Specimen 772 does not have appreciable influence on damping capacity as is evidenced by Figure R-14.

"Preformed" cables* possess slightly less damping

*Twist in the constituent wires was formed before they were stranded together.

capacity than the non-preformed ones (Specimen 771) as shown on Figure R-15. Pre-stretching of 3-stranded cable over 90% its breaking strength considerably reduces its damping capacity whereas prestretching up to 70% breaking strength has no apparent effect as revealed by Figure R-16. Energy dissipation due to inter-strand friction is believed to have been reduced through either the "preform" process or prestretching over the yield point of the stranded cable.

Frictional resisting moment M_f (derived and defined in Section A, p. 12) and spring coefficient (flexural rigidity per unit length) of three cable specimens are plotted against amplitudes ϕ_1 in Figures R-17, R-18 and R-19. The frictional moment M_f is obtained by measuring the width of the hysteresis loops on the moment axes (Figures R-5, R-6, R-7). The value of M_f increases with amplitudes ϕ_1 and approaches a constant as the amplitude ϕ_1 exceeds the "critical amplitude". This phenomenon is somewhat less apparent in the case of the 3-strand cable than in the 7-strand ones. Based on the straight-line boundaries of the hysteresis loops shown on Figures R-5, R-6 and R-7, we may conclude the following

(1) Below a "critical amplitude", the frictional resisting moment M_f increases with deformation.

(2) Above the critical amplitude, the friction resisting moment M_f is independent of deformation.

The values of spring coefficient were obtained from

both dynamic and static tests as follows

$$k = \frac{2EI}{L} \qquad (s)$$

$$k = I_c\left(\frac{2\pi}{T}\right)^2 \qquad (d)$$

where T is the period of vibration and I_c is the solid moment of inertia of the cylinders.

The value of k obtained from both methods tends to be a constant above critical amplitude; and the ones obtained from dynamic tests are slightly higher than those from static tests.

The horizontal width of the hysteresis loops ($2\phi_o$) and decay of amplitude per half-cycle ($\Delta\phi_1$) for three specimens 771, 772 and 351 were plotted against ϕ_1 on Figures R-20, R-21 and R-22. The general shape of the two curves for each specimen checked fairly well with each other, and the values of the two checked nearly exactly in the case of Specimen 772. In the case of Specimens 771 and 351, where the hysteresis loops are large (see Figures R-5, R-6 and R-7), the fact that $2\phi_o$ as obtained from forced steady cycles always is a higher value than $\Delta\phi_1$ (obtained from free decay tests) may be explained by the following diagram:

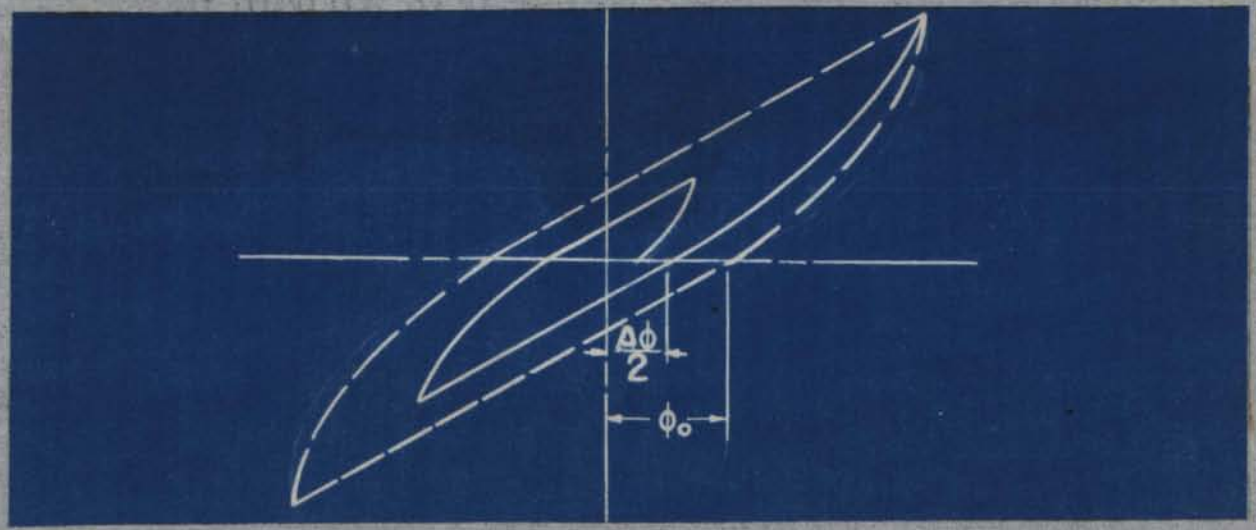

Thus the relations

$$\Delta\phi_i = 2\phi_o$$

as given by (13) and (17c) holds only for cases of ideal dry friction (where there is no initial slipping) and where damping is small as in the case of Specimen 772; Eq. (13) or (17c) is an approximate expression for the latter case.

All the dynamic test results were evaluated by the potential energy method from decay per half-cycle ϕ_i and the spring coefficient in the cycle k with the help of Equations (14), (20) or (20a). Since the internal damping in the cases of both 3-strand and 7 strand cables are small, the approximate formula checked very well with the static tests. For cases of high damping where the deviation of decay path from steady sustained path becomes appreciable, it is believed that point to point energy evaulation along both the M-ϕ and ϕ-t paths is necessary for reliable results - see Section (A).

(C)

EFFECT OF TENSION

Analysis

Thus far the effect of tension has been intentionally eliminated in the investigation of the basic nature of internal damping in stranded cables. In actual applications, cables are always strung under tension, and the effect of the latter should by no means be neglected.

Since it has been established from the foregoing investigations that the internal damping consists nearly solely of dry friction between strands, it will be only necessary to determine the effect of tension on inter-strand dry friction.

The exact analysis of the effect of tension on inter-strand dry friction must be based on the geometrical shape of the cable, its elastic property and the coefficient of friction of the wire surface. The problem is again complicated by the variation of inter-strand pressure upon bending. An approximate solution, however, may be achieved very readily as follows:

Consider a thin wire stretched on both ends by tension S on a cylinder with radius of curvature R. The normal pressure exerted by the wire on the surface due to S is

$$N = \frac{S}{R} \tag{24}$$

FIGURE 6

If this cylinder is replaced by another piece of wire bent into the same contour as the cylinder, Eq. (24) will still hold. Now if the two wires twists around each other uniformly along the span to form a stranded cable, the normal pressure between them no longer remains constant along the span.

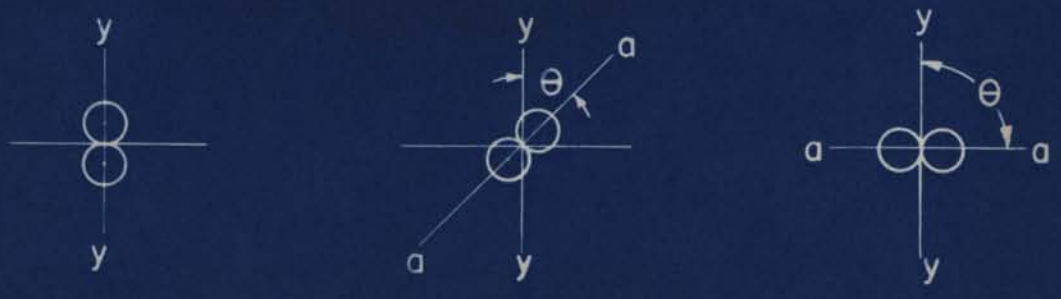

FIGURE 7

Figure 7 shows cross-sectional views of the two-stranded cable at three locations along the span. The line $\overline{ww}$ connecting the centers of the circular sections rotates about the point of contact as it proceeds along the axis of the two-stranded cable with the twist. At location (a) where $\overline{ww}$ lies in the plane of bending yy, the normal pressure N' reaches its maximum value given by Eq. (24). In general, $\overline{ww}$ intersects yy at an angle θ, and the normal pressure N' between the two wires at any location along the span is given by

$$N' = N \left| \cos \theta \right| \qquad (24\text{-a})$$

The lay length λ of a cable is defined as the length along the span which corresponds to each 2π of θ, thus Eq. (24-a) may be expressed as a function of x as follows:

$$N' = \frac{S}{R} \left| \cos \theta \right|$$

$$= \frac{S}{R} \left| \cos \frac{2\pi x}{\lambda} \right| \qquad (24\text{-b})$$

where λ is the lay length of the cable. The value of N' will repeat itself periodically along the span after every half lay length $\frac{\lambda}{2}$.

When the cable under tension is deformed into a sinusoidal loop, its curvature of bending along the span will be proportional to its deflection as evidenced by the following relations:-

$$y = a \sin \frac{\pi x}{L}$$

$$\frac{1}{R} = y'' = -a \frac{\pi}{L} \sin \frac{\pi x}{L}$$

$$\therefore y = \frac{a \pi^2}{L^2} \frac{1}{R}$$

$$y = c_1 \frac{1}{R} \qquad (a)$$

The normal pressure in between wires of (24-b) thus becomes

$$N' = c_1 S y \left| \cos \frac{2\pi x}{\lambda} \right| \qquad (24\text{-}c)$$

Now since dry friction is directly proportional to normal pressure between contact surfaces, the inter-strand friction force per unit length of the cable, in general, is the sum of a term independent of tension (see the previous section) plus the term proportional to tension given by (24-c) which yields

$$f = f(x) + f' S y \left| \cos \frac{2\pi x}{\lambda} \right| \qquad (25)$$

where $f(x)$ = unit inter-strand friction force when there is no tension

f' = constant, a function of the coefficient of friction of the wire surface

λ = pitch length of strand

As the number of wires in the cable increases, $\cos \frac{2\pi x}{\lambda}$ in the second term on the right of (25) should be

generalized as

$$\sum_{r=0}^{n-1} \cos \frac{2\pi}{\lambda} \left(x - \frac{r\lambda}{2n} \right)$$

where n is the number of wires in the multi-stranded cable. As the number of wires in the strand approaches infinity, the summation becomes a constant independent of x. For multi-stranded cable, (25) thus may take the approximate form

$$f = f(x) - f_1 S.y \qquad (25\text{-a})$$

which gives the unit inter-strand friction of a multi-stranded cable as a linear function of deflection.

The exact value of the relative displacement of two contacting elements of the two stranded wires upon variation of the deformed shape of the twisted strand again requires complicated manipulation. For small deformations, assume this relative displacement to be a linear function of the deflection, thus

$$u = c_2 y \qquad (26)$$

and

$$du = c_2 dy \qquad (26\text{-a})$$

where u represents the unit relative displacement of the contacting elements of the two wires.

Energy dissipated by inter-strand friction in a segment of cable dx deflected from y to y+dy is

$$d(\Delta W_1) = f\, du\, dx \qquad (27)$$

where f is given by (25-a).

By Eq. (26-a),

$$d(\Delta W_1) = f\, c_2\, dy\, dx \qquad (27\text{-a})$$

Call

$$F = c_2 f \tag{28}$$

for multi-stranded cables,

$$F = F(x) + F_1 S\, y \tag{29}$$

and

$$F(x) + F_1 S\, y = c_2 f(x) + c_2 f_1 S\, y \tag{28-a}$$

Hence

$$f\, du\, dx = F\, dy\, dx$$

and (27) becomes

$$d(\Delta W_i) = F\, dy\, dx \tag{27-b}$$

Total energy dissipation for a multi-stranded cable in one complete cycle in span L is (assume deformation and tension to remains constant throughout the cycle)

$$\begin{aligned}
\Delta W_i &= 4 \int_0^L \int_0^{y_i} F\, dy\, dx \\
&= 4 \int_0^L \int_0^{y_i} \left[F(x) + F_1 S\, y\right] dy\, dx \\
&= 4 \int_0^L \left[F(x) \cdot y_i + \tfrac{1}{2} F_1 S\, y_i^2\right] dx \\
&= 2 \int_0^L \left[2F(x)\, a_i \sin \frac{\pi x}{L} + F_1 S (a_i \sin \frac{\pi x}{L})\right] dx
\end{aligned} \tag{30}$$

When $F(x) = F_o \sin \frac{\pi x}{L}$, (where F_o is a constant), then (30) becomes

$$\begin{aligned}
\Delta W_i &= 2a_i (2F_o + F_1 S a_i) \int_0^L (\sin \frac{\pi x}{L})^2\, dx \\
&= a_i L\, (2F_o + F_1 S \cdot a_i)
\end{aligned} \tag{30-a}$$

where a_i = maximum amplitude

F_o, F_i = coefficient of damping function

L = span

S = tension

(30-a) gives the energy dissipation per cycle as a quadratic function of maximum amplitude, and, at the same time, a linear function of tension.

Experiments

Tests were carried out to determine energy dissipation per cycle of a 3/8" 7-strand steel cable strung under tension (same sample as No. 771 in the previous section, see p. 39). Figure T-8 is a picture of the test set-up. Transverse loads were applied at the mid-span by a load pan and dead-weights. Mid-span deflections were measured by an Ames dial gage. Lenght of span may be adjusted at will by merely shifting the roller end supports.

Hysteresis loops were obtained for various tension loads and maximum deflections. A typical example of the hysteresis loops is shown on Figure R-23. Energy dissipation per cycle was determined from the hysteresis loop areas and plotted against maximum deflections for various values of tension loads. Figure R-24 is such a diagram obtained for 40" span whereas Figure R-26 is a similar diagram for 60" span. The relations of energy dissipation per cycle and tension loads are shown on Figure R-25 and R-27, where energy is plotted against tension for various maximum deflections. Figures R-25 and R-27 were obtained directly from Figures R-24 and R-26.

The basic nature of energy dissipation per cycle for small deformations of a stranded cable under tension

(a linear function of tension and a quadratic function of maximum deflection as given by Eq. 30-a) is evidenced by the test results shown in these figures in spite of the fact that the deformed shape of the cable in the tests were by no means sinusoidal. Henceforth it will be assumed that Eq. 30-a shall hold for cases where the deformed shape of cable is or nearly sinusoidal provided the deformation is small.

From the test results, with the help of Eq. (30-a), the damping coefficients F_o and F_1 may be readily determined. The average of these constants, as determined from Figures B-24 for Specimen 771 are as follows

$$F_o = 4.05 \times 10 \qquad \text{lb./in.}$$

$$F_1 = 0.201 \times 10 \qquad 1/\text{in.}$$

Since damping force proportional to tension is also a linear function of amplitude; as amplitude increases, for a cable strung under tension, the part of damping proportional to tension becomes predominant. As an example, consider the case when S = 1000 lb. at amplitude a_i = 0.3", then

$$\text{Max. } F(x) = F_o = 4.05 \times 10^{-3} \quad \text{lb/in}$$

$$F_1 S.a_i = \quad 60.3 \times 10^{-3} \quad \text{lb/in}$$

the latter part being nearly fifteen times as large as the part independent of tension.

(D)

CONCLUSIONS

On basic properties:-

(1) The source of internal damping of stranded cables consists essentially of the interstrand dry friction. The solid internal friction of the wire materials is small. For practical purposes, it may be assumed that only dry friction exists.

(2) Without tension, the basic behavior of the internal dry friction damping in the cable are as follows:-

(a) Damping capacity (energy dissipation per cycle) is a linear function of amplitude.

(b) Frictional resisting moment against bending increases with amplitude below a small "critical amplitude" but tends to assume a constant value above this amplitude.

(3) When a stranded cable is strung under tension, the internal damping consists of two parts:

(a) Constant frictional damping ---- independent of tension.

(b) Linear frictional damping ---- a linear function of tension.

(4) The linear frictional damping in cables deformed into a near-sinusoidal shapes possesses the following characteristics:

(a) Damping capacity is a quadratic function of

amplitude and a linear function of tension.

(b) Frictional force function is a linear function of both tension and amplitude.

(5) As tension increases, linear frictional damping becomes predominent as constant damping reduces to insignificance.

(6) The equivalent flexural rigidity of cables approaches a constant above critical amplitude.

(7) Factors that may influence internal damping:

(a) Increase of lay length reduces damping capacity.

(b) Greater number of constituent wires in stranded cables of comparable sizes provides higher damping capacity.

(c) Prestressing of stranded cables below yield point has no effect on damping capacity; whereas prestressing over yield point considerably reduces damping capacity.

(d) "Preformed" cables possess less damping capacity than the non-preformed.

On technique of analysis:

(1) Satisfactory agreement has been achieved between the static and dynamic test results. Since dry friction is practically the sole source of internal damping, a simple static test may well be utilized to simulate both the sustained and the free decay vibrations for the study

of internal damping of cables.

(2) Although the free decay and the sustained steady vibrations are basically different in nature, no significant difference was observed in the energy evaluation from the two processes. As the magnitude of damping becomes small, the difference approaches zero.

(3) The technique of investigation developed proved to be adequate to provide reliable information on the internal damping of stranded cables. It therefore may be applied for the further analysis of all other influencing factors and should consequently result in better design and the development of preventive measures against vibration fatigue failures of stranded cable.

PART II

ANALYSIS OF DAMPED VIBRATIONS

(A) ANALYSIS OF THE MOTION

Simplifying Assumptions

(1) The internal damping of stranded cable is due to dry friction in between strands which consists of two parts:—
   (a) linear damping proportional to tension
   (b) constant damping independent of tension

(2) Energy dissipation at the end connections and in the frame structures are neglected.

(3) Air resistance is assumed to be small.

(4) The variation of tension during the formation of vibration loops is neglected.

(5) The cable is assumed to be straight at its neutral position (when amplitude is zero), hence the effect of sagging in the span is neglected.

(6) The bending flexural rigidity of stranded cable is assumed to be constant throughout each cycle of vibration.

Formulation of the Problem

Consider a piece of stranded cable strung under tension S and having the following properties:

Equivalent flexural rigidity EI (lb-in.^{2})

Mass per unit length μ (slug/in.)

Internal damping functions:--

(a) Linear damping coefficient = P_1 (in.$^{-2}$)

(b) Unit constant damping = F (x) (lb/in.)

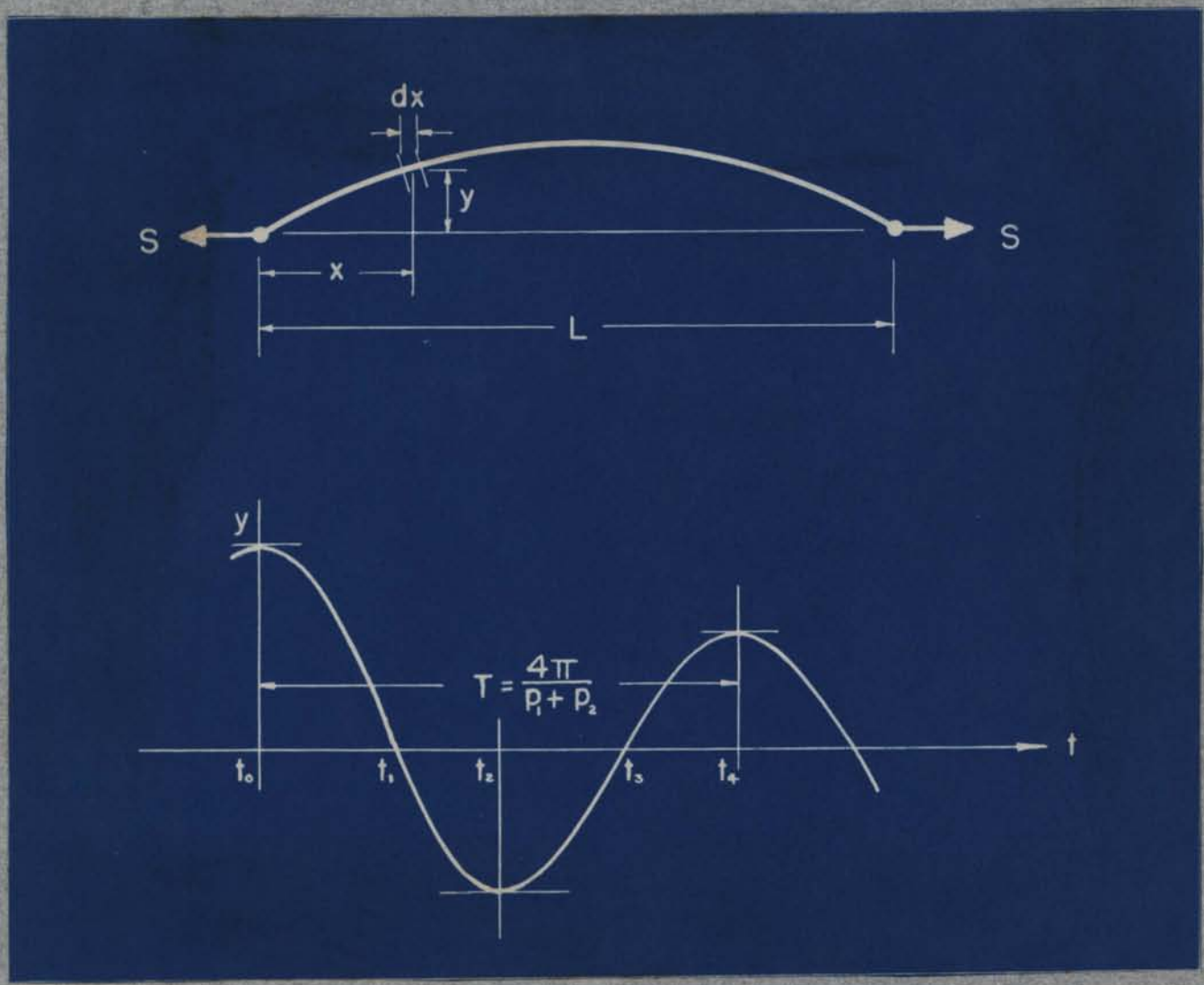

Figure 8

Figure 8 shows the cable vibrated in one loop at the position returning from the upper peak. In the first quarter-cycle, when the cable moves from the upper peak to neutral, forces acting on a segment of cable dx are the following (assume positive sign in the +y direction)

(1) Spring force:

due to flexural rigidity (acting downward, see p. 185, Ref. 6)

$$-EI \cdot \frac{\partial^4 Y}{\partial x^4} \cdot dx$$

due to tension (proportional to the difference in slope at the ends of the segment dx, acting downward, p. 170, Ref. 6)

$$+S \frac{\partial^2 Y}{\partial x^2} \cdot dx$$

The negative sign is cancelled because y'' is also negative in the first quarter cycle.

(2) Damping force:

linear damping (proportional to amplitude and tension, acting upward-against motion)

$$+F_1 \cdot Sy \cdot dx$$

constant damping (acting upward-against motion)

$$+F(x) \cdot dx$$

(3) Inertial force (proportional to acceleration, hence negative in the first quarter-cycle)

$$-u \frac{\partial^2 Y}{\partial t^2} dx$$

By D'Alembert's principle (Ref. 4) for dynamic equilibrium, we may equate all the forces acting on the element (then divide through by dx and transpose terms) to obtain the equation of motion for the first quarter-cycle.

$$m\frac{\partial^2 y}{\partial t^2} + EI\frac{\partial^4 y}{\partial x^4} - S\frac{\partial^2 y}{\partial x^2} - F_1 Sy - F(x) = 0$$

Equations for the ensuing three quarter-cycles from t_1 to t_4 may be obtained in a similar manner. After a full cycle, the equations will again repeat themselves. The four equations are essentially the same except for the combination of signs before the damping terms which varies in every quarter-cycle.

$$m\frac{\partial^2 y}{\partial t^2} + EI\frac{\partial^4 y}{\partial x^4} - S\frac{\partial^2 y}{\partial x^2} \mp F_1 Sy - F(x) = 0 \quad (31a)$$

$$m\frac{\partial^2 y}{\partial t^2} + EI\frac{\partial^4 y}{\partial x^4} - S\frac{\partial^2 y}{\partial x^2} \mp F_1 Sy + F(x) = 0 \quad (31b)$$

where $F(x)$ = Damping force function independent of tension

F_1 = Coefficient for damping proportional to tension

Equation (31a) gives motion from t_0 to t_2 for a unit segment of cable moving in the -y direction, whereas (31b) is for the second half-cycle from t_2 to t_4 when the unit segment moves in the +y direction. The "-" sign before the damping force "$F_1 Sy$" holds when the unit segment moves towards neutral position, and the sign is "+" when it moves away from neutral.

Equations (31) reveal a very interesting and unique characteristic of vibration of stranded cable as influenced by its internal damping, namely, the fact that the equation of motion differs for each quarter cycle.*

General Solution

The general solution of Eq. (31) (a linear partial differential equation), may be expressed in the form,

$$y = y_c(x,t) - y_f(x) \qquad (32)$$

in which $y_f(x)$ is a particular solution induced by the constant dry friction damping term $F(x)$.

We shall first proceed to determine $y_f(x)$. Since $y_f(x)$ is independent of t, $\frac{\partial^2 y_f}{\partial t^2}=0$, and Equation (31) is reduced to an ordinary linear differential equation:

$$EI\, y_f^{iv} - S\, y_f'' \mp F_1 S y_f \mp F(x) = 0 \qquad (33)$$

If $F(x)$ is linear or of the form e^{bx} where b is a constant, the solution of (33) is (see Appendix C)

$$y_f(x) = y_f(x) \mp BF(x) \qquad (34)$$

where $y_f(x)$ = solution of the homogeneous differential equation

$$EI\, y_f^{iv} - S y_f'' \pm F_1 S y_f = 0$$

---

*Although the "$\mp$" discontinuity may be replaced by Fourier's series, yet the physical picture will not be as clear as it is and the solution will not be as convenient for numerical computations (see Ref.9).

B= A constant determined by the damping function F(x)

Now if we substitute (34) into (32) and again into (31) we obtain

$$u\frac{\partial^2 y_c}{\partial t^2} + EI\frac{\partial^4 y_c}{\partial x^4} - S\frac{\partial^2 y_c}{\partial x^2} \pm SF_1 y_c = 0 \qquad (31\text{-}1)$$

Assume $y_c(x,t) = X(x) \cdot T(t)$ and substitute into (31-1), we get

$$u X \ddot{T} + T(EI X^{iv} - SX'' \pm F_1 SX) = 0$$

where $\ddot{T} = \frac{d^2T}{dt^2}$

$$X^{iv} = \frac{d^4X}{dx^4}$$

$$X'' = \frac{d^2X}{dx^2}$$

Divide through by X*T and transpose terms,

$$u\frac{\ddot{T}}{T} = -\frac{1}{X}(EI X^{iv} - SX'' \pm F_1 SX) \qquad (35)$$

Since the left member of (35) does not involve x and the right member does not involve t, they must both equal a constant $-K^2$: then, Eq. (31-1) is reduced to two separate ordinary differential quations,

$$u\ddot{T} + K^2T = 0 \qquad (35a)$$

$$EIX^{iv} - SX'' \pm F_1 SX + K^2X = 0 \qquad (35b)$$

The solutions of (35a) and (35b) are (assume $F_1 S < K^2$):

$$T(t) = b_1 \cos pt + b_2 \sin pt \qquad (36)$$

where $p^2 = \frac{K^2}{u}$

b_1, b_2 = arbitrary constant

$$X(x) = c_1 \cos a_r x + c_2 \sin a_r x + c_3 \cosh a_s x + c_4 \sinh a_s x \qquad (37)$$

where $a_r^2 = \sqrt{\left(\frac{S}{2EI}\right)^2 + \frac{K^2 + P_1 S}{EI}} - \frac{S}{2EI}$

$$a_s^2 = \sqrt{\left(\frac{S}{2EI}\right)^2 + \frac{K^2 + P_1 S}{EI}} + \frac{S}{2EI}$$

c's = arbitrary constants

For simply supported ends, assume

at $x = o$, $y(o) = o, y''(o) = o$

at $x = L$, $y(L) = o$, $y''(L) = o$

In Appendix C, we have determined $y_f(x)$ so that it satisfies the same boundary conditions. Thus $y_c(x,t)$ and hence $X(x)$ must satisfy the same boundary conditions, namely

at $x = o$, $X(o) = o$, $X''(o) = o$ (i)

at $x = L$, $X(L) = o$, $X''(L) = o$ (ii)

Boundary condition (i) gives

$$c_1 = c_3 = o \qquad (37a)$$

and (ii) yields

$$c_4 = o \text{ and } \sin a_r L = o \qquad (37b)$$

from (37a) and (37b), we get the following:

$$X(x) = c_2 \sin a_r x \qquad (37c)$$

$$a_r L = r\pi$$

or

$$a_r = \frac{r\pi}{L} \qquad (37d)$$

where r is an integer

From Eq. (37) and (37d), we equate the values of a_r,

$$\frac{r^2\pi^2}{L^2}=\sqrt{\left(\frac{S}{2EI}\right)^2+\frac{K^4\pm F_1S}{EI}}-\frac{S}{2EI}$$

$$\therefore K^4=EI\frac{r^4\pi^4}{L^4}+S\frac{r^2\pi^2}{L^2}\pm F_1S \qquad (33)$$

and the natural frequency of vibration becomes

$$q=\frac{p}{2\pi}=\frac{1}{2\pi}\sqrt{\frac{K^2}{A\rho}} \qquad (33a)$$

Combining equations (34), (36), and (37c,d), the general solution of Eq. (31) becomes

$$y=\sum_{r=1}^{\infty}(C_r\cos p_r t+C_r'\sin p_r t)\sin\frac{r\pi x}{L}+y_{f_1}(x)\pm BF(x) \qquad (32a)$$

where C_r, C_r' = constants to be determined by initial conditions

$$p^2=\frac{K^4}{A\rho}=\frac{1}{\rho I}(k'\pm F_1S)$$

$$k'=EI\,\pi^4\frac{r^4}{L^4}+S\,\frac{\pi^2r^2}{L^2}$$

$y_f(x)$ = particular solution induced by constant damping function

B = constant to be determined by constant damping function

F(x) and boundary conditions

Equation (32a) is a general solution for the vibration of stranded cable strung under tension. The expression was

obtained for simply-supported ends, it may, however, be generalized for any type of end conditions by merely varying the boundary conditions below Eq. (37).

The coefficients C_r and C'_r may be determined for any initial shape of vibration by Fourier's method.

At the end of each quarter cycle, the sign in front of "F_1S" changes, as a consequence, Eq. (32a) takes on a different form; and the motion of the cable can be completely determined only by studying Eq. (32a) in each consecutive quarter cycle. In order to do this, we will have to first specify the dry friction damping function F(x).

Specific Cases

(a) F(x) is a Function of the Deformed Shape of Cable

Let $F(x) = \pm F_o \sin \frac{r\pi x}{L}$, hence $y_{f_1}(x)$ of Eq. (34) vanishes (see Eq. 12 Appendix C), and (34) becomes

$$y_f(x) = \pm a_f \sin \frac{r\pi x}{L} \qquad (39)$$

$$\text{where } a_f = \frac{F_o}{EI\frac{\pi^4 r^4}{L^4} + S\frac{\pi^2 r^2}{L^2} + F_1 S)}$$

then (32a) for four consecutive quarter cycles from t_o to t_4 becomes,

$$y_1(x,t) = \sum_{r=1}^{\infty}(C_r \cos pt + C'_r \sin pt) \sin \frac{r\pi x}{L} + \sum a_{f_1} \sin \frac{r\pi x}{L}$$

$$= \sum_{r=1}^{\infty} (C_{r_1} \cos p_1 t + C'_{r_1} \sin p_1 t + a_{f_1}) \sin \frac{r\pi x}{L} \quad (40a)$$

$$y_2(x,t) = \sum_{r=1}^{\infty} (C_{r_2} \cos p_2 t + C'_{r_2} \sin p_2 t + a_{f_2}) \sin \frac{r\pi x}{L} \quad (40b)$$

$$y_3(x,t) = \sum_{r=1}^{\infty} (C_{r_3} \cos p_1 t + C'_{r_3} \sin p_1 t + a_{f_1}) \sin \frac{r\pi x}{L} \quad (40c)$$

$$y_4(x,t) = \sum_{r=1}^{\infty} (C_{r_4} \cos p_2 t + C'_{r_4} \sin p_2 t + a_{f_2}) \sin \frac{r\pi x}{L} \quad (40d)$$

where $p_1^2 = \frac{K_1^2}{a} = \frac{1}{a}(k' - F_1 S)$

$$p_2^2 = \frac{K_2^2}{a} = \frac{1}{a}(k' + F_1 S)$$

$$a_{f_1} = \frac{P_0}{k' - F_1 S}$$

$$a_{f_2} = \frac{P_0}{k' + F_1 S}$$

$$k' = Er^2 \frac{\pi^4 r^4}{L^4} + S \frac{\pi^2 r^2}{L^2}$$

The Fourier coefficient C_r's of Equations (40) are to be determined by initial conditions.

We shall now proceed to analyze the motion of the cable in one complete cycle when its shape at $t=t_0$ is one single sine wave. This can only be done by investigating its behavior step by step through four consecutive quarter cycles (from t_0 to t_1, t_1 to t_2, t_2 to t_3 and t_3 to t_4). Assume at $t = t_0$,

$$y_1(x_1, t_0) = a_1 \sin \frac{\pi x}{L}$$

$$\dot{y}_1(x_1, t_0) = 0 \quad (a)$$

From (40a),

$$r = 1$$

$$C_{r_1} = (a_1 - a_{f_1}) \cos p_1 t_o \qquad (a-1)$$

$$C'_{r_1} = (a_1 - a_{f_1}) \sin p_1 t_o$$

and the solution for the first quarter-cycle becomes

$$y_1(x,t) = \left[(a_1 - a_{f_1})(\cos p_1 t \cos p_1 t_o + \sin p_1 t \sin p_1 t_o) + a_{f_1}\right] \sin \frac{\pi x}{L}$$

$$= \left[(a_1 - a_{f_1}) \cos p_1 (t - t_o) + a_{f_1}\right] \sin \frac{\pi x}{L}$$

$$= \left\{a_1 \cos p_1 (t - t_o) + a_{f_1}\left[1 - \cos p_1 (t - t_o)\right]\right\} \sin \frac{\pi x}{L} \qquad (41)$$

The instant t_1 at the end of the first quarter cycle is defined as the time when $y(x,t)$ of Eq. (41) reaches neutral, or

$$y_1(x,t_1) = 0 \qquad (a-2)$$

From Eq. (41) and condition (a-2), we obtain time t_1 at the end of the first quarter of the i-th half cycle,

$$t_1 = t_o + \frac{1}{p_1} \cos^{-1}\left(-\frac{a_{f_1}}{a_1 - a_{f_1}}\right) \qquad (42)$$

Equation (40b) for the second quarter-cycle (from t_1 to t_2) must satisfy the following boundary conditions at t_1 in order to maintain continuous motion:

at $t = t_1$,

$$y_2(x,t_1) = y_1(x,t_1)$$

$$\dot{y}_2(x,t_1) = \dot{y}_1(x,t_1)$$
$$= - p_1(a_1 - a_{f_1}) \sin p_1(t_1 - t_o) \sin \frac{\pi x}{L} \quad .. (b)$$

Making use of the above boundary conditions, the coefficients C_{r_2} and C'_{r_2} of (40b) are determined:

$$C_{r_2} = - a_{f_2} \cos p_2 t_1 + Q\sqrt{a_1(a_1 - 2a_{f_1})} \sin p_2 t_1$$
$$C'_{r_2} = - a_{f_2} \sin p_2 t_1 + Q\sqrt{a_1(a_1 - 2a_{f_1})} \cos p_2 t_1 \qquad (b\text{-}1)$$

$$\text{where} \quad Q = \frac{p_1}{p_2}$$

The solution for the second quarter-cycle becomes

$$y_2(x,t) = \left\{ - Q\sqrt{a_1(a_1 - 2a_{f_1})} \sin p_2(t - t_1) + a_{f_1}\left[1 - \cos p_2(t - t_1)\right] \right\} \sin \frac{\pi x}{L} \qquad (43)$$

Maximum amplitude at the end of a half-cycle (which is also the end of the second quarter-cycle) is reached when $t = t_2$, where

$$\dot{y}_2(x,t_2) = o, \text{ and}$$
$$y_2(x,t_2) = - a_{i+1} \sin \frac{\pi x}{L} \qquad (c)$$

From the first of the above conditions, we get

$$t_2 = t_1 + \frac{1}{p_2} \tan^{-1} \frac{Q\sqrt{a_1(a_1 - 2a_{f_1})}}{a_{f_2}} \qquad (44)$$

Substituting (44) into (43), we obtain,

$$a_{i+1} = Q\sqrt{a_i\,(a_i - 2a_{f_1})}\,\sin p_n(t_n - t_1) - a_{f_1}\left[1 - \cos p_n(t_n - t_1)\right]$$

$$a_{i+1} = \sqrt{Q^2\,a_i\,(a_i - 2a_{f_1}) + a_{f_n}^2} - a_{f_n} \tag{45}$$

Decay of maximum amplitude in the first half-cycle is,

$$\begin{aligned}\Delta a_i &= a_i - a_{i+1}\\ &= a_i - \left(\sqrt{Q^2\,a_i\,(a_i - 2a_{f_1}) + a_{f_n}^2} - a_{f_n}\right)\\ &= (a_i + a_{f_n}) - \sqrt{Q^2\,a_i\,(a_i - 2a_{f_1}) + a_{f_n}^2}\end{aligned} \tag{46}$$

where a_i = initial maximum amplitude

$$a_{f_1} = \frac{F_0}{k' - F_1 S}$$

$$a_{f_n} = \frac{F_0}{k' + F_1 S}$$

$$k' = \left(\frac{\pi^4}{L^4} \cdot EI + \frac{\pi^2}{L^2} \cdot S\right)$$

$$Q^2 = \frac{a_{fn}}{a_{f_1}}$$

When tension is reduced to zero, and the part of internal damping proportional to amplitude vanishes, $F_1 = 0$ and $Q = 1$, $a_{f_1} = a_{f_n} = a_f = \frac{F_0}{k'}$, and (46) becomes

$$\Delta a_i = 2a_f = 2\left(\frac{F_0}{k'}\right)$$

which is similar to the expression in the case of single degree of freedom harmonic vibrations with constant damping (compare with Eq. 13, Part I).

When $F_1 = 0$, $p_2 = p_1 = p$, from (42) and (44), we obtain

$$t_2 = t_0 + \frac{\pi}{p} \tag{44a}$$

which indicates that the period of vibration of a half-cycle is not altered by the part of dry friction independent of tension and amplitude.

Second Half-cycle

By taking conditions (c) at the end of the second quarter-cycle as the initial conditions for the third quarter cycle, procedures similar to those from conditions (a) throughout Eq. (46) may be applied for the second half-cycle (ranging from $t = t_2$ to $t = t_4$). Thus we obtain from (40c) and (40d),

$$\begin{aligned} C_{r_2} &= (-a_{i+1} - a_{f_1}) \cos p_1 t_2 \\ C_{r_2}' &= (-a_{i+1} - a_{f_1}) \sin p_1 t_2 \end{aligned} \tag{c-1}$$

and

$$\begin{aligned} y_2(x,t) &= -\left\{(a_{i+1} - a_{f_1}) \cos p_1(t-t_2) + a_{f_1}\right\} \sin \frac{\pi x}{L} \\ &= -\left\{a_{i+1} \cos p_1(t - t_2) + \right. \\ &\quad \left. + a_{f_1}\left[1 - \cos p_1(t - t_2)\right]\right\} \sin \frac{\pi x}{L} \end{aligned}$$

At the end of third quarter-cycle,

$$y_2(x,t_2) = 0 \tag{c-2}$$

and

$$t_3 = t_2 + \frac{1}{p_1}\cos^{-1}\left(-\frac{a_{f_1}}{a_{i+1} - a_{f_1}}\right) \qquad (48)$$

At $t = t_3$,

$$y_4(x,t_3) = y_3(x,t_3) = 0$$

$$\dot{y}_4(x,t_3) = \dot{y}_3(x,t_3)$$

$$= p_1 (a_{i+1} - a_{f_1}) \sin p_1(t_3 - t_2) \sin \frac{\pi x}{L} \qquad (d)$$

From which,

$$C_{r_4} = a_{f_2} \cos p_2 t_3 - Q\sqrt{a_{i+1}\,(a_{i+1} - 2a_{f_1})} \sin p_2 t_3$$

$$C'_{r_4} = a_{f_2} \sin p_2 t_3 + Q\sqrt{a_{i+1}\,(a_{i+1} - 2a_{f_1})} \cos p_2 t_3 \qquad (d\text{-}1)$$

and

$$y_4(x,t) = -\left\{-Q\sqrt{a_{i+1}\,(a_{i+1} - 2a_{f_1})} \sin p_2 (t - t_3) + a_{f_2}\left[1 - \cos p_2 (t - t_3)\right]\right\} \sin \frac{\pi x}{L} \qquad (49)$$

Maximum amplitude at the end of the second half-cycle (also the end of the fourth quarter) is reached at $t = t_4$, where

$$\dot{y}_4(x,t_4) = 0, \text{ and}$$

$$y_4(x,t_4) = a_{i+2} \sin \frac{\pi x}{L} \qquad (e)$$

The first condition of (e) gives

$$t_4 = t_3 - \frac{1}{p_2} \tan^{-1} \frac{Q\sqrt{a_{i+1}\,(a_{i+1} - a_{f_1})}}{a_{f_2}} \qquad (50)$$

Substituting (50) into (49), it yields

$$a_{i+2} = e\sqrt{a_{i+1}\,(a_{i+1} - 2a_{f_1})}\,\sin p_2\,(t_2 - t_2) - a_{f_2}\left[1 - \cos p_2(t_2 - t_2)\right]$$

$$= \sqrt{e^2\, a_{i+1}(a_{i+1} - 2a_{f_1}) + a_{f_2}^2} - a_{f_2} \qquad (51)$$

If we replace a_{i+1} by a_i in Equations (47) and (49) for the third and fourth quarter cycles, we find that they become exactly the same expression as (41) and (43) for the first and second quarter cycles only with the signs of y changed. Equations (48), (50) and (51) for time elapsed and amplitude decay are identical with their counterparts (42), (44) and (45) in the first half-cycle. The vibration characteristics of the stranded cable considered, therefore, repeat itself in every half-cycle. To determine its motion, it is only necessary to investigate two consecutive quarter cycles represented by two of the four partial differential equations given by Equations (31a) and (31b). For further discussions, it will only be sufficient to deal with the first half-cycle alone.

One of the most outstanding characteristics of damping proportional to amplitude is its effect on the variation of circular frequency of vibration. As the vibration proceeds, the circular frequency takes on alternatively the values of $p_1 = \sqrt{\frac{k' - F_1 S}{u}}$ and $p_2 = \sqrt{\frac{k' + F_1 S}{u}}$ in each quarter cycle, the average frequency in each half-cycle $\frac{p_1 + p_2}{2}$ remaining constant. The phenomenon may readily be visualized if we recall that "$F_1 S$"

is the coefficient of y and thus may be taken as a spring coefficient having the property of changing signs at the end of each quarter-cycle. When the cable moves towards neutral, the F S-term retards the motion hence is working against the rest of the spring forces k' in the system, as a result, the circular frequency of vibration is reduced. On the other hand, as the cable moves away from neutral, the rest of the spring forces are acting against the motion, thus the F S-term adds to the effect of k' and makes the circular frequency higher.

The natural frequency of the cable is obtained by taking the average of the values given by (38-a) for two consecutive quarter cycles, thus

$$q = \frac{1}{2\pi} p$$

$$= \frac{1}{4\pi} (p_1 + p_2)$$

$$= \frac{1}{4\pi} \left(\sqrt{\frac{k' - F_1 S}{M}} + \sqrt{\frac{k' + F_2 S}{M}} \right) \qquad (38\text{-b})$$

where q = natural frequency of cable in c. p. s.

$$k' = \frac{\pi^4}{L^4} EI + \frac{\pi^2}{L^2} S$$

The decay of maximum amplitude in one half-cycle is a linear function of the initial amplitude as evidence by Eq. (46).

The solution presented is for the case of single sinusoidal loop, it may be generalized for the case of n-sinusoidal loops without much trouble. Vibrations in other

shapes may also be analyzed by the use of Fourier's series in Equation (40).

(b) F(x) is a Constant (a general discussion)

Let $F(x) = F_o$*, the value of $y_f(x)$ may be determined for specified boundary conditions as it was carried out for the case in the previous section (see Appendix C)

General solution for the first quarter cycle when the cable is vibrated in one loop is

$$y_1(x,t) = \sum_{r=1}^{\infty} (C_{r_1} \cos p_1 t + C'_{r_1} \sin p_1 t) \sin \frac{r\pi x}{L} + y_f(x) \quad (52)$$

At $t = t_o$, assume

$$y_1(x,t_o) = a_1 \sin \frac{\pi x}{L} + y_f(x) \quad (a')$$
$$\dot{y}_1(x,t_o) = 0$$

Now if $t_o = 0$, from (52) it yields

$$r = 1$$
$$C'_{r_1} = 0 \quad (a'-1)$$
$$C_{r_1} = a_1$$

Hence,

$$y_1(x,t) = a_1 \sin \frac{\pi x}{L} \cos p_1 t + y_f(x) \quad (53)$$

---

*Although F_o may be approached by a Fourier's series in the form of $\sum_{r=1,3,\cdots}^{\infty} \frac{4F_o}{\pi} \frac{1}{r} \sin \frac{r\pi x}{L}$, it is not adopted because of its lack of clarity in presenting the physical picture.

Comparing (53) with (41), it is seen that the general form of the solution remains largely the same as that of the case when damping is a function of the deflected shape of the cable. The frequency of vibration is exactly the same in both cases.

The instant at the end of the first quarter cycle is defined as time t_1 when $y_1(x,t)$ reaches neutral, or

$$y_1(x,t) = 0 \qquad (a'-2)$$

From (a'-2) and (53), we get

$$t_1(x) = \frac{1}{p_1}\cos^{-1}\left(\frac{-y_0(x)}{a_1 \sin\frac{\pi x}{L}}\right) \qquad (54)$$

Eq. (54) gives time t_1 as a function of x. This means that points along the span of the cable will not reach neutral at the same time. Now since Eq. (53) is true only for $y(x) \geq 0$, as soon as the first particle in the span reaches neutral (say at $t = t_{11}$), Eq. (53) ceases to function. Equation and solution for the second quarter cycle (as may be derived from Eq. 32-a), however, will not begin to become in effect until $t = t_{12}$ at which instant the last particle in the span has just passed neutral. During the "transition period t_t" defined by $t_{11} < t_t < t_{12}$, a part of the span is above the neutral axis where $y \geq 0$ and the rest of the span lies below the neutral axis where $y \leq 0$.

The behavior of the cable in the transition stage is relatively irregular. Exact solution of its motion in this

state furnishes a very interesting and yet mathematically involved problem. Since the transition period is usually small compared with the complete period of vibration, an approximate solution may be obtained by taking*

$$t_{11} = t_t = t_{12} \tag{55}$$

Thus we have

$$t_t = t_1\left(\frac{L}{2}\right) = \frac{1}{p_1}\cos^{-1}\left\{\frac{-y_f\left(\frac{L}{2}\right)}{a_0}\right\} \tag{55a}$$

Substituting (55a) into (53), we get

$$y_1(x,t_1) = 0 \text{ and}$$

$$\dot{y}_1(x,t_1) = -a_1 p_1 \sin\frac{\pi x}{L} \sin p_1 t_1 \tag{b'}$$

which may then be utilized as the initial condition for the second quarter cycle. A transition period will again appear at the end of the second quarter cycle where neither of the Equations (31a) and (31b) will hold. Approximate solution, however, may readily be obtained by taking $t_2(x) = t_2\left(\frac{L}{2}\right)$, and decay of amplitude in the half-cycle may thus be obtained.

(c) F(x) vanishes

In most of the actual cases, where stranded cables are

---

* A closer approximation may be obtained as follows: (1) determine t_{11} from $\frac{d}{dx} t_1(x) = 0$, (2) use Eq. 31-a with the term "$F_1 \delta y$" dropped out (y is close to zero in transition) and determine the motion, (3) determine t_{12} when every point in span has passed neutral.

strung under high tension, the part of damping independent of tension as represented by $F(x)$ becomes insignificant, compared with the term proportional to it. Hence a close approximation may be obtained by putting

$$F(x) = 0 \tag{56}$$

The solution for this case may be obtained as in the two previous cases by starting from the general solution -- given by (32-a). The same results, however, may be readily achieved by puting

$$F_0 = 0 \quad (\because \ a_f = 0) \tag{56-a}$$

in Equations (40) through (51).

The following are thus obtained:

(1) Solution for the first quarter-cycle:

$$y_1(x,t) = a_1 \cos p_1(t-t_0) \sin \frac{\pi x}{L} \tag{57}$$

where $p_1^2 = \frac{1}{M}(k'-F_1 S)$

$$k' = EI \frac{\pi^4}{L^4} + S \frac{\pi^2}{L^2}$$

at the end of the first quarter-cycle,

$$t_1 = t_0 + \frac{1}{p_1} \cos^{-1}(0) = t_0 + \frac{\pi}{2p_1} \tag{58}$$

(2) Solution for the second quarter-cycle:

$$y_2(x,t) = -Qa_1 \sin p_2(t-t_1) \sin \frac{\pi x}{L} \tag{59}$$

$$\text{where } p_s^2 = \frac{1}{m}(k' + P_1 S)$$

at the end of the second quarter-cycle,

$$t_s = t + \frac{\pi}{2p_2} \tag{60}$$

Maximum amplitude at the end of half-cycle,

$$a_{i+1} = Q a_i \tag{61}$$

$$\text{where } Q^2 = \frac{k' - P_1 S}{k' + P_1 S}$$

Amplitude decay in one half-cycle

$$\Delta a_i = (1-Q)\, a_i \tag{62}$$

Percentage decay in one half cycle,

$$\frac{\Delta a_i}{a_i} = 1 - Q \tag{63}$$

Equation (63) gives the percentage decay of amplitude as a constant $(1-Q)$, and (62) reveals that decay per half-cycle is a linear function of vibration amplitude.

Now if we assume the term which contains flexural rigidity in k' to be small compared with the term which contains tension (on account of the high value of the latter), an approximate formula for natural frequency is obtained by putting

$$k' = \frac{\pi^2}{L^2} S \tag{64}$$

and the natural frequency becomes

$$q = \frac{1}{4\pi}\left(\sqrt{\frac{k' - F_1 S}{\lambda}} + \sqrt{\frac{k' + F_1 S}{\lambda}}\right)$$

$$= \frac{1}{4L}\left(\sqrt{1 - \frac{F L^2}{\pi^2}} + \sqrt{1 + \frac{F L^2}{\pi^2}}\right)\sqrt{\frac{S}{\lambda}} \qquad (65)$$

When the approximate form (64) is used,

$$Q^2 = \frac{k' - F_1 S}{k' + F_1 S}$$

$$= \frac{\pi^2 - F S}{\pi^2 + F S}$$

and it follows that the percentage decay of amplitude is independent of tension.

Numerical Example

(a) Sample Cable

Designation	771	
Nominal Dia.	3/8	in.
Number of Wires	7	
Dia of Wire	0.120	in.
Lay Length	5.5	in.
Material	Carbon Steel	
Weight	0.273	lb/ft.
Breaking Strength	10,800	lb.
Flexural Rigidity	2.32×10^3	lb-in.*

Damping Constants (from Part I, p.56)

---

*From Figure R-17, use average value of k (0.116×10^3),
$EI = \frac{kL}{2} = \frac{40}{2} \times 0.116 \times 10^3 = 2.32 \times 10^3$ lb.- in.

$$F_o = 4.05 \times 10^{-3} \text{ lb./in.}$$

$$F_1 = 0.201 \times 10^{-3} \text{ 1/in.}$$

(b) Natural Frequency

For any type of damping function F(x), the natural frequency of the cable vibrated under tension S in loop lengths L is given by (38-b), p.76

When the cable is vibrated into loops of 38" lengths,

$$q = \frac{1}{2} \left(1.65\sqrt{17.2 + S} + 1.78\sqrt{14.9 + S}\right) \qquad (66)$$

Under high tension, where flexural rigidity is relatively insignificant, the approximate formula (65) gives

$$q = 1.713\sqrt{S} \qquad (66\text{-a})$$

(66) and (66-a) are both plotted in Figure R-50 for comparison. The approximate formula gives slightly lower natural frequency, the maximum difference being less than 3% above 500 lb. tension. As tension S and loop length L increases, the difference becomes less noticeable.

Natural frequencies for loop lengths 50", 70" and 85" were evaluated by formula (38-b), p.76 , the results are as follows:

$$L = 50", \quad q = 0.61\sqrt{10.45 + S} + 0.688\sqrt{8.16 + S} \qquad (67\text{-a})$$

$$L = 70", \quad q = 0.405\sqrt{6.14 + S} + 0.516\sqrt{3.76 + S} \qquad (67\text{-b})$$

$$L = 85", \quad q = 0.307\sqrt{2.46 + S} + 0.445\sqrt{2.33 + S} \qquad (67\text{-c})$$

Equations (67) are plotted on Figure E-31 for the comparison with the experimental results.

(c) Amplitude Decay

Decay of maximum amplitude per half-cycle for the case of $P(x) = P_o \sin \frac{\pi x}{L}$ is given by (46), namely

$$\Delta a_i = a_i + a_{f_s} - \sqrt{Q^2 a_i \ (a_i - 2a_f) - a_{fs}^2} \qquad (46)$$

Take $l = 38"$, $S = 1{,}000$ lb, from the previous paragraph,

$$k' = \frac{\pi^2}{L^2} \left(\frac{\pi^2}{L^2} EI + S\right)$$

$$= 6.85 \times 10^{-3} \ (15.9 + S) = 6.950$$

$$a_f = \frac{P_o}{k' + P_1 S} = \frac{4.05}{6.749} \times 10^{-3} = 6.000 \times 10^{-4}$$

$$a_{f_s} = \frac{P_o}{k' + P_1 S} = \frac{4.05}{7.151} \times 10^{-3} = 5.67 \times 10^{-4}$$

$$Q^2 = \frac{k' - P_1 S}{k' + P_1 S} = \frac{6.749}{7.151} = 0.944$$

$$Q = 0.971$$

$$\Delta a_i = a_i + 0.00056 - \sqrt{0.944 \ a_i \ (a_i - 0.00119) + 3.12 \times 10^{-7}} \qquad (68)$$

Neglecting the terms of secondary magnitude, (68) may be simplified to a linear expression

$$\Delta a_i = 0.029 \ a_i + 0.00056 \qquad (68a)$$

Decay of mid-span amplitude in a full cycle is twice the value of (68a)

(B) EXPERIMENTAL WORK

Motion and vibration characteristics were observed for a stranded cable vibrated in near-sinusoidal loops under tension. The test set-up used (Figure T-9) was primarily designed for the purpose of vibration fatigue tests of stranded cables (Ref. 12). A 3/8" 7-wire specimen (same as No. 771 used in Part I, see p. 39) vibrated at its resonance was driven near one end of the span by an electro-dynamic motor connected to a 145-watt power amplifier with a built-in audio oscillator.

Decay of maximum amplitude was recorded by a movie camera described in Part I (p. 37). Figure T-10 is a picture of the set-up of the recording system.

Principle and details of the operation were the same as those described in Part I, p. 35. The scale screen is mounted on the frame structure to avoid the extensive heat of the flood light (a G. E. No. 4 flood light bulb rated at 2,000 watts was used in this set-up). A 1/2000 H.P. D.C. motor with a speed range of 2000 - 3000 rpm was used as a timing gear. The propeller casts a vertical black line on the film every time it swings across the front of the lens. The speed of the motor is controlled by a rheostat and calibrated by a stroboscope.

Natural frequencies for various loop lengths of the

cable at various tensile loads were determined by the criterion of maximum amplitude of steady sustained vibrations. The results are shown in Figure R-30 and Figure R-31. The observed frequencies checked very well with the computed values for all the loop lengths recorded. The consistent higher observed values were presumably due to the end conditions of the cable tested which were actually partially restrained (computed values were based on the assumption of simply-supported ends).

The decay pictures were obtained by first obtaining the steady sustained vibrations at a certain amplitude and then shut off the input signal of the power amplifier. Two examples of the pictures thus obtained are presented.

Figure R-28 shows a few cycles of the steady sustained vibrations while Figure R-29 represents the beginning of the damped motion. Amplitude decay and percentage decay are plotted on Figure R-32 against vibration amplitude. Below a_i = 0.20", decay of amplitude hovers around a straight line having nearly the same slope as the theoretical value given by Equation (68-a). Amplitude decay in each cycle obtained from tests assumes a higher value than that given by the theory. This is probably due to the external sources of damping which have not been taken into account in the theory (e.g., air resistance, loss in the frame, loss in drive motor, etc.) The basic linear relations as shown in Figure R-32, however, agreed very satisfactorily with the theory.

As amplitude of vibration exceeds 0.20", the linear relations given by (62), (63) and (68-a) based on the assumption of small deformations no longer hold. It is believed that the amplification of other sources of damping and the variation of tension at high amplitudes may have caused the deviation. Further investigation, however, is required at high amplitudes to ascertain the causes.

(C) CONCLUSIONS

(1) Based on results from Part I and several simplifying assumptions, an analytic solution for damped vibrations of a stranded cable strung under tension has been obtained. The experimental results at low amplitudes agreed very well with the theory.

(2) In the field, where vibration amplitudes of cable are usually very small (the maximum value rarely exceeds the diameter of the cable -- see Reference 1 and the Bibliography on vibration of cable and conductors in the Appendix), the analysis and solution presented is justified to be used for purposes of practical application.

REFERENCES

1. Bonneville Power Administration, U. S. Department of Interior "Conductor Vibration Manual" Nov. 1947, pp. 8-11

2. Bate, E. :"Vibration of Transmission Line Conductors", Inst. of Engineers, Australia, Trans. VII, 1930, pp. 279-282

3. Sturm, R. G. : "Vibration of Cables and Dampers". Electrical Engineering, June 1936, pp. 673-88

4. Synge, J. L. & Griffith, B. A. : "Principles of Mechanics", McGraw Hill 1942, pp. 64-66 and p. 138

5. Sokonikoff, I. S. : "Mathematical Theory of Elasticity" McGraw Hill, 1946, p. 264

6. Den Hartog, J. P. : "Mechanical Vibrations" McGraw Hill, 1947, p. 71

7. von Heydekampf, G. S. : "Damping Capacity of Materials" Proc. A.S.T.M. Part II, Vol. 31, 1931 p. 157

8. Kimball, A. L. : "Friction and Damping in Vibrations" Trans. A.S.M.E. Vol. 63, 1941, A-37 and A-135

9. Den Hartog, J. P. : "Forced Vibrations with Combined Coulomb and Viscous Damping" Trans. A.S.M.E. Vol. 53, 1931, APM-53

10. Timoshenko, S.: "Vibration Problems in Engineering" Van Nostrand Co., New York, 1937, p. 54

11. Searle, G. F. C.: "Experimental Elasticity", Cambridge Univ. Press, 1933, pp. 107-110

12. Yu, Ai-Ting and Johnston, B. G.: "A Method for Vibration Fatigue Tests of Stranded Conductor" Proc., Society for Experimental Stress Analysis, No. II, Vol. VI, pp. 1-6

13. Churchill, R. V. : "Complex Variables and Applications" McGraw Hill, 1948, p. 12

APPENDICES

APPENDIX A

CURVATURE, SLOPE AND DEFLECTION OF A CIRCULAR ARC

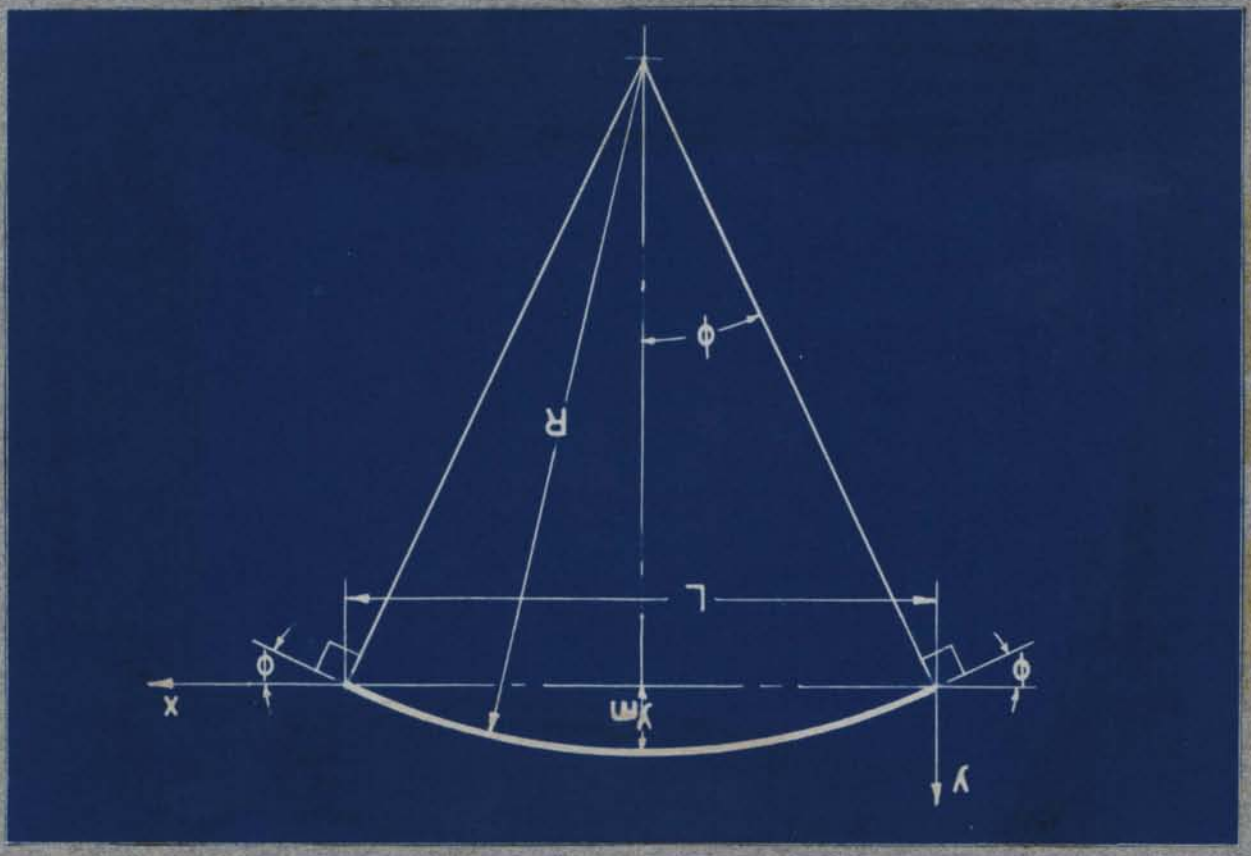

Assume deflection to be small

Let R = radius of curvature

y_m = deflection at mid-span

$y'_o = \phi$ = slope at ends

$y''_m = \frac{1}{R}$ = curvature

L = length of span

By relations in a right triangle, it may be easily verified that

$$(R-y_m)^2 = R^2 - (\frac{L}{2})^2 \qquad (1)$$

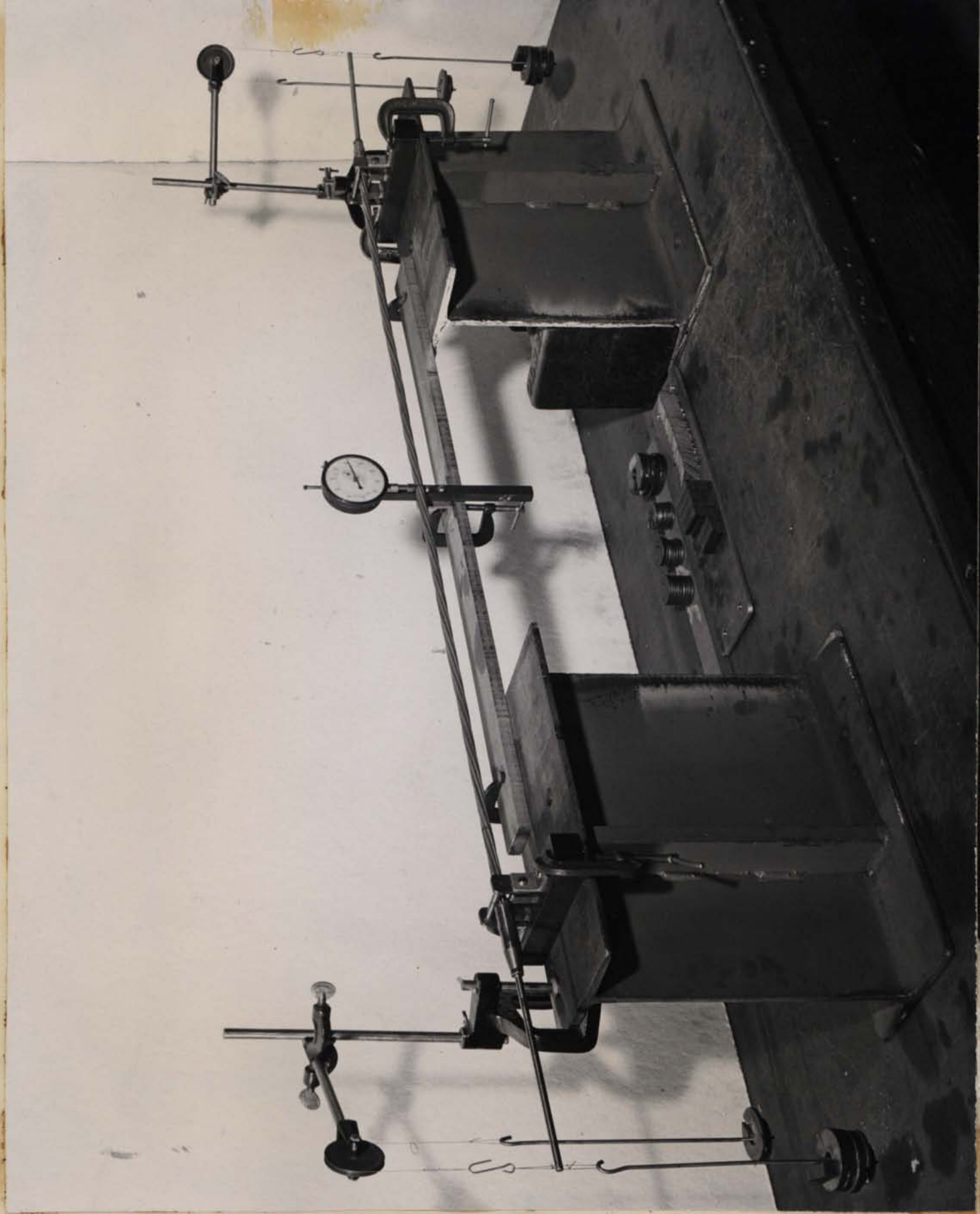

Figure T-1 Complete View of the
Static Hysteresis Test Set-up

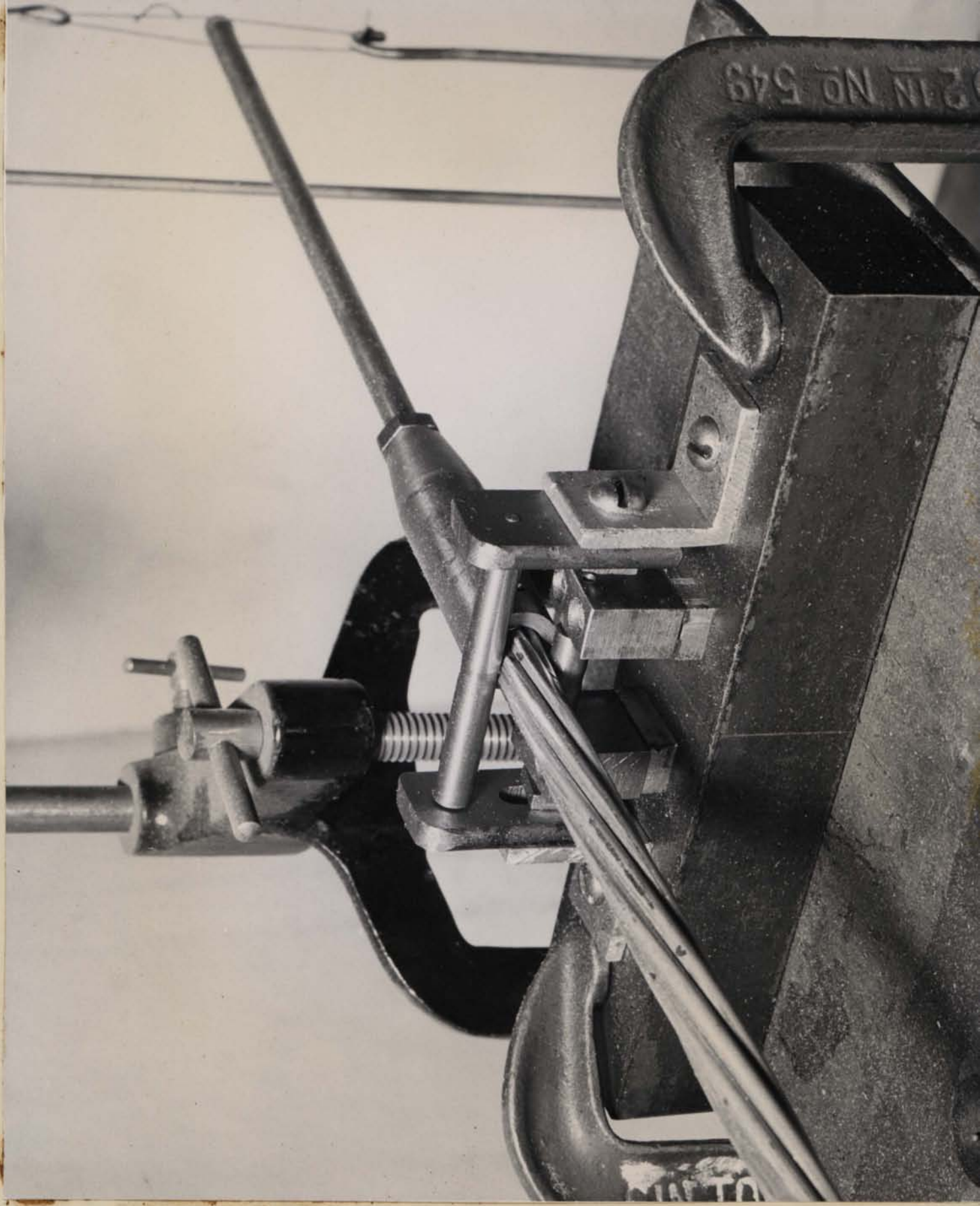

Figure T-2 Details of End Support for Static Hysteresis Test

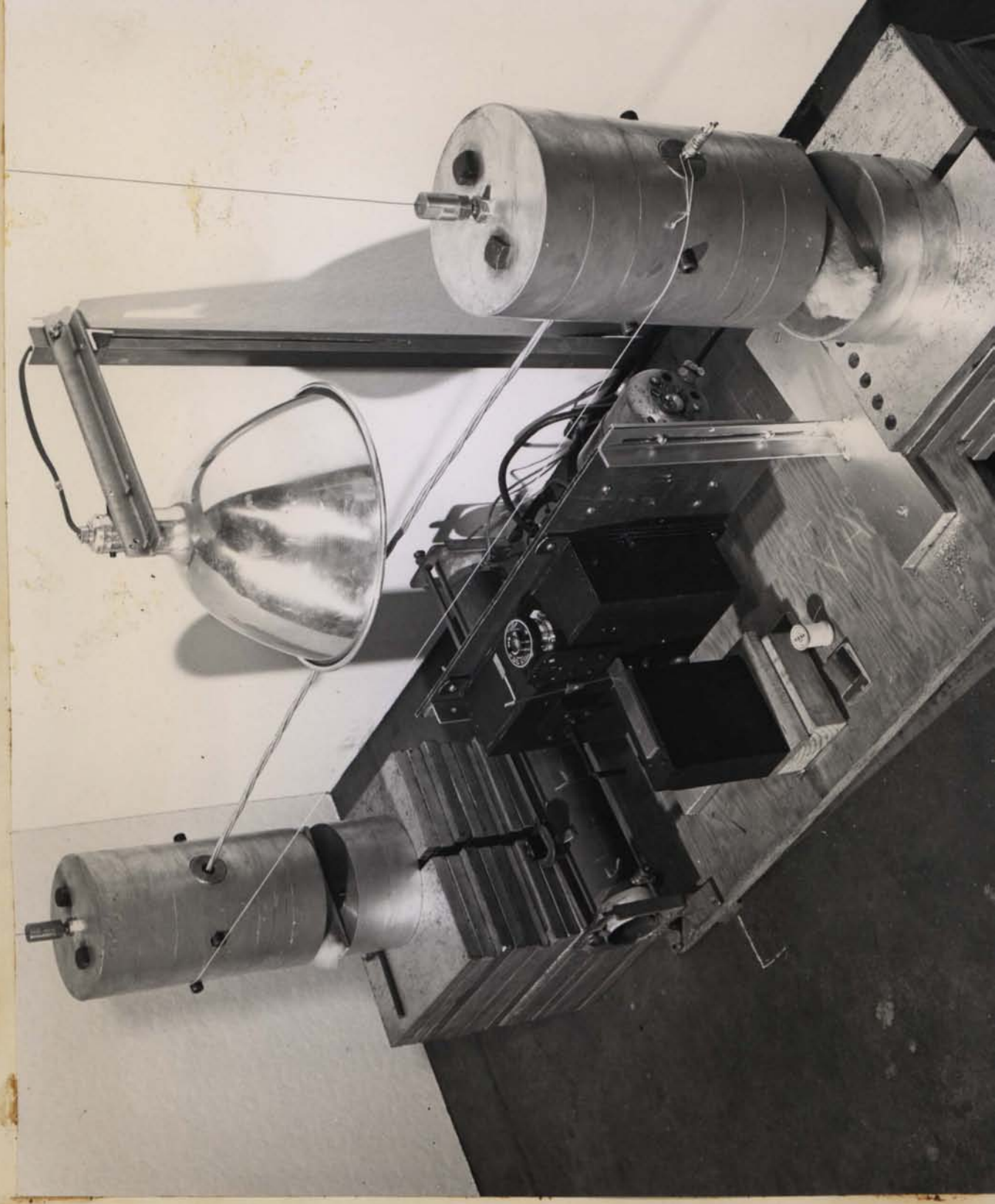

Figure T-3 General View of the
Free Decay Test Set-up

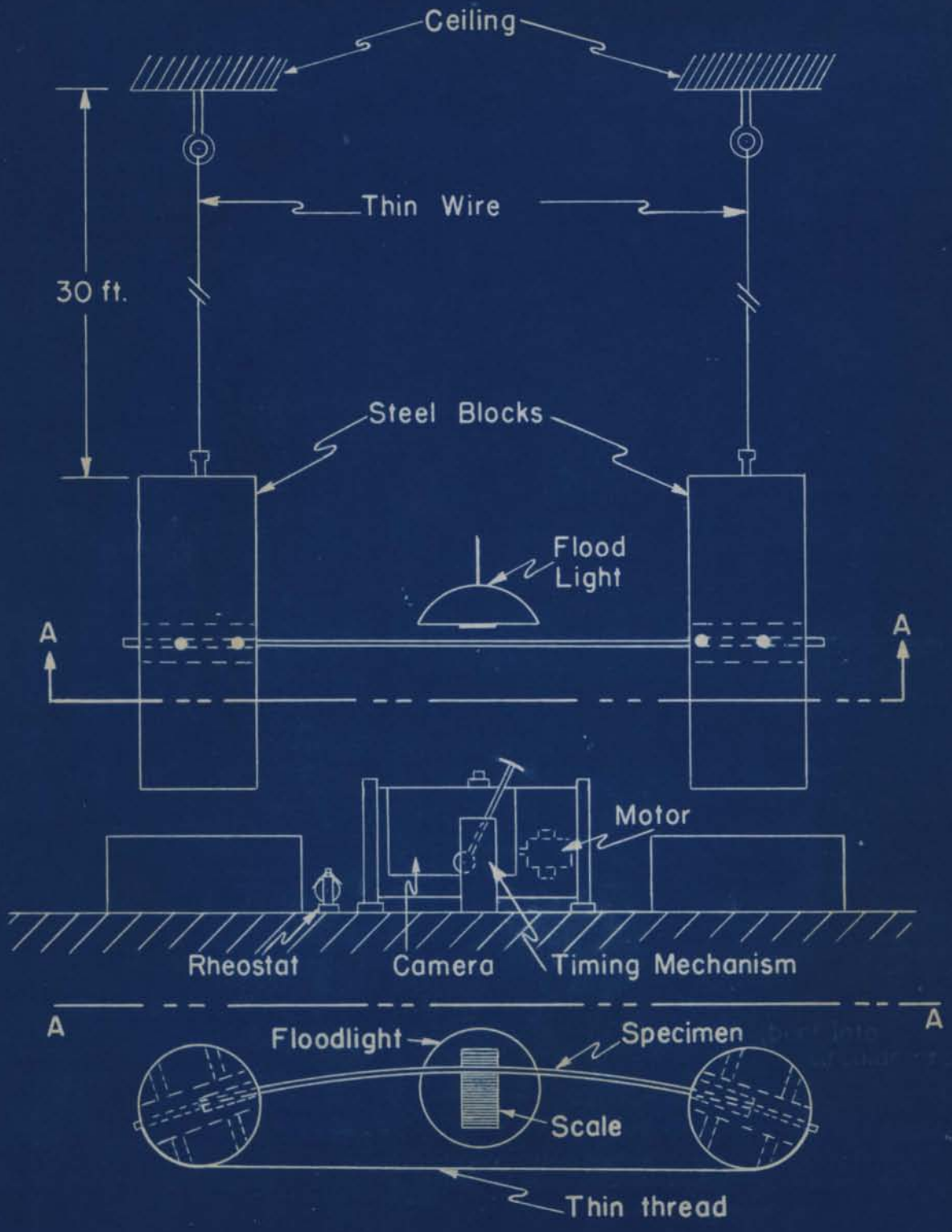

SCHEMATIC DIAGRAM FOR
BENDING DECAY TEST SET-UP

Fig. T-4

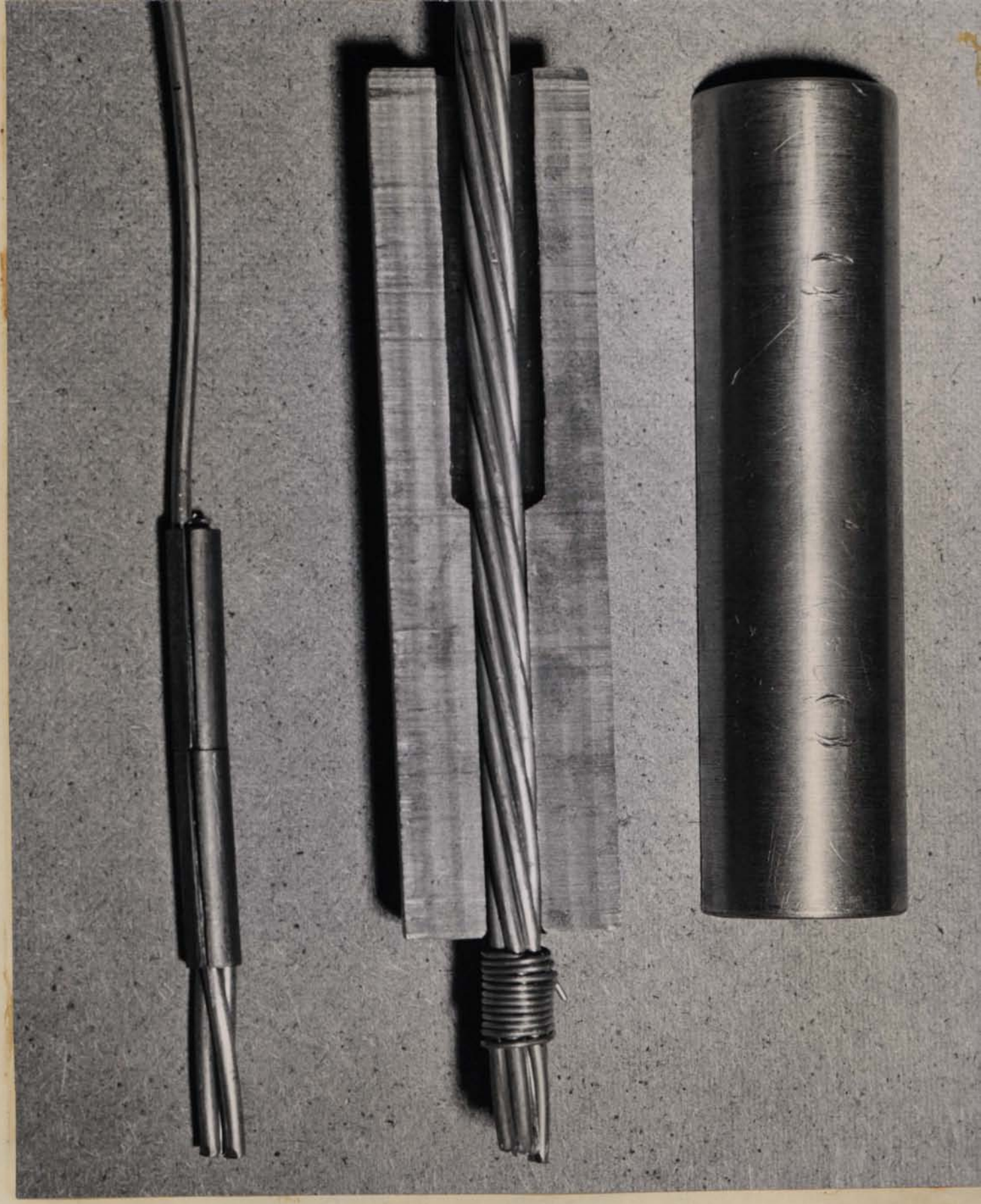

Figure T-5 Details of End-clamp for Cable Specimen in Free Decay Test

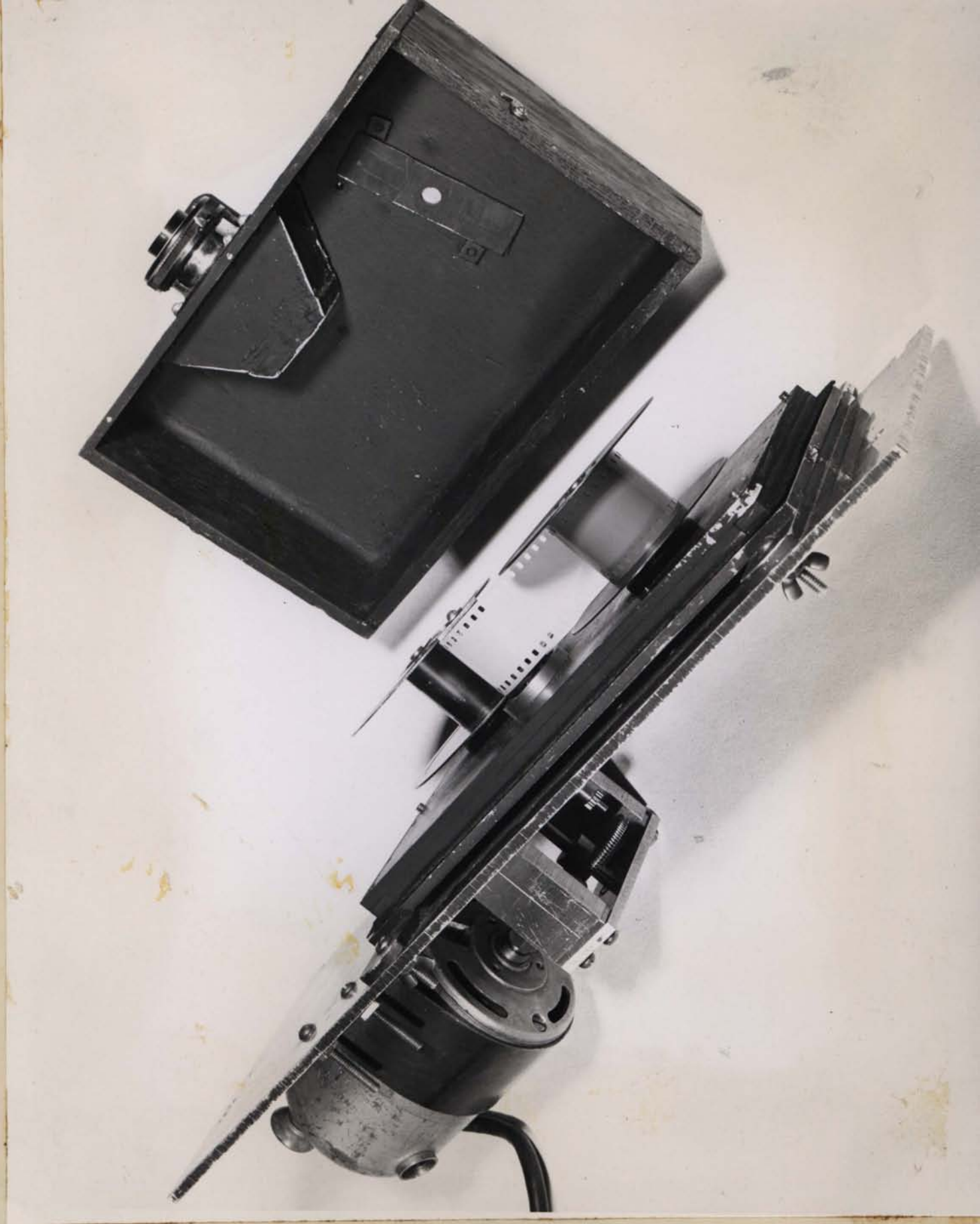

Figure T-6 Motion Picture Camera
(recorder of free decay
vibrations)

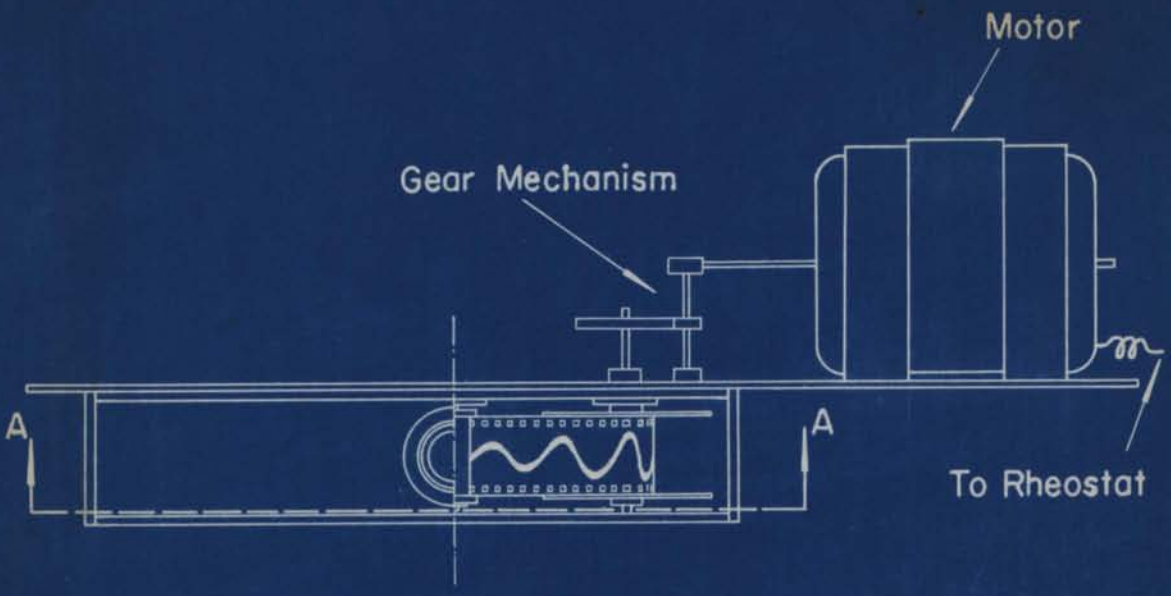

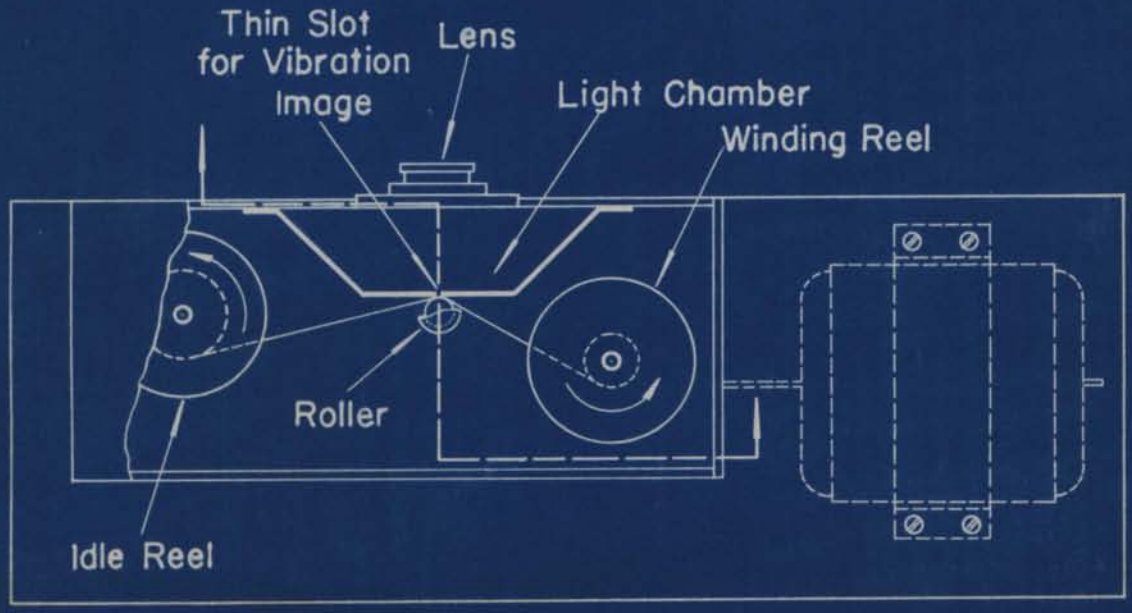

DETAILS OF MOTION PICTURE CAMERA

FIGURE T-7

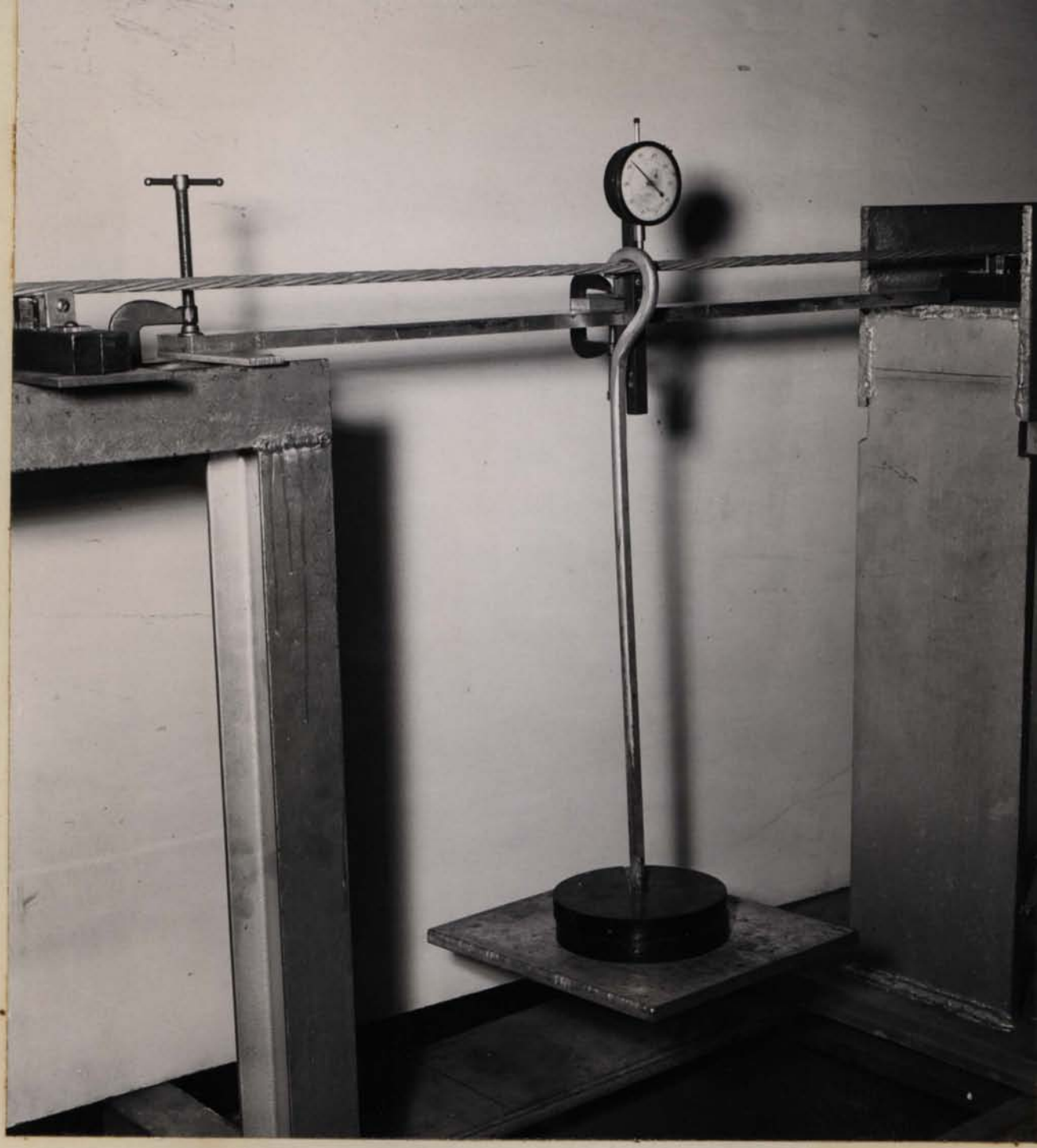

Figure T-8 Hysteresis Test Set-up for Cable Under Tension

Figure T-9 General view of Test Set-up for Vibration of Stranded Cable Under High Tension

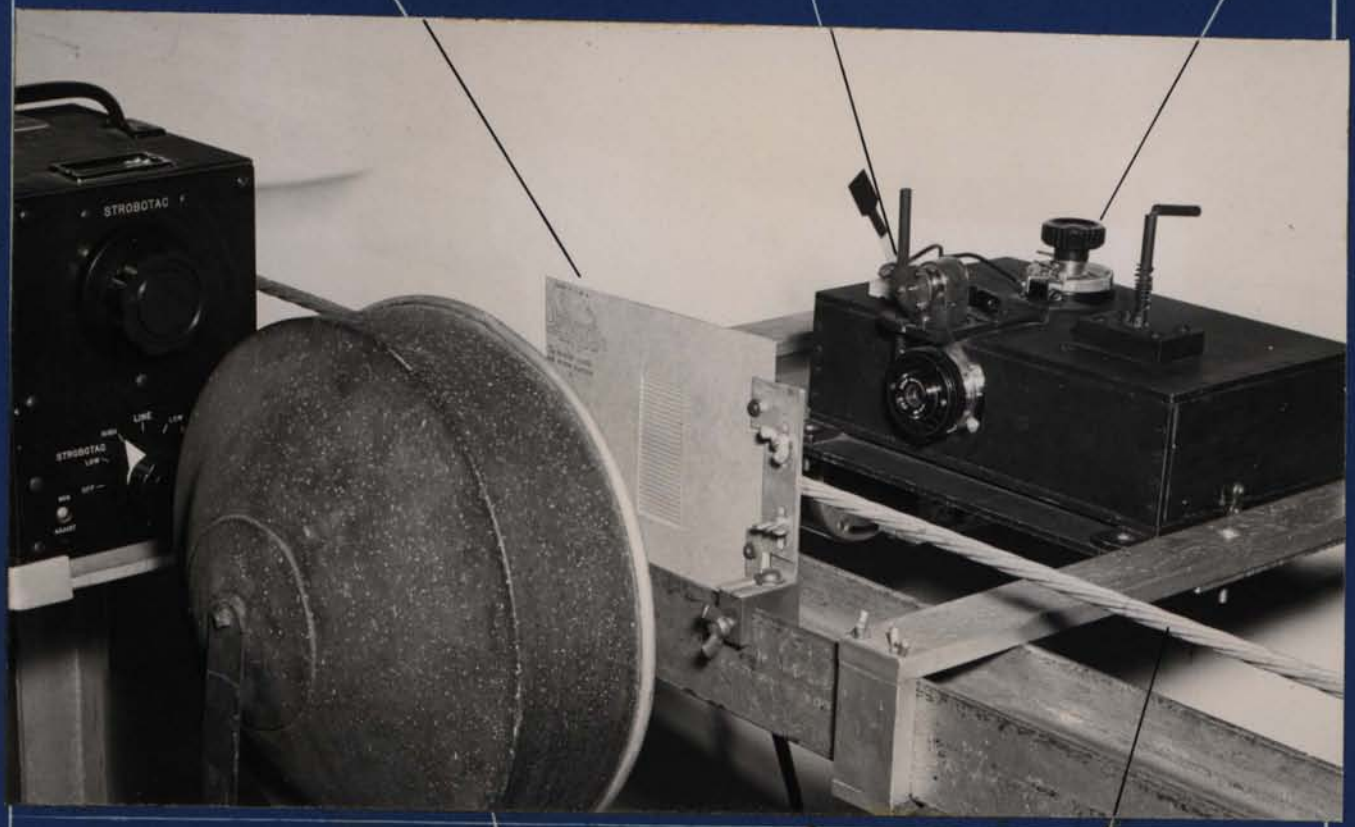

Figure T-10 Set-up for Recording Amplitude Decay of Cable Under Tension

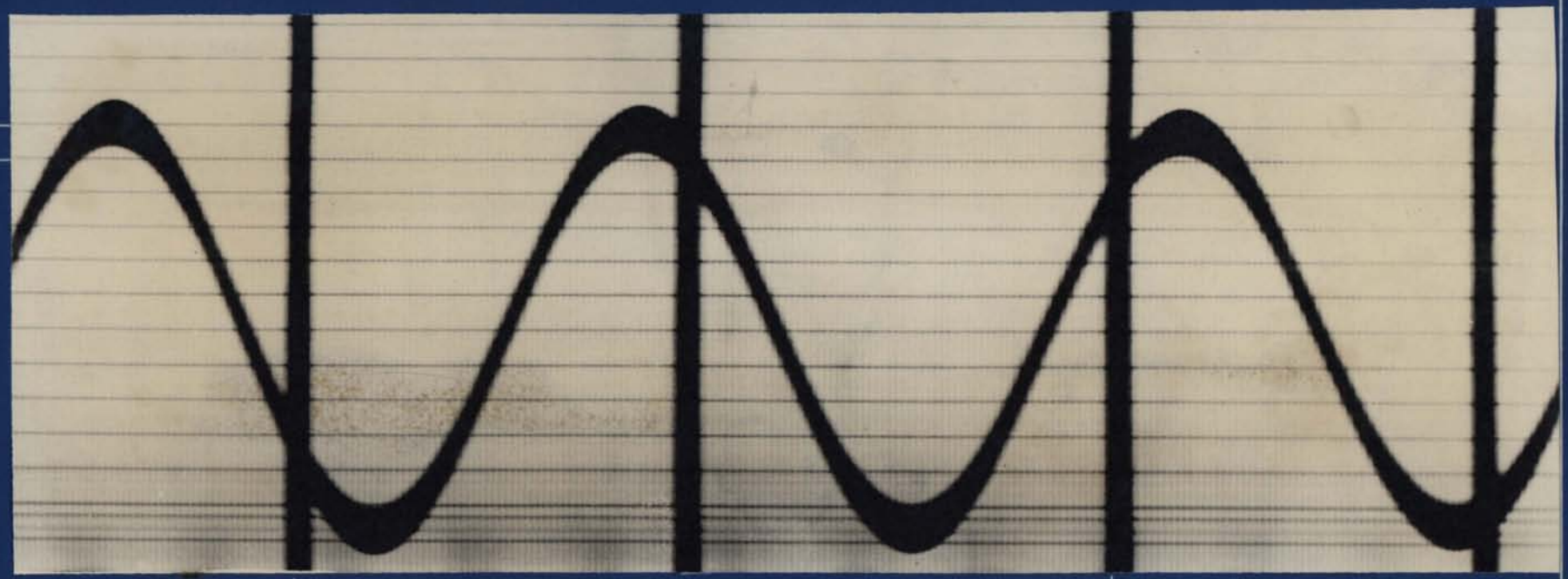

SPECIMEN 301 Wire dia. = 0.138"

FIGURE R-1 DECAY OF SINGLE WIRE

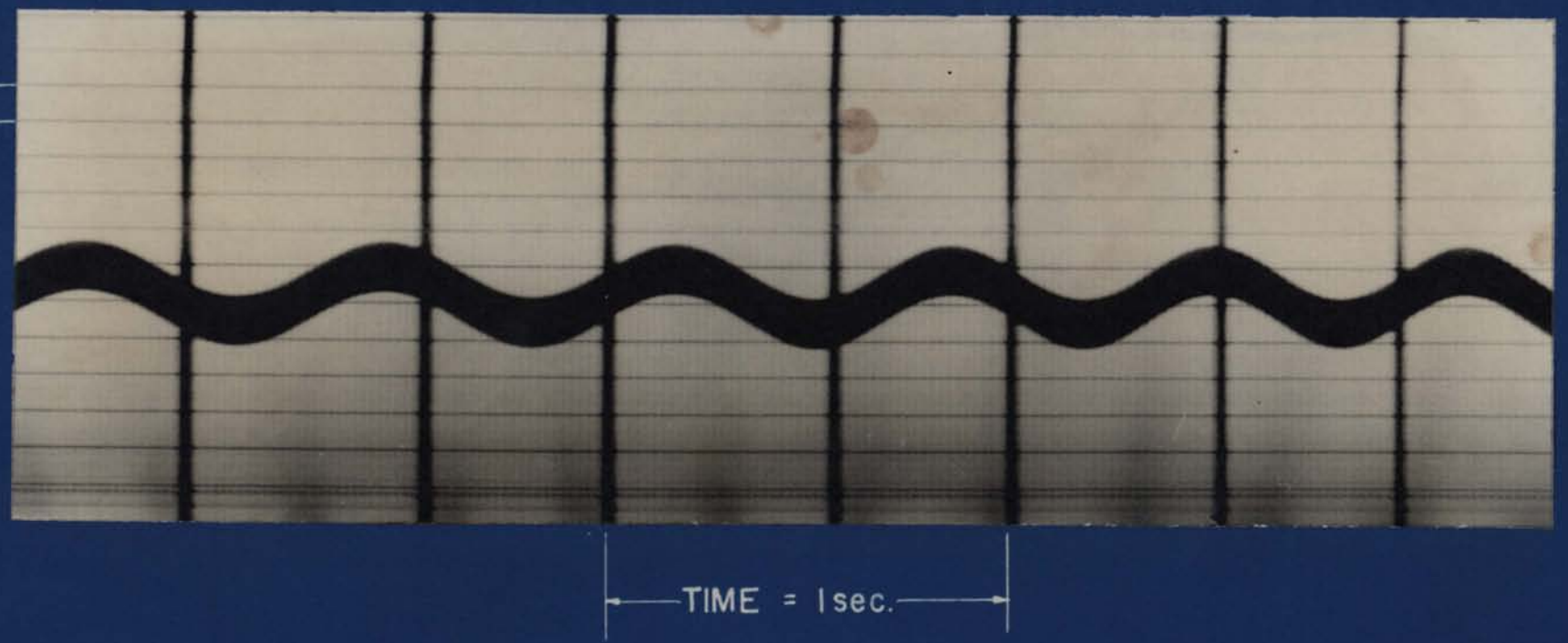

SPECIMEN 301 Wire dia. = .138"

FIGURE R-1a DECAY OF SINGLE WIRE
(200 cycles after FIGURE R-1)

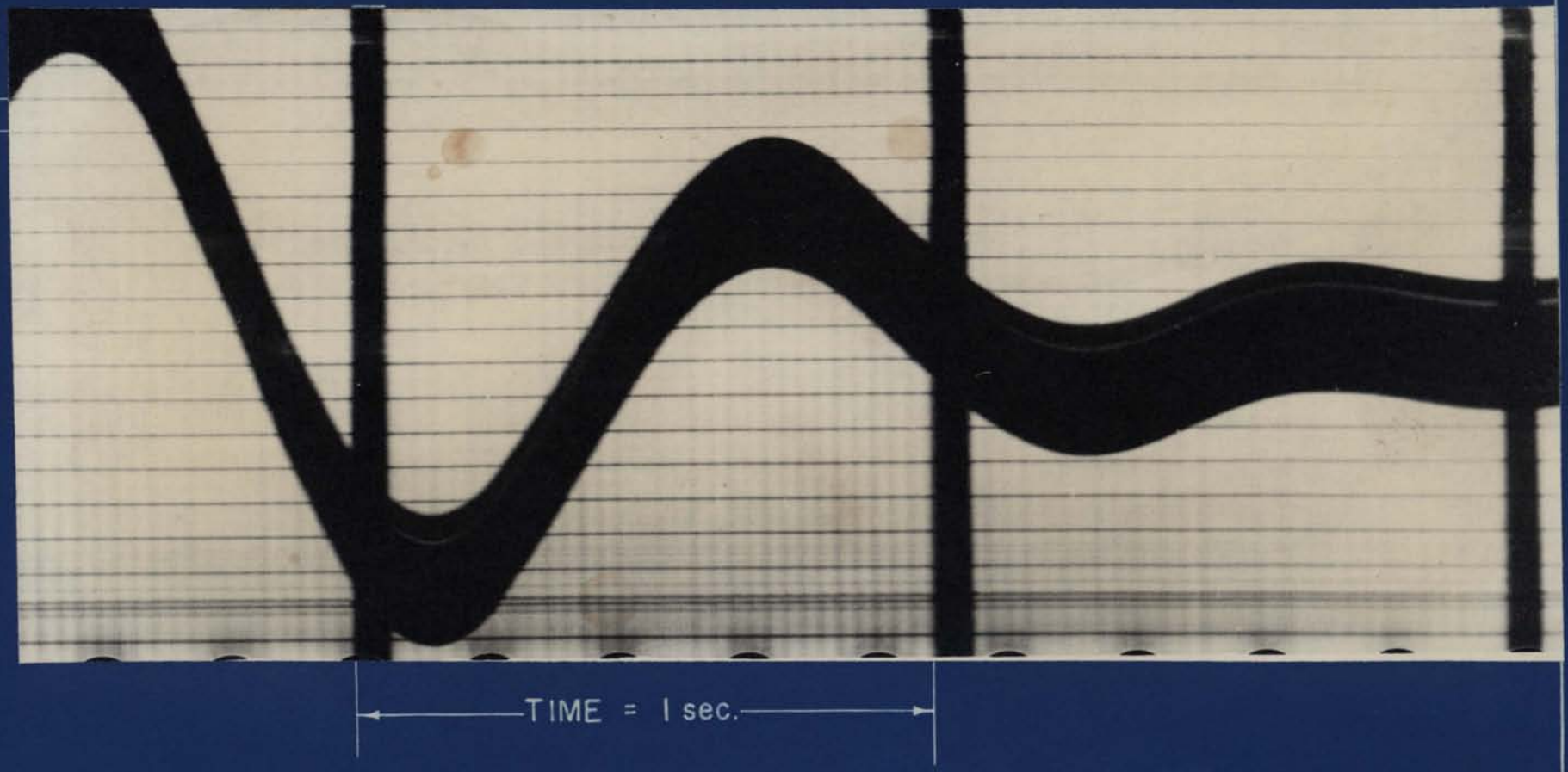

SPECIMEN 771 3/8" 7-strand

FIGURE R-2 DECAY OF STRANDED CABLE (a)

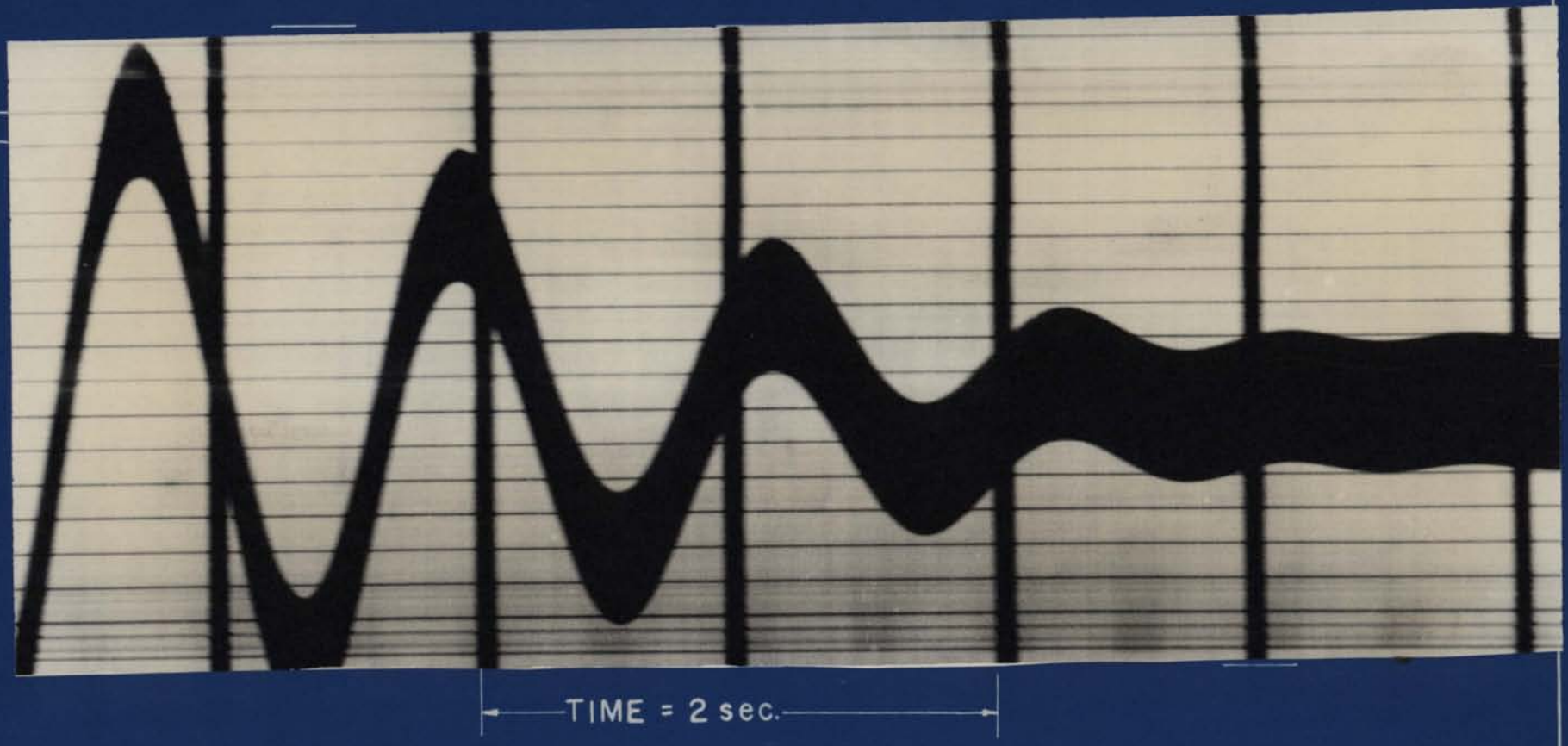

SPECIMEN 772 3/8" 7-strand

FIGURE R-3 DECAY OF STRANDED CABLE (b)

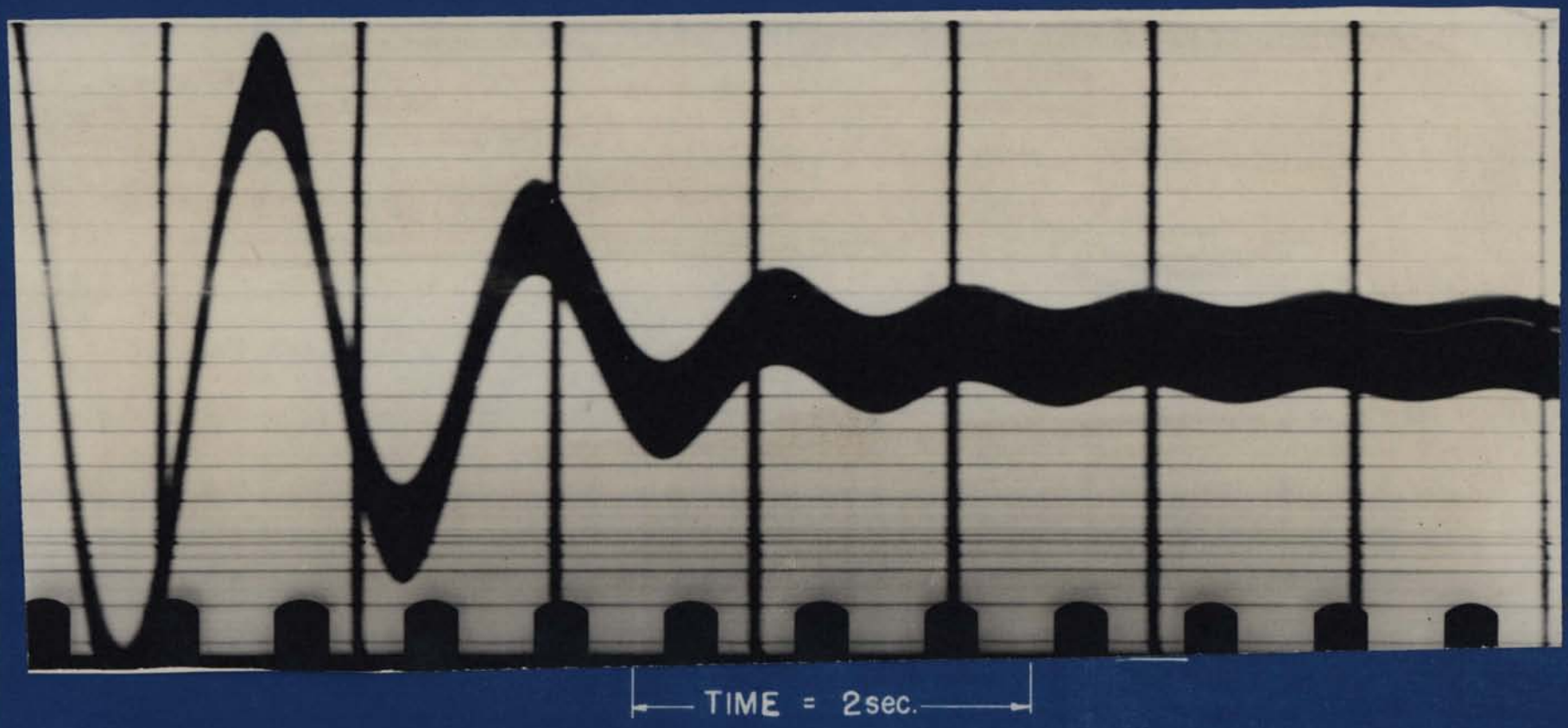

SPECIMEN 331 .297" 3-strand

FIGURE R-4 DECAY OF STRANDED CABLE (c)

STATIC HYSTERESIS LOOPS

SPECIMEN 771

3/8" 7-strand

Lay length 5.5 in.

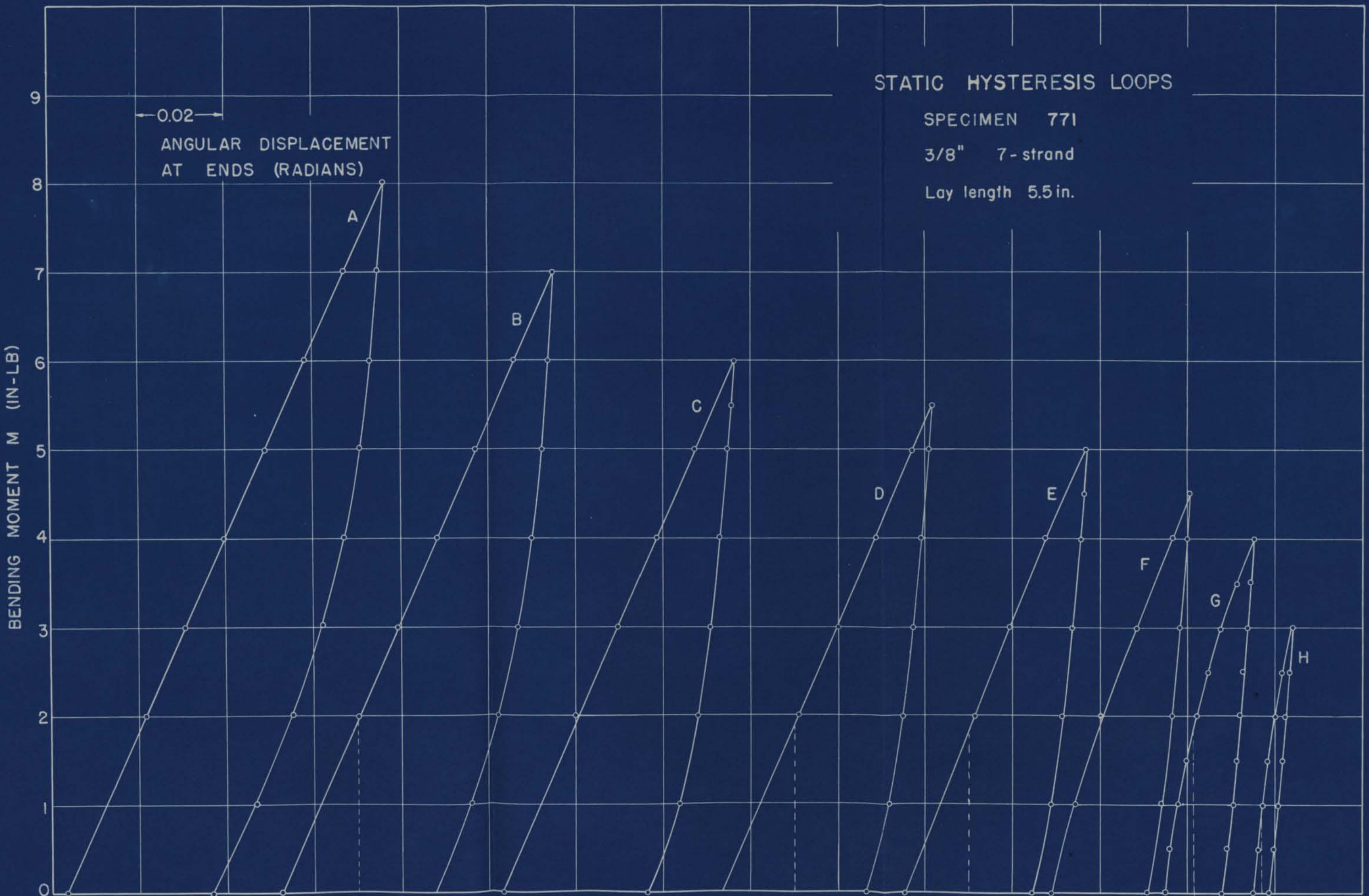

FIGURE R-5

STATIC HYSTERESIS LOOPS

SPECIMEN 772

3/8" 7-strand

Lay length 8.4 in.

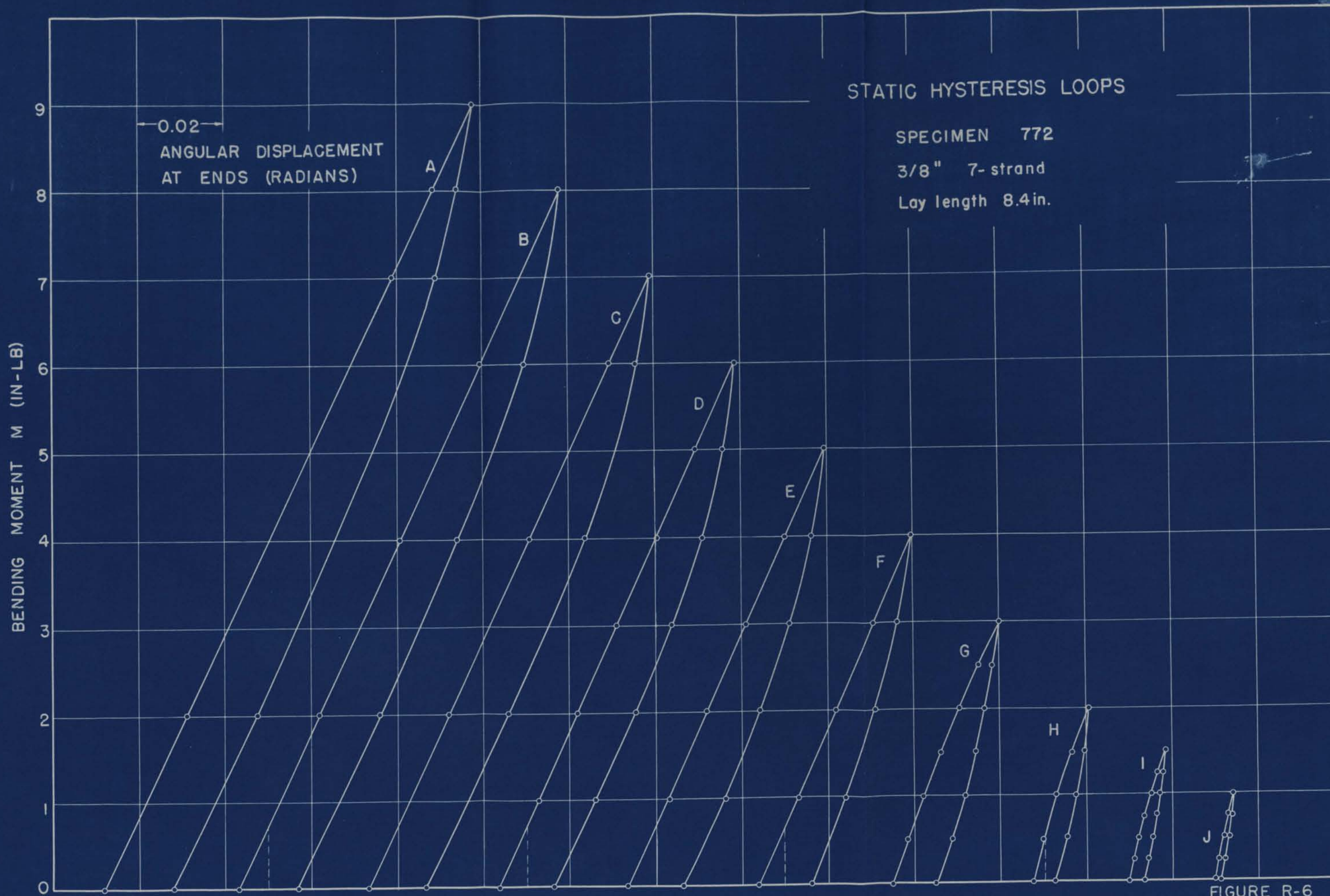

FIGURE R-6

STATIC HYSTERESIS LOOPS

SPECIMEN 331

0.297" 3-strand

Lay length 5.0 in.

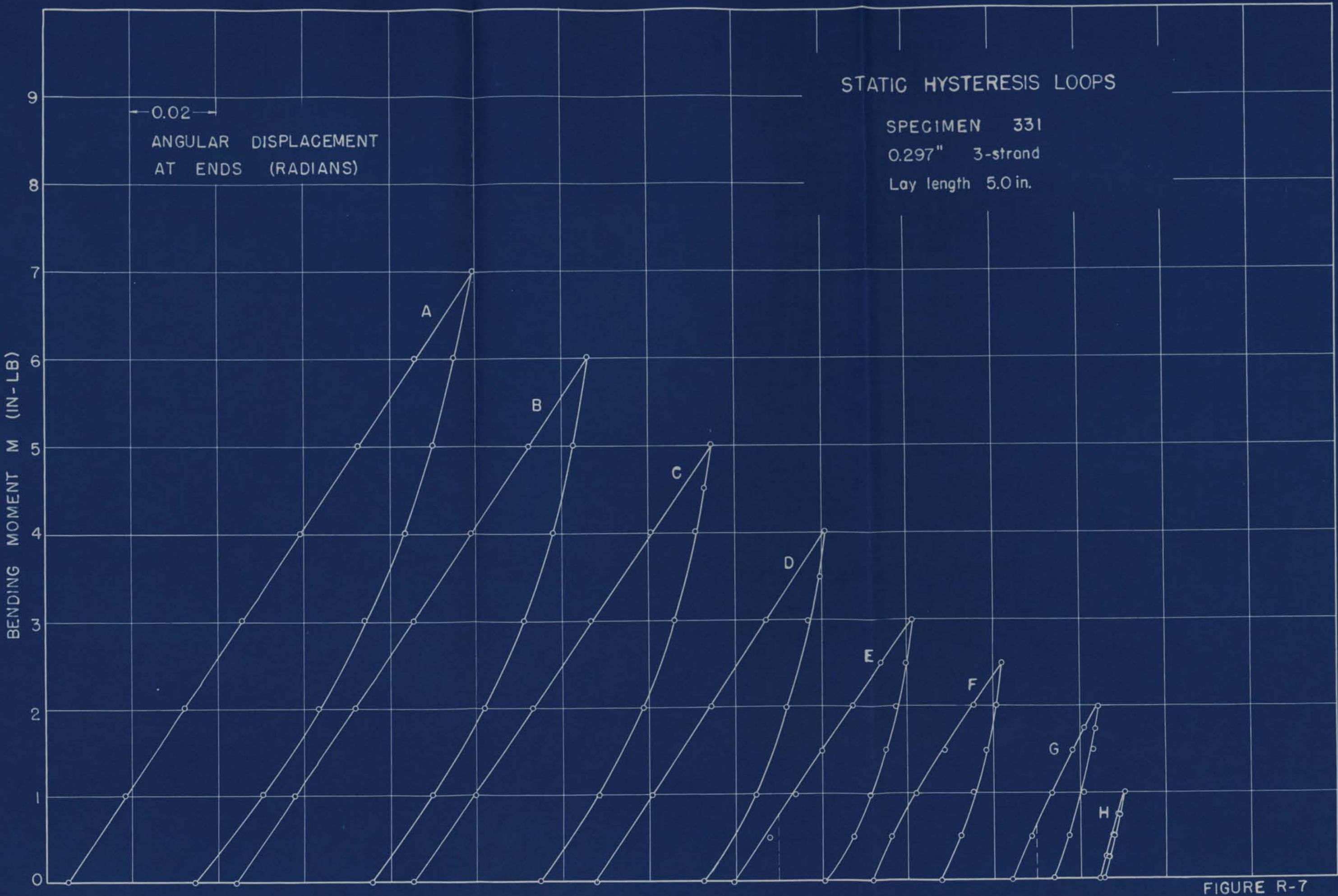

FIGURE R-7

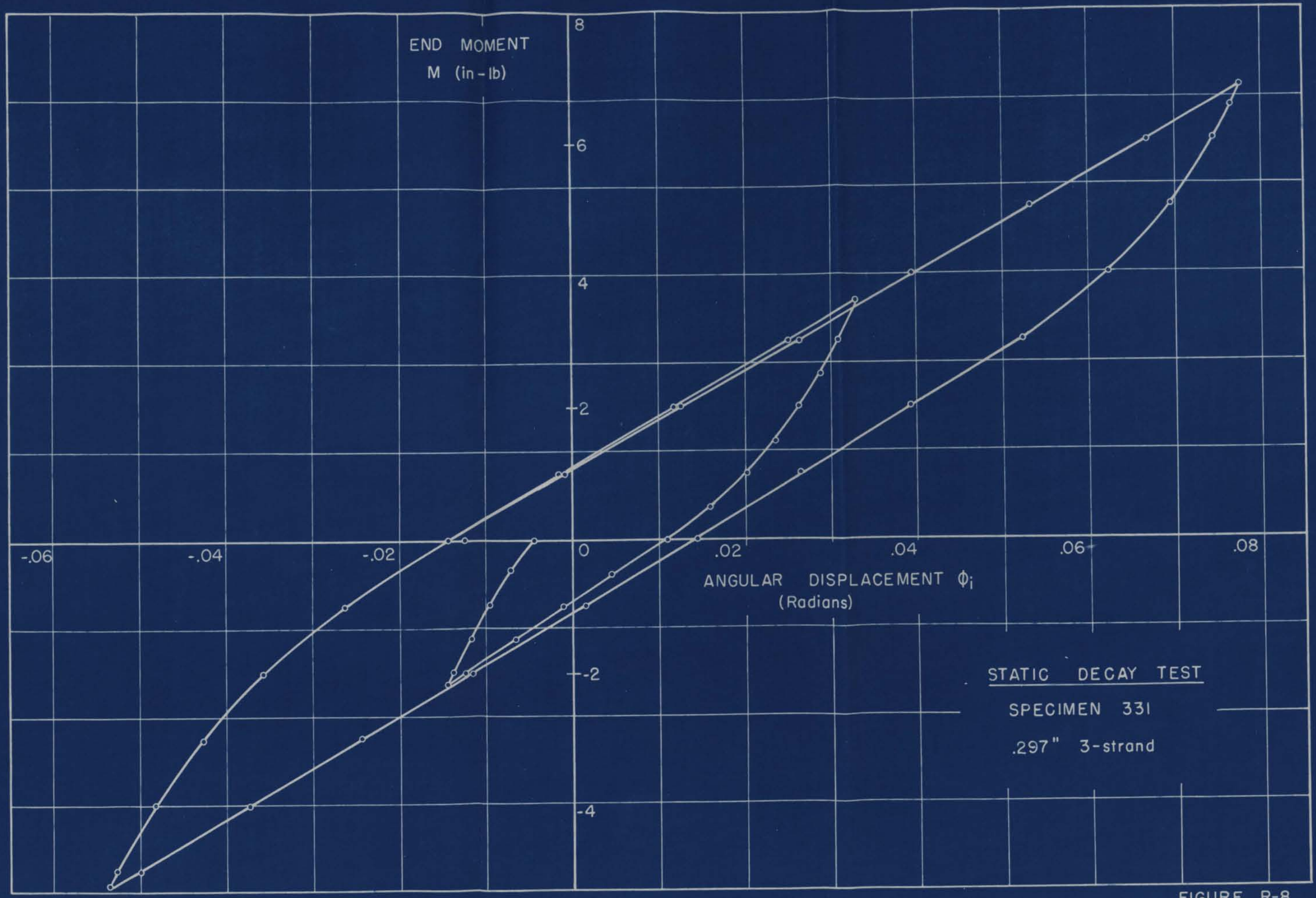
END MOMENT
M (in-lb)
8
6
4
2
-2
-4
-.06
-.04
-.02
0
.02
.04
.06
.08
ANGULAR DISPLACEMENT ϕ_i
(Radians)
STATIC DECAY TEST
SPECIMEN 331
.297" 3-strand

FIGURE R-8

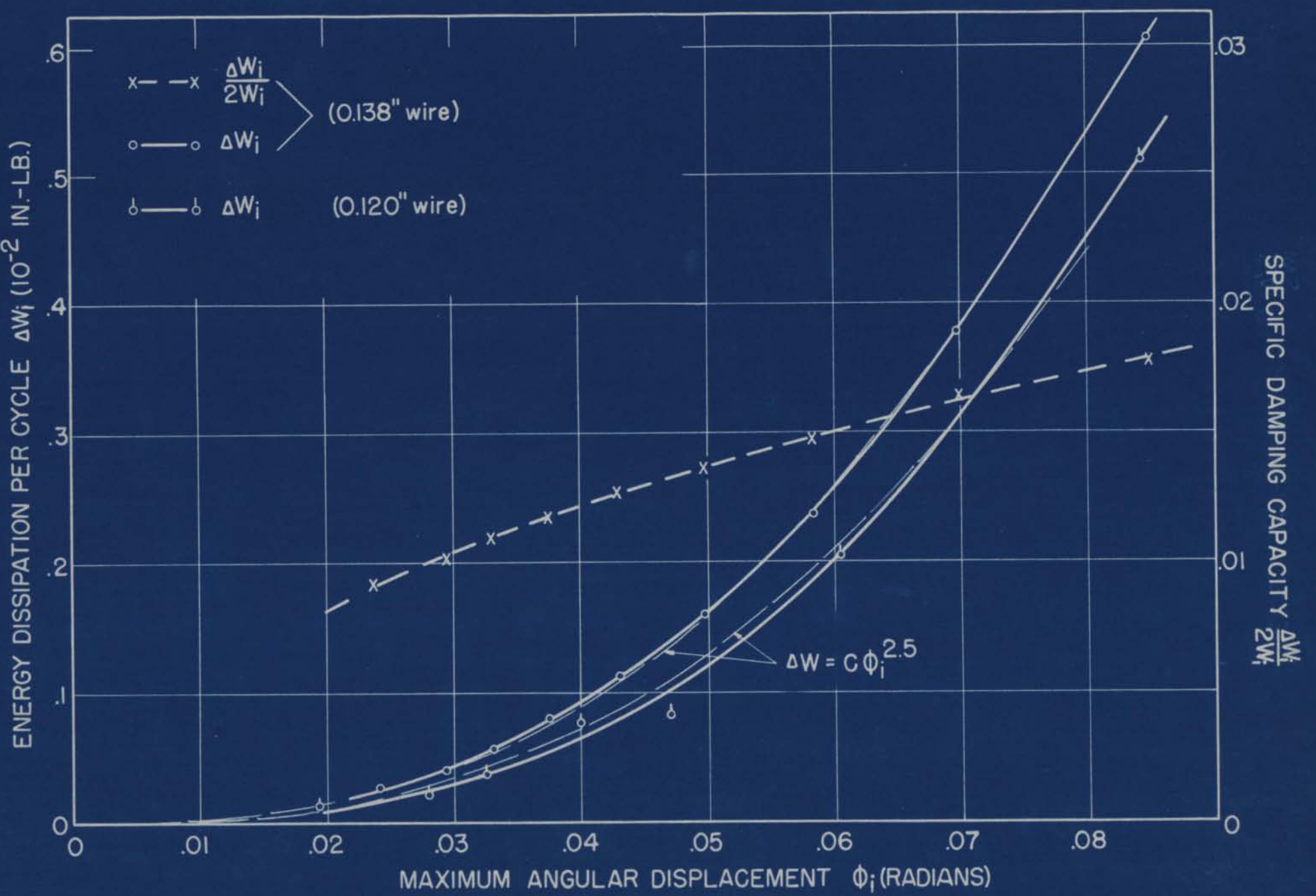

FIGURE R-9 DAMPING OF SINGLE WIRES (40" SPAN, FREE DECAY TEST)

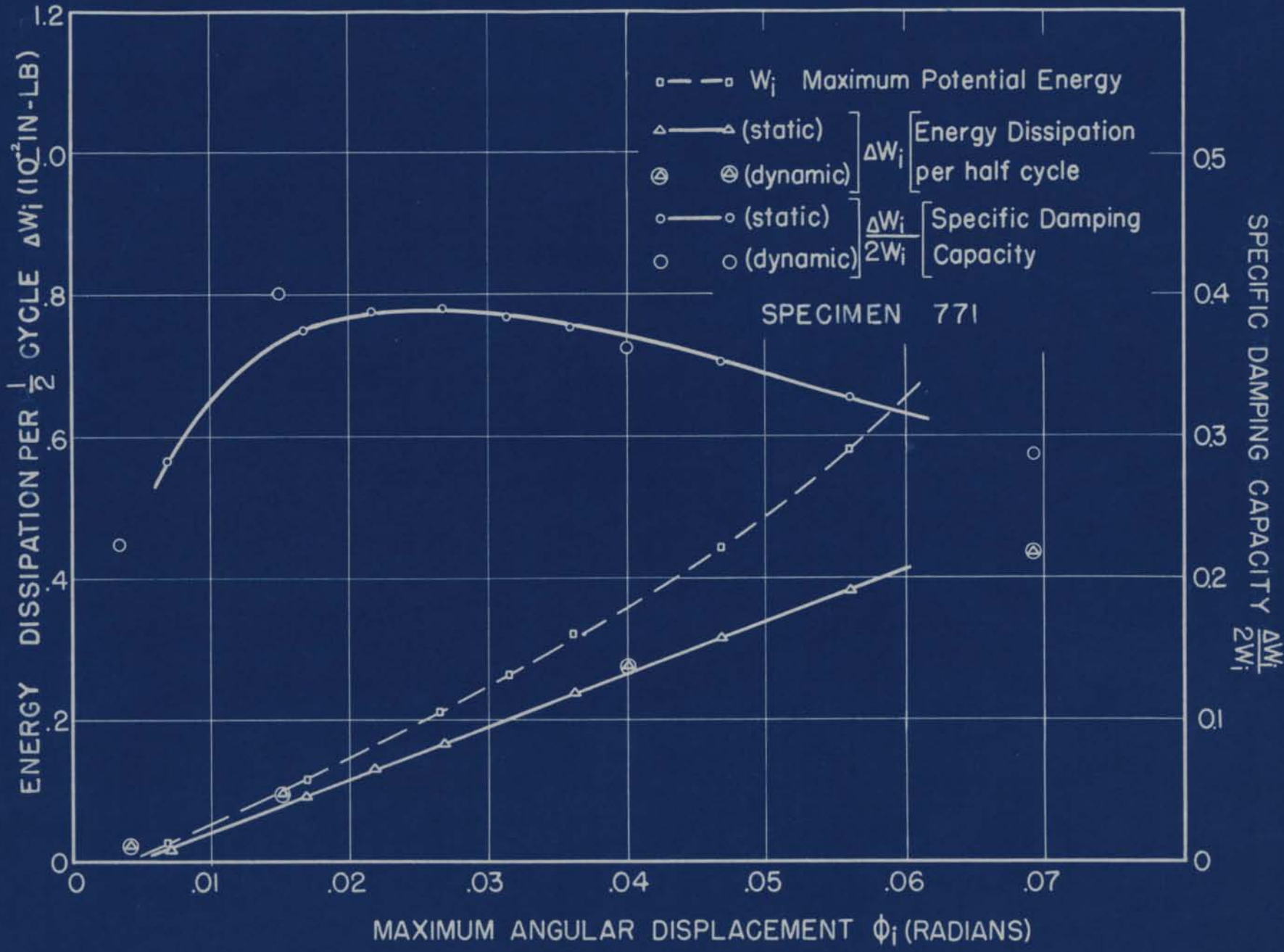

FIGURE R-10 ENERGY RELATIONSHIPS OF 7-STRAND CABLE

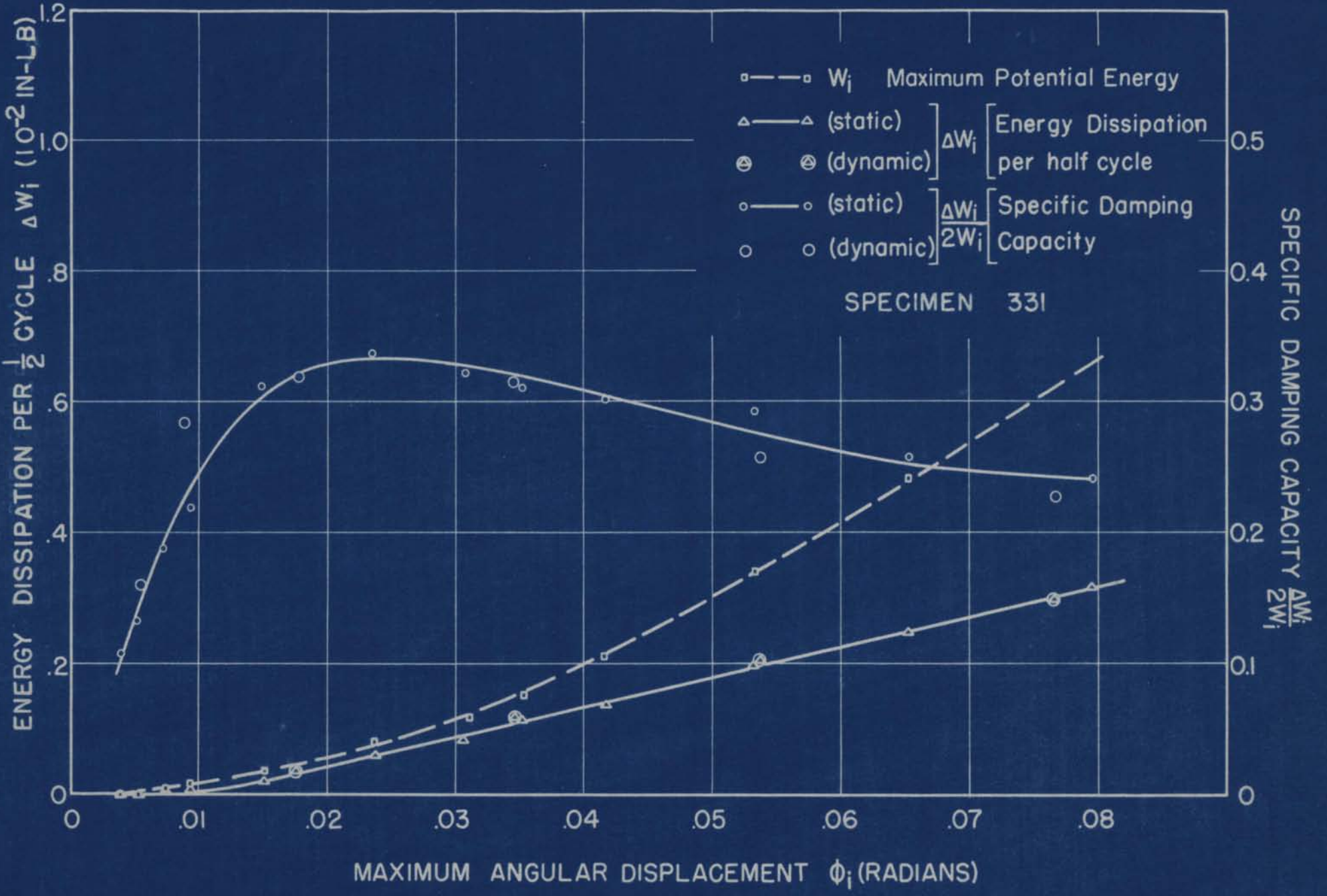

FIGURE R-11. ENERGY RELATIONSHIPS OF 3-STRAND CABLE

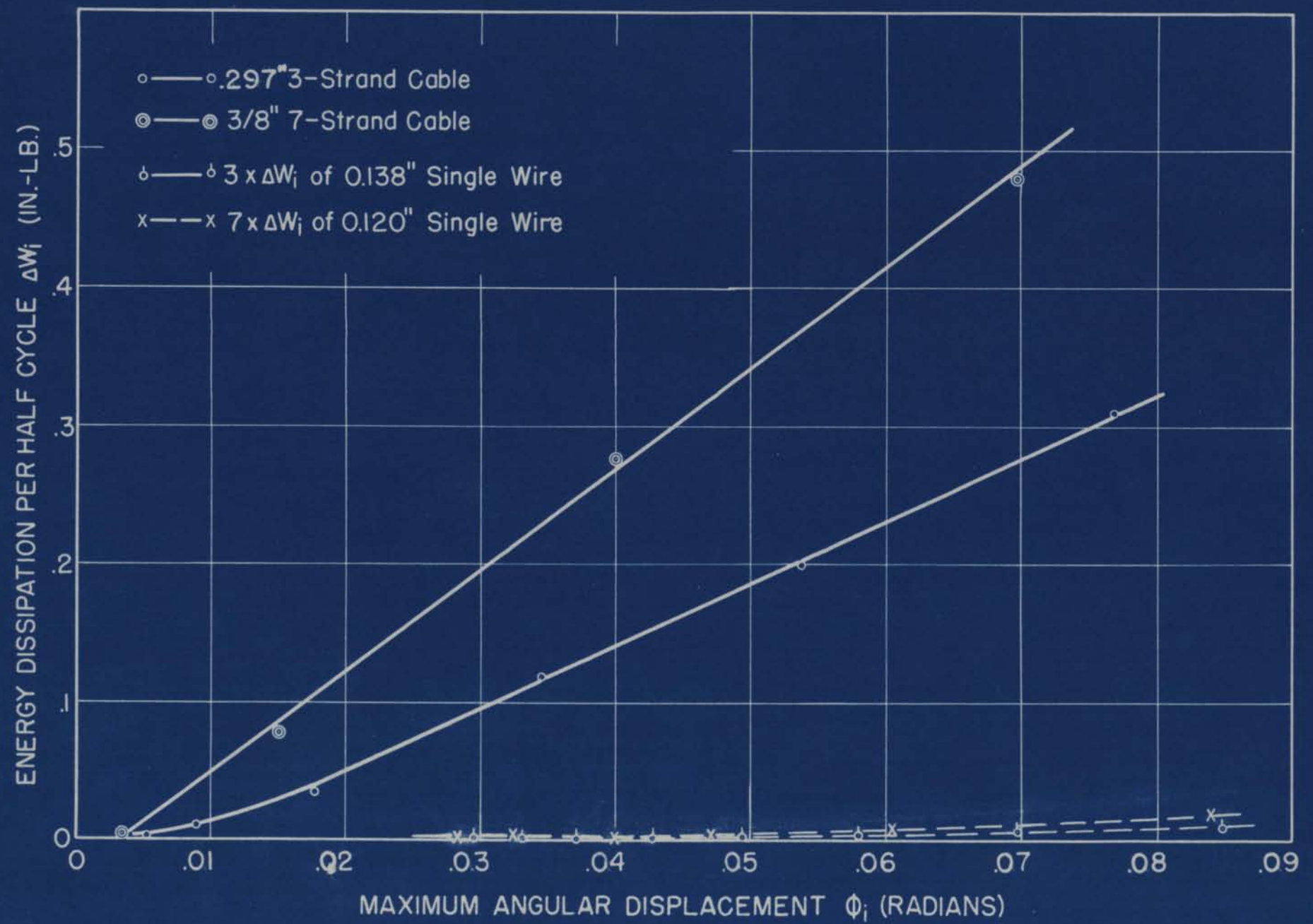

FIGURE R-12. ENERGY DISSIPATION OF STRANDED CABLE COMPARED WITH SINGLE WIRE (FREE DECAY TEST)

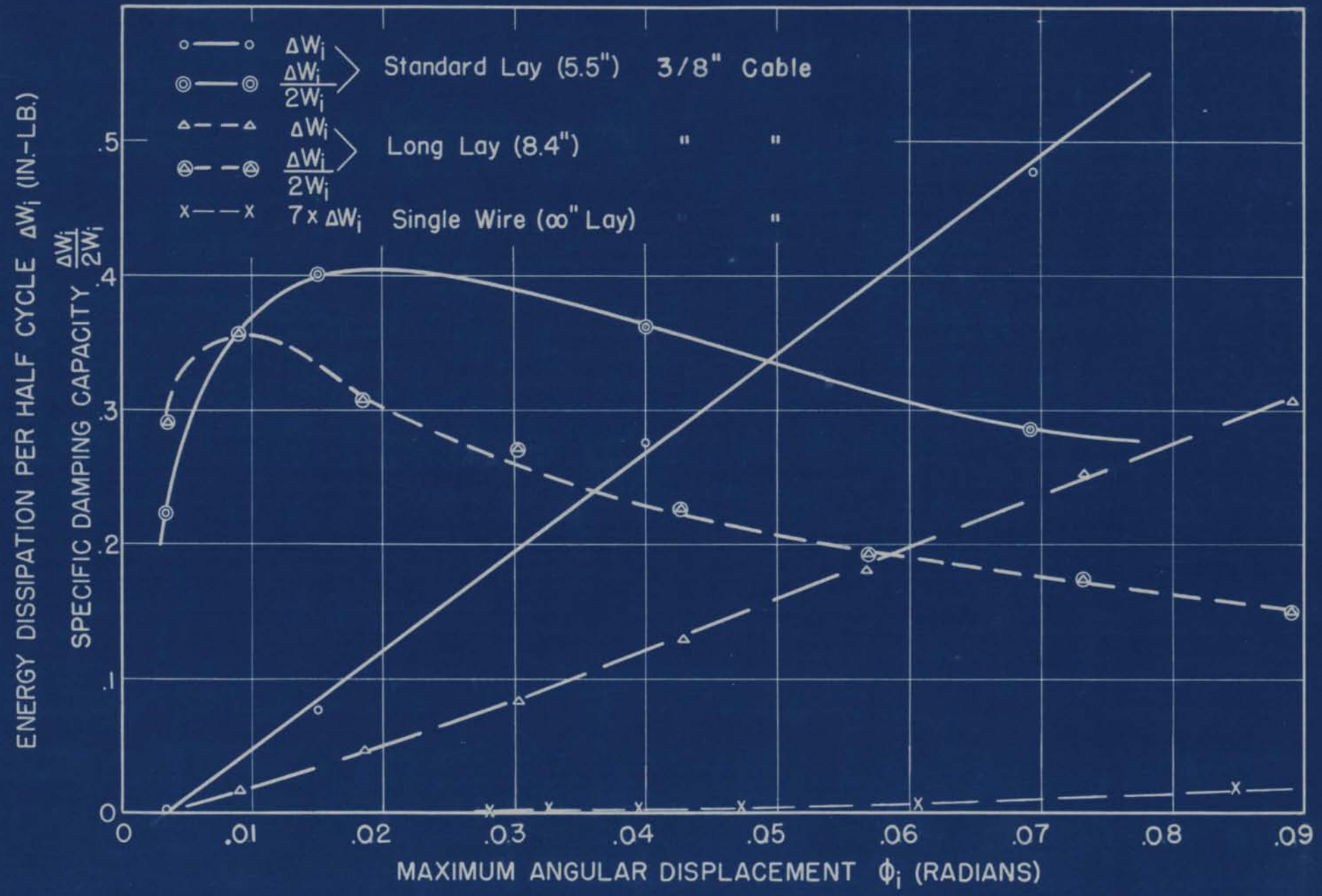

FIGURE R-13. EFFECT OF LAY LENGTH ON DAMPING

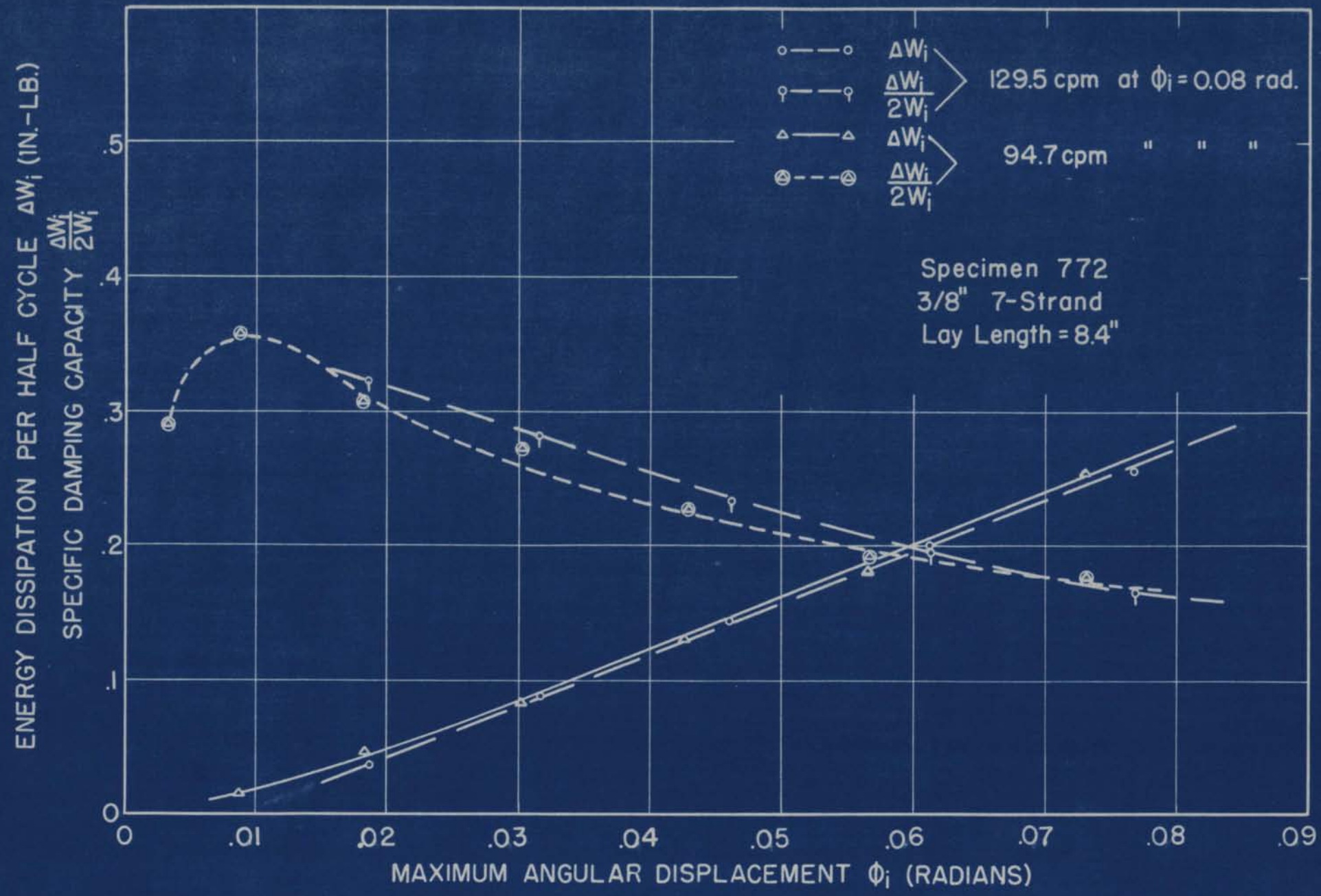

FIGURE R-14. EFFECT OF VIBRATION SPEED ON DAMPING

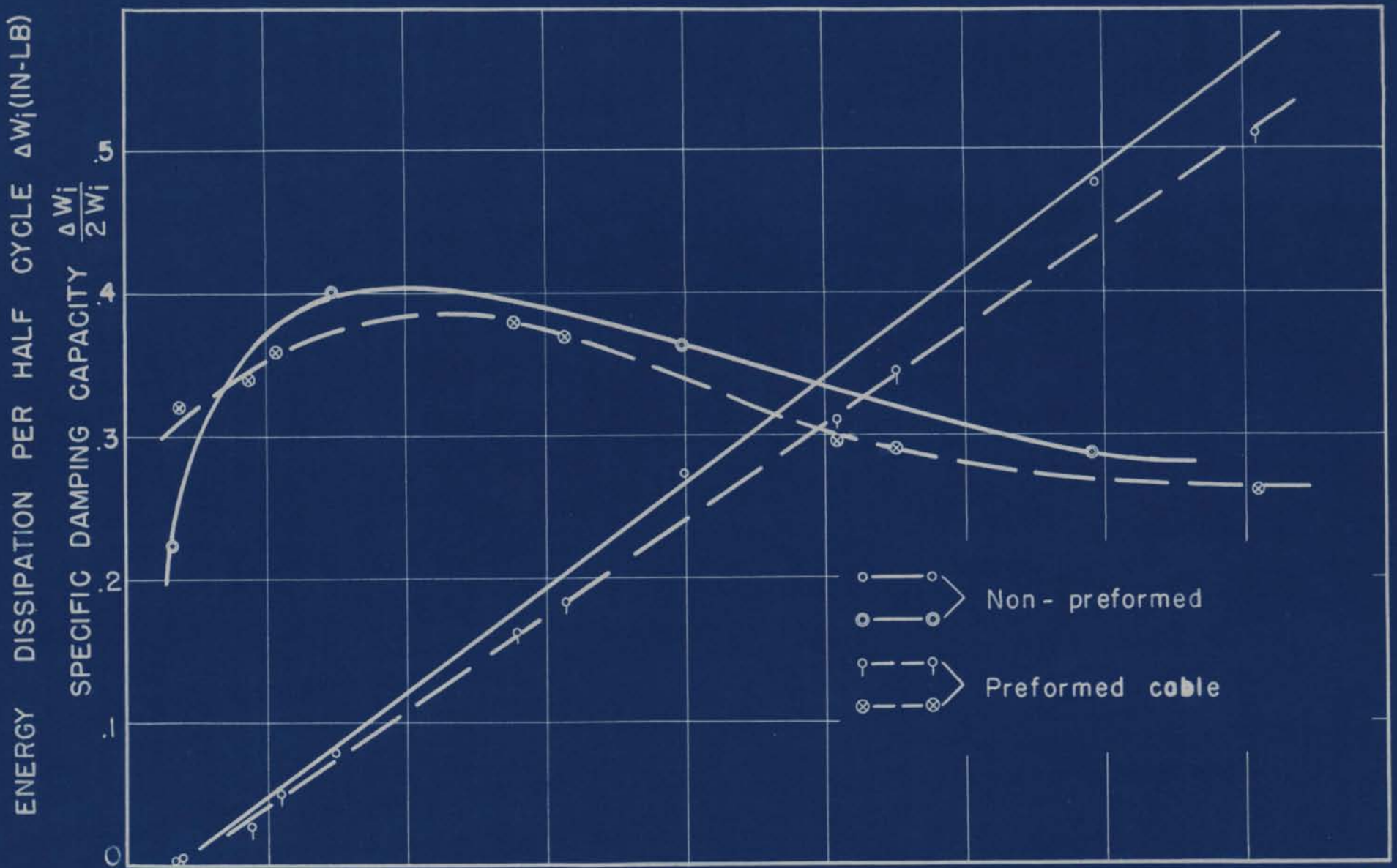

FIGURE R-15 EFFECT OF FORMING PROCESS ON DAMPING

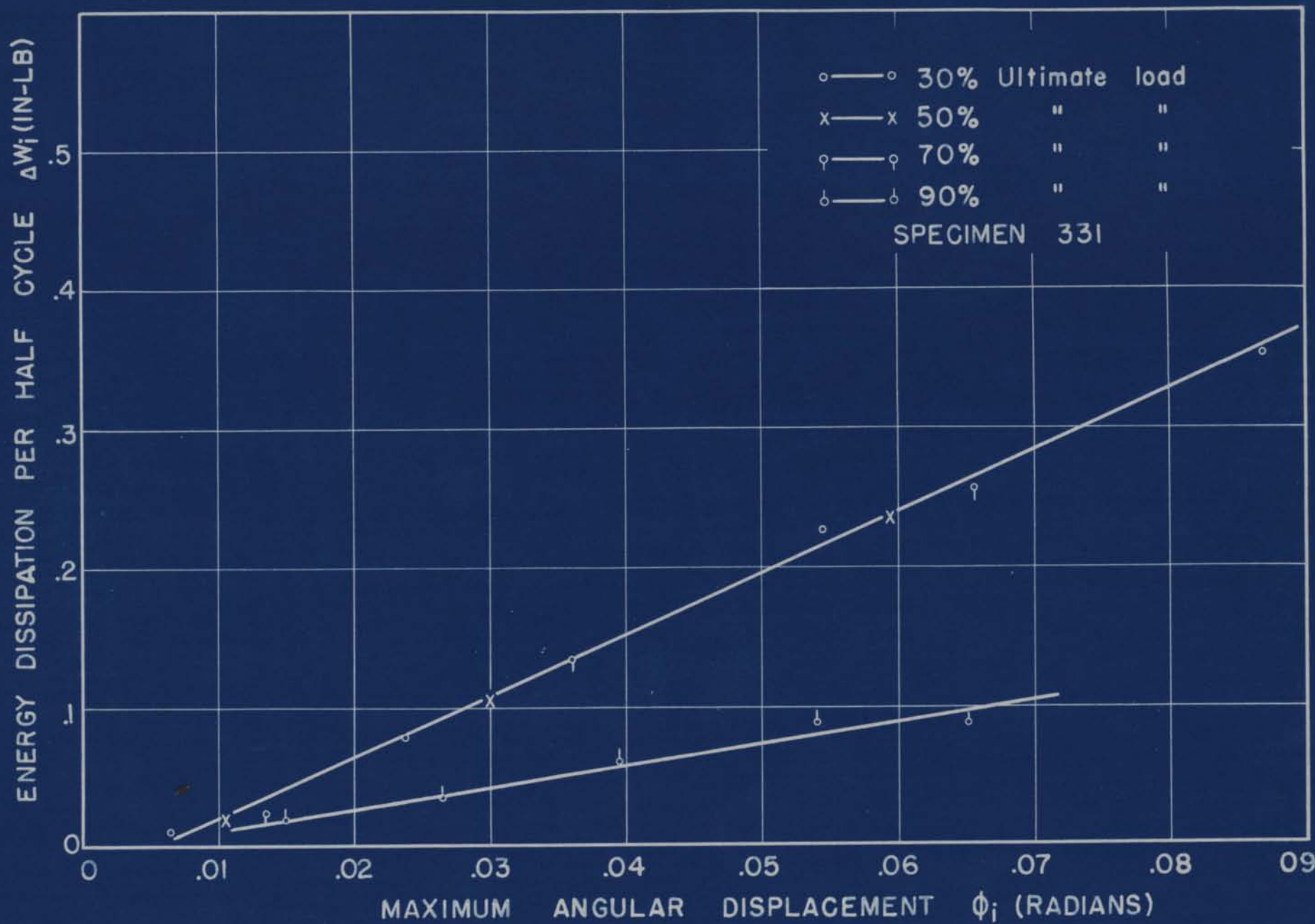

FIGURE R-16. EFFECT OF PRE-STRESSING ON DAMPING

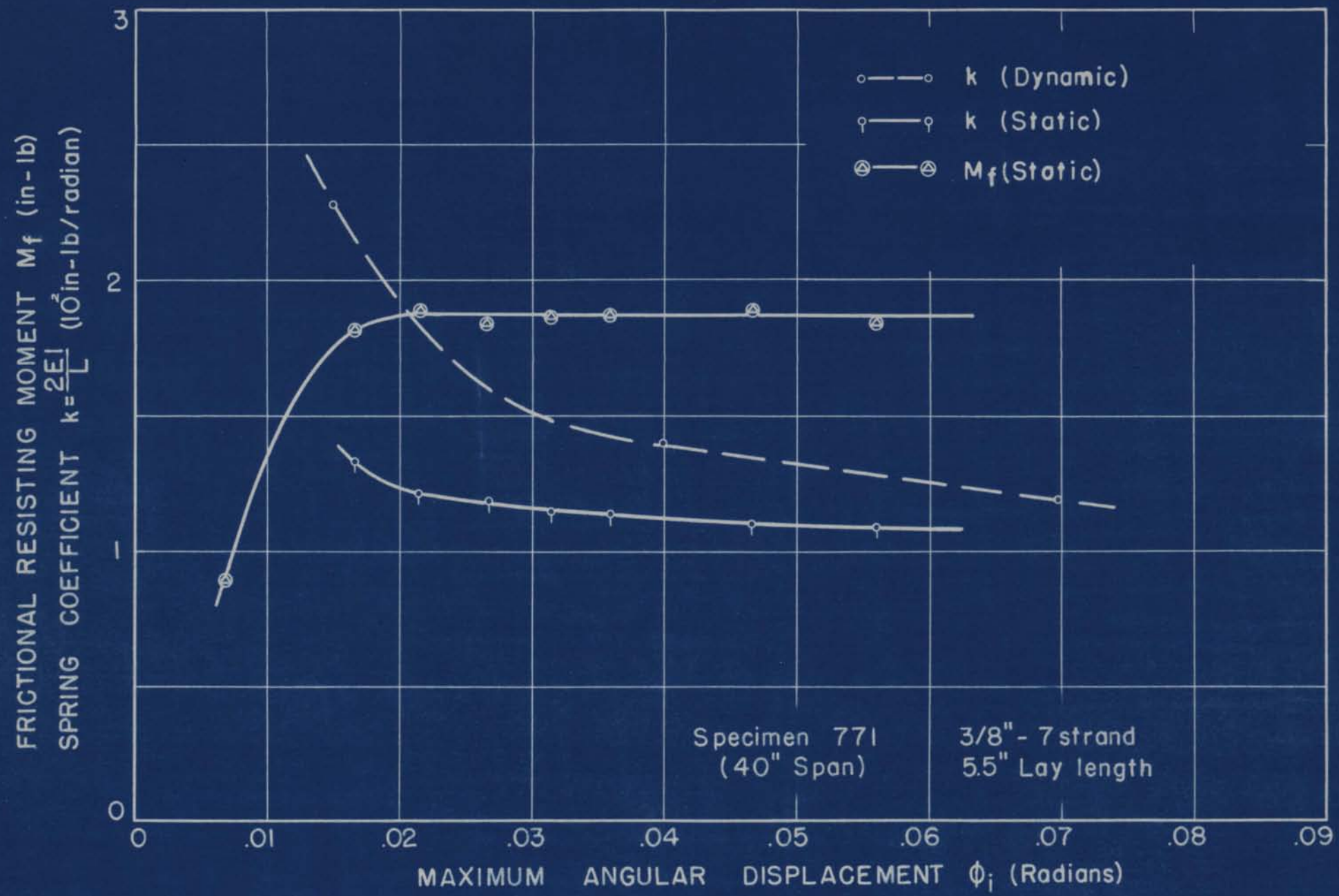

FIGURE R-17 FRICTION FORCE AND SPRING (a)

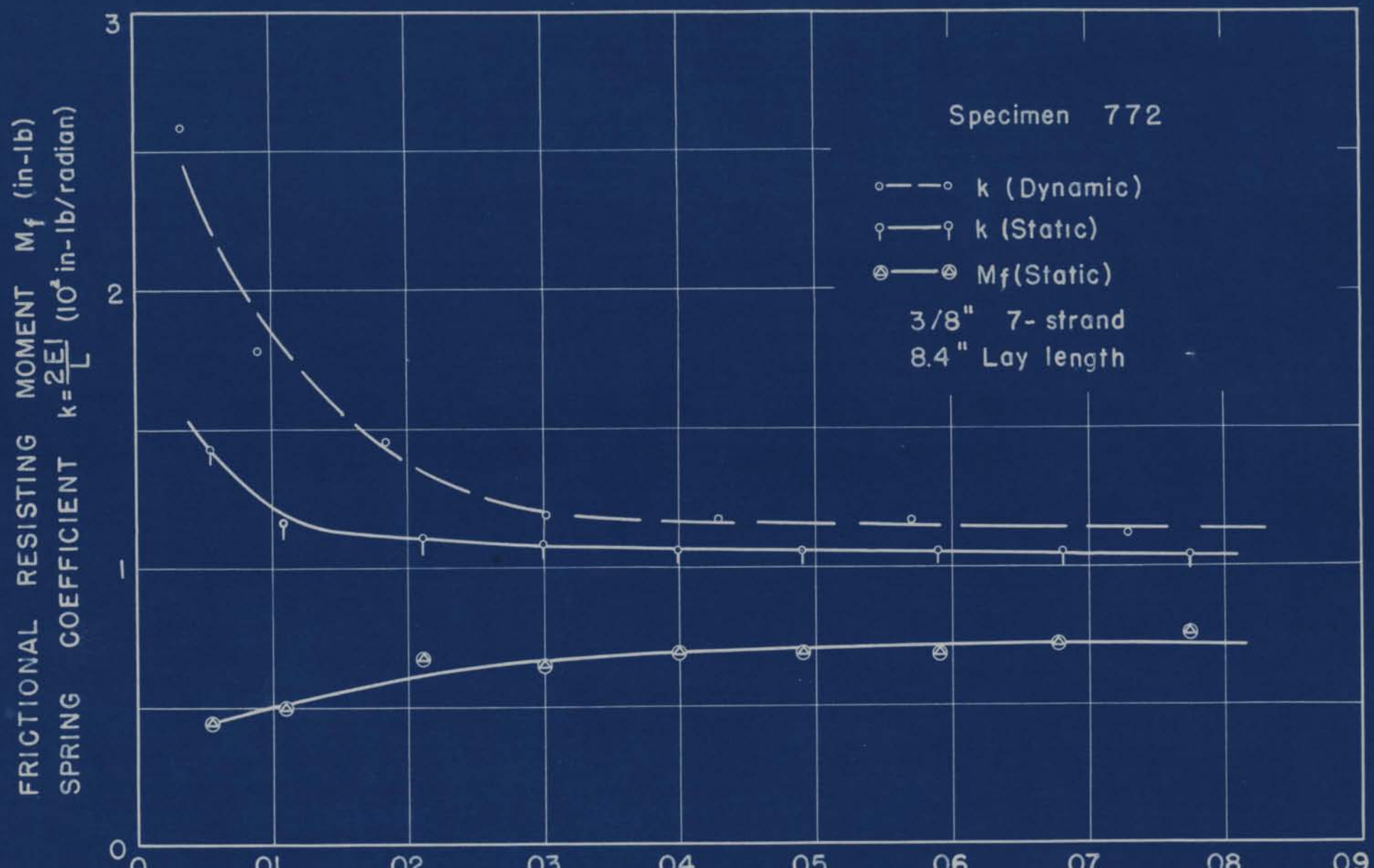

FIGURE R-18 FRICTION FORCE AND SPRING (b)

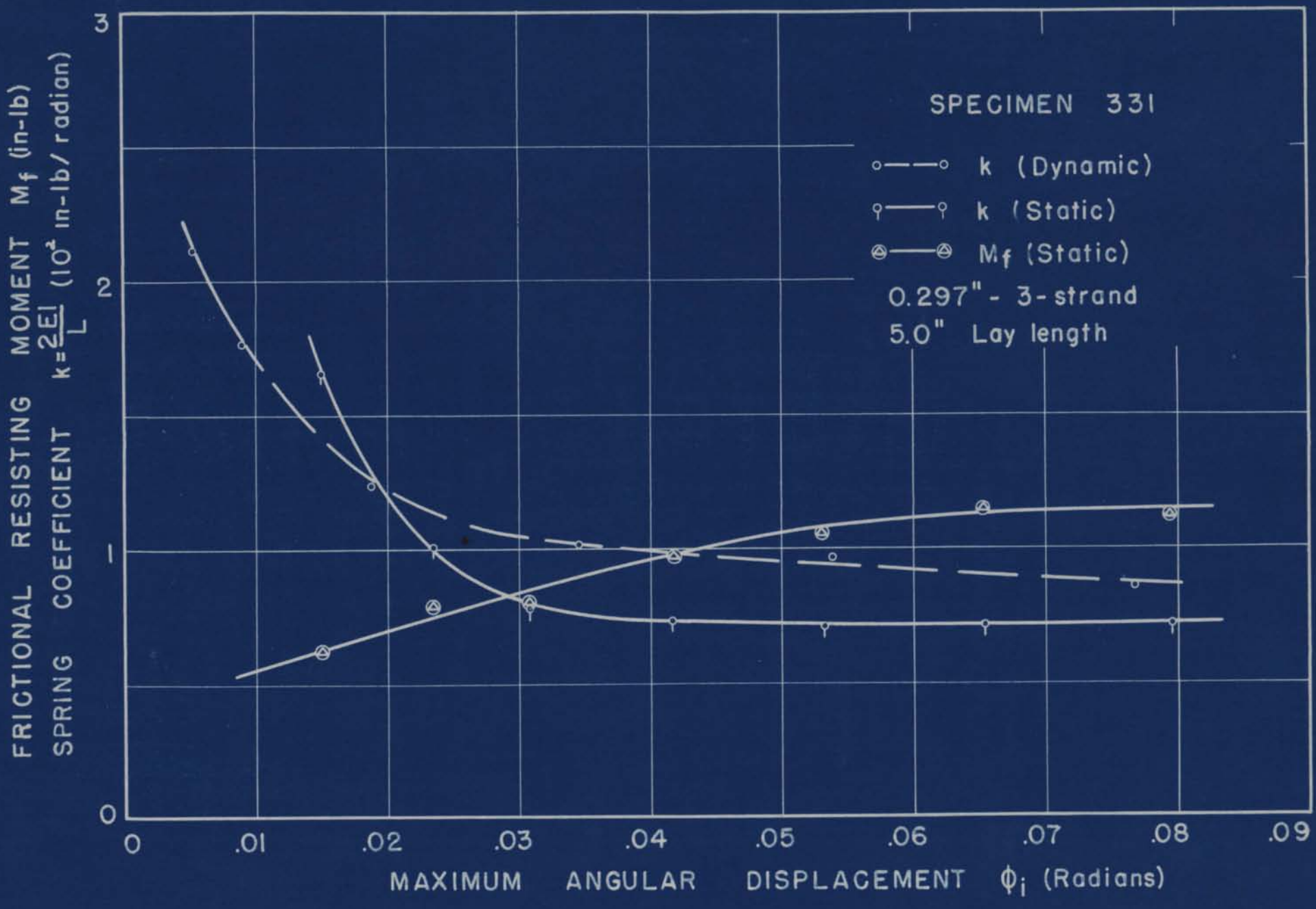

FIGURE R-19 FRICTION FORCE AND SPRING (c)

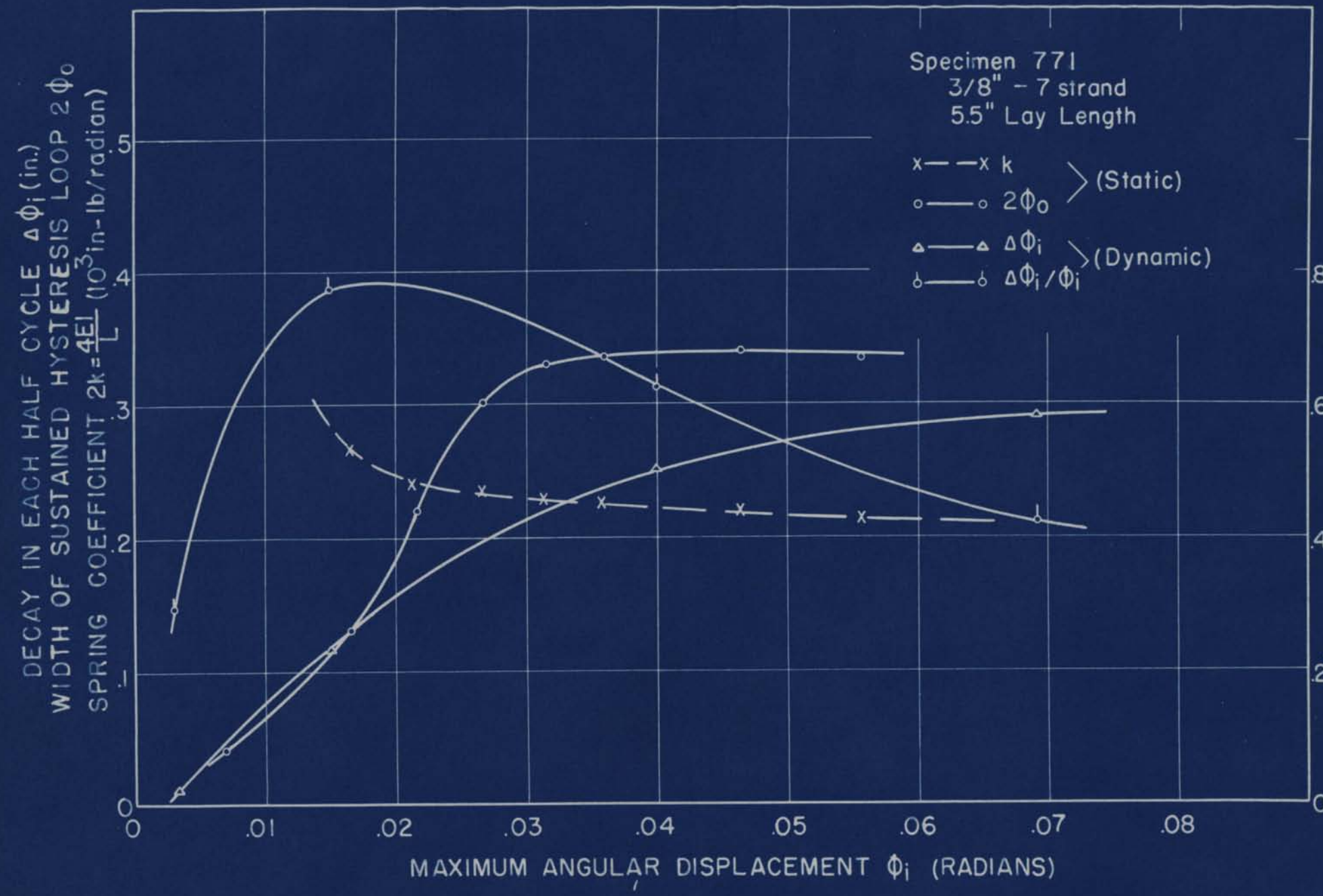

FIGURE R-20 DECAY AND HYSTERESIS LOOP WIDTH (a)

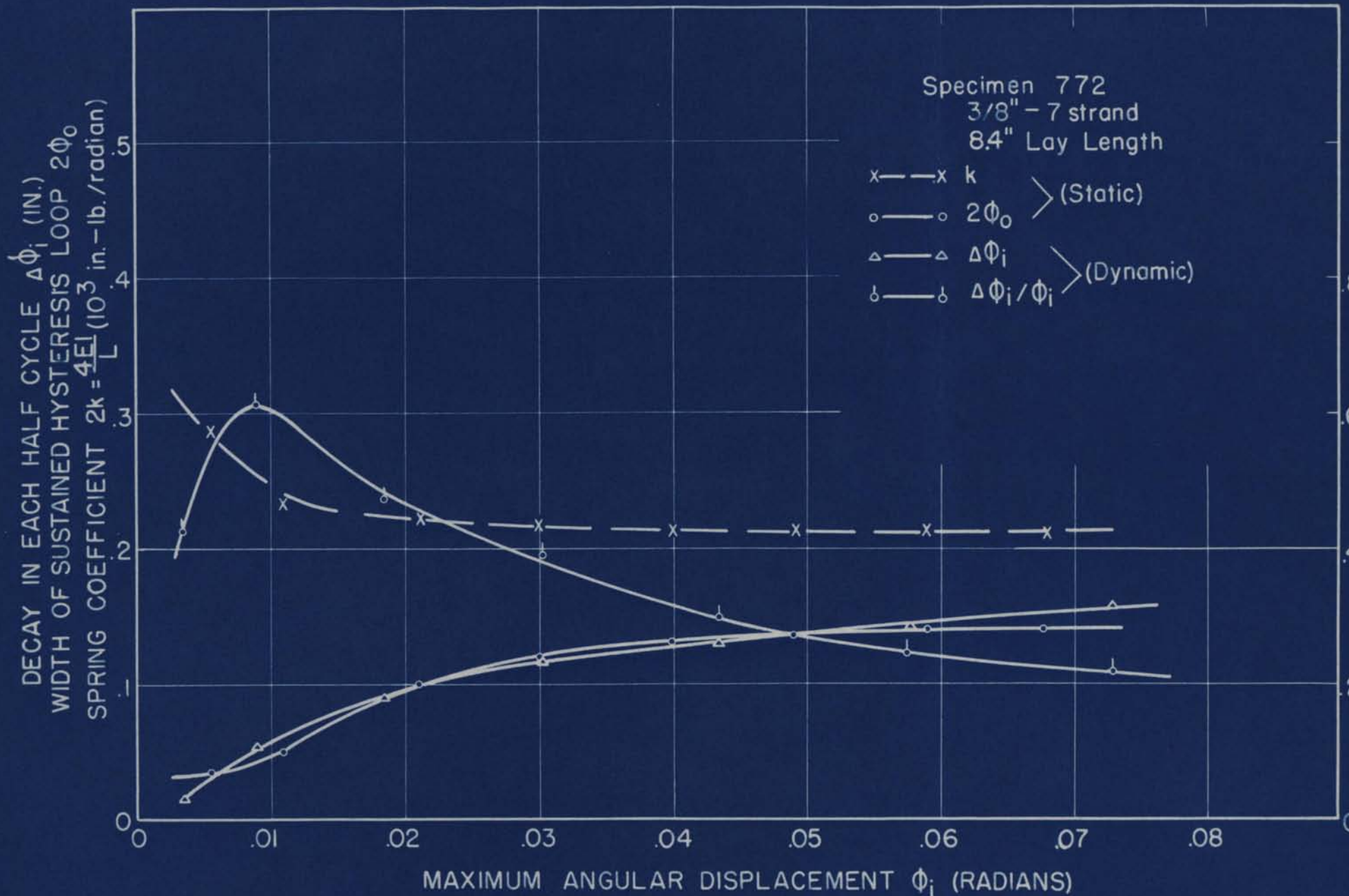

FIGURE R-21 DECAY AND HYSTERESIS LOOP WIDTH (b)

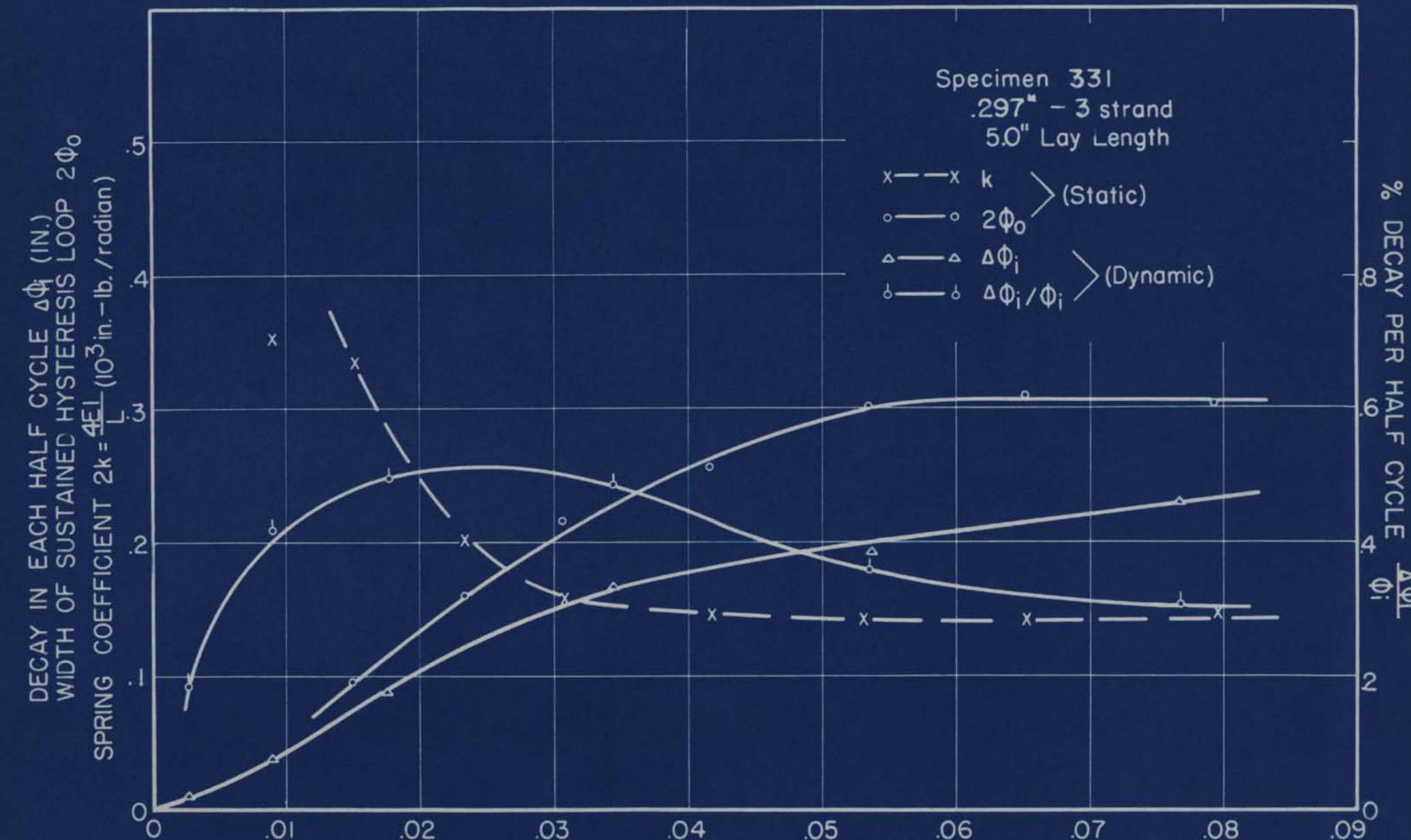

FIGURE R-22. DECAY AND HYSTERESIS LOOP WIDTH (c)

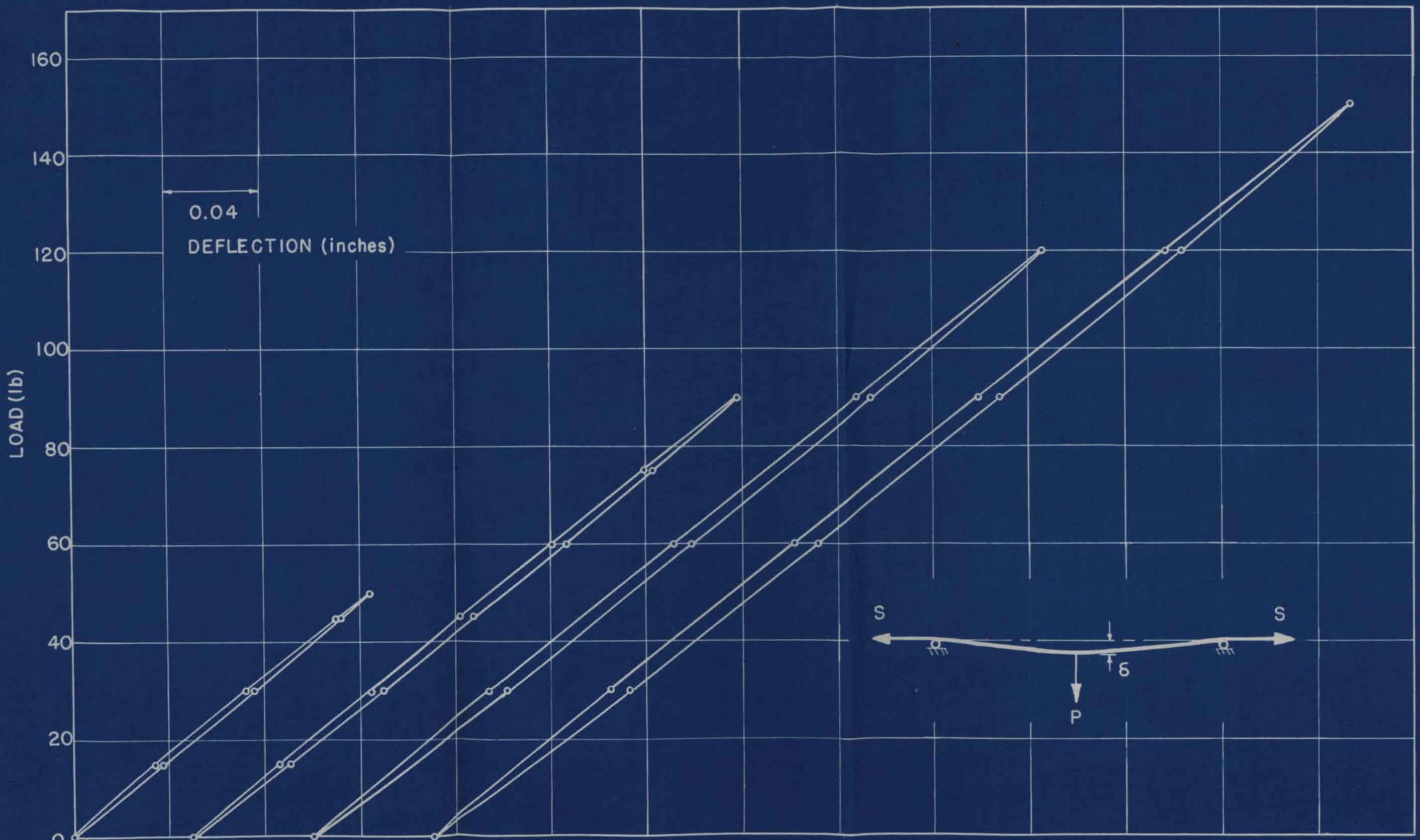

FIGURE R-23 TYPICAL HYSTERESIS LOOPS OF CABLE
(SPECIMEN 771 — 3500lb. TENSION)

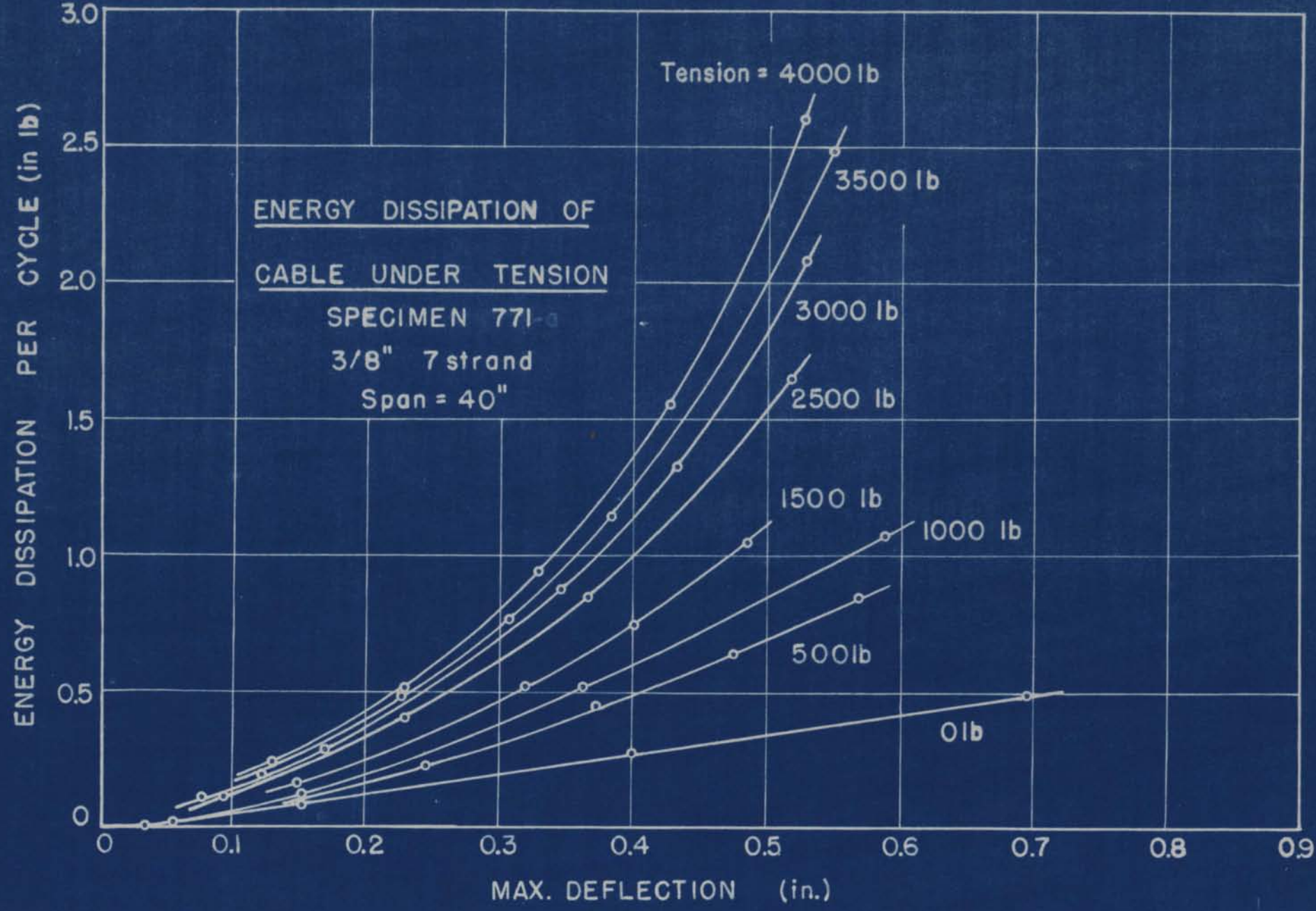
ENERGY DISSIPATION OF
CABLE UNDER TENSION
SPECIMEN 771-a
3/8" 7 strand
Span = 40"
Tension = 4000 lb
3500 lb
3000 lb
2500 lb
1500 lb
1000 lb
500 lb
0 lb
ENERGY DISSIPATION PER CYCLE (in lb)
MAX. DEFLECTION (in.)
0
0.5
1.0
1.5
2.0
2.5
3.0
0.1
0.2
0.3
0.4
0.5
0.6
0.7
0.8
0.9

FIGURE B-24

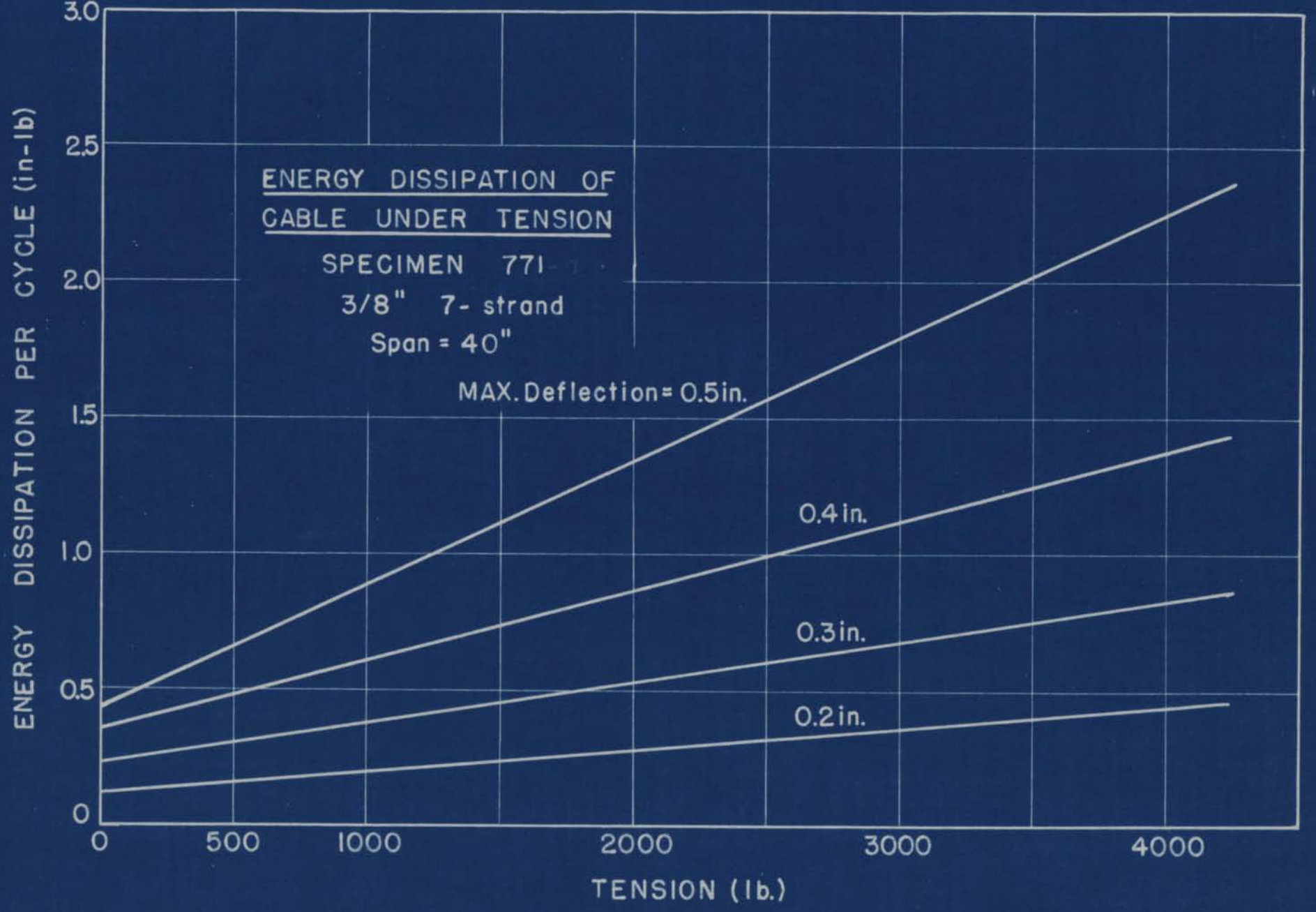
ENERGY DISSIPATION OF
CABLE UNDER TENSION
SPECIMEN 771
3/8" 7- strand
Span = 40"
MAX. Deflection = 0.5in.
0.4 in.
0.3 in.
0.2 in.
ENERGY DISSIPATION PER CYCLE (in-lb)
TENSION (lb.)
0
0.5
1.0
1.5
2.0
2.5
3.0
0
500
1000
2000
3000
4000

FIGURE R-25

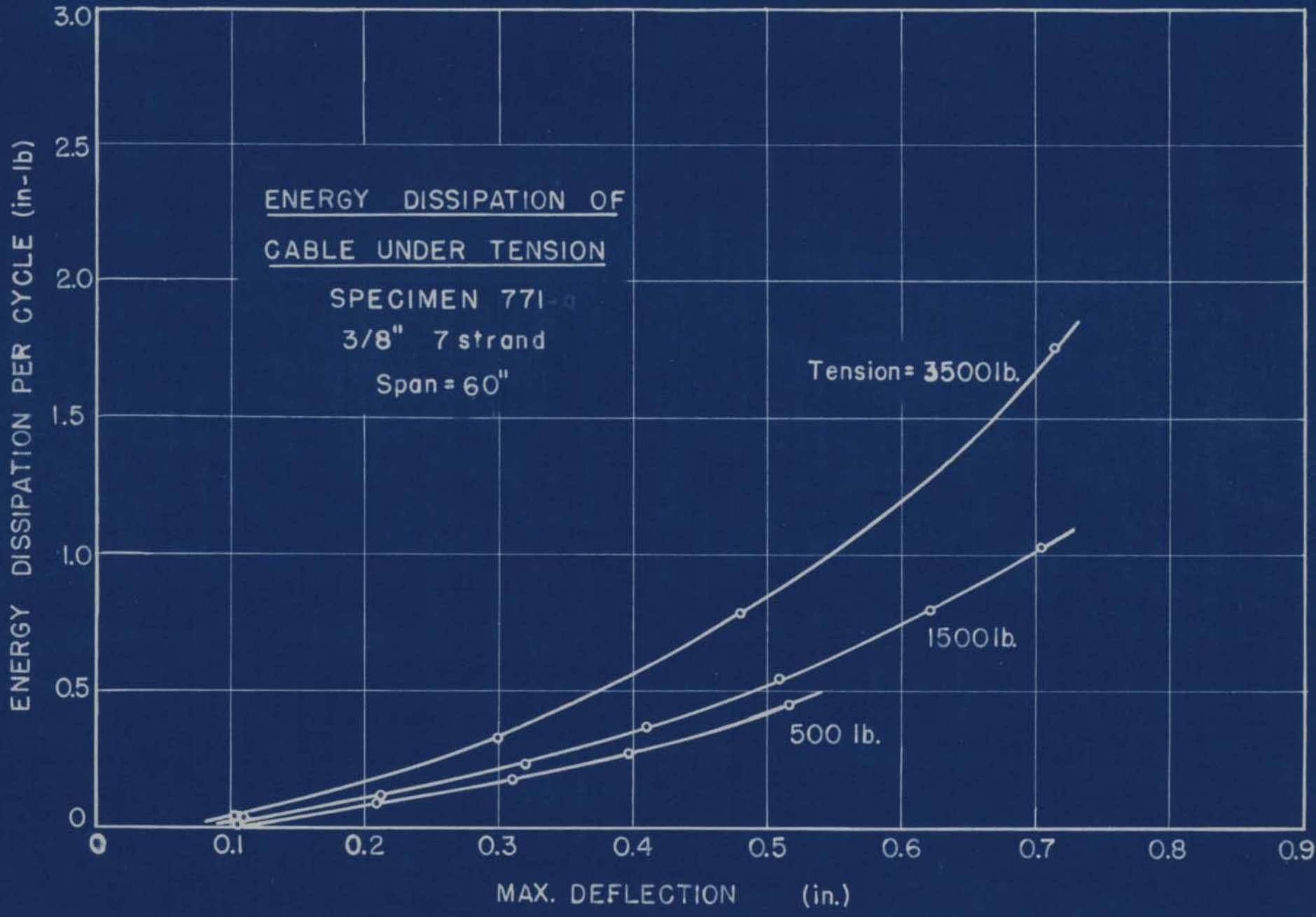
ENERGY DISSIPATION OF
CABLE UNDER TENSION
SPECIMEN 771-a
3/8" 7 strand
Span = 60"
Tension = 3500 lb.
1500 lb.
500 lb.
ENERGY DISSIPATION PER CYCLE (in-lb)
MAX. DEFLECTION (in.)
0
0.5
1.0
1.5
2.0
2.5
3.0
0.1
0.2
0.3
0.4
0.5
0.6
0.7
0.8
0.9

FIGURE R-26

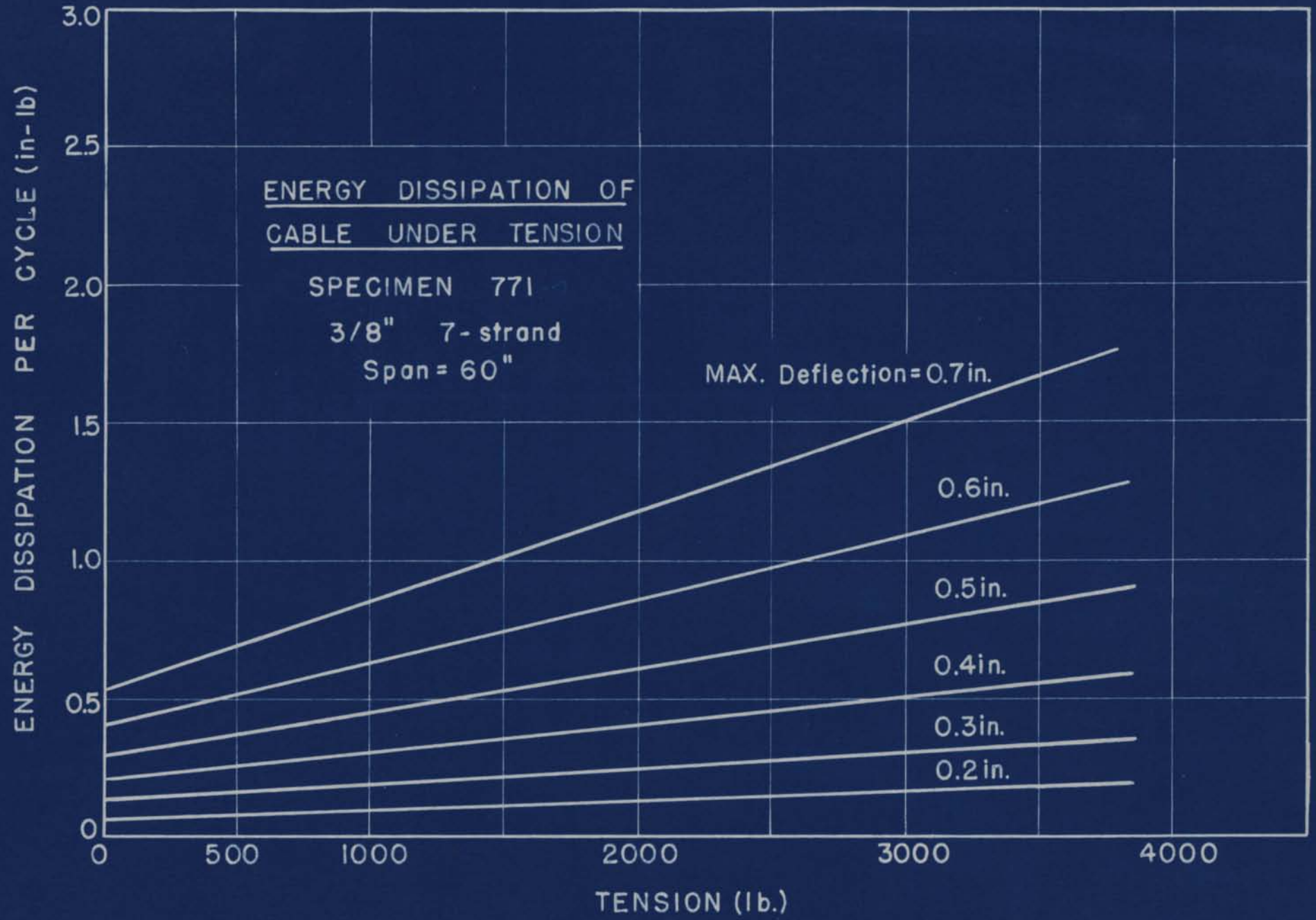
ENERGY DISSIPATION OF
CABLE UNDER TENSION
SPECIMEN 771
3/8" 7-strand
Span = 60"
MAX. Deflection = 0.7 in.
0.6 in.
0.5 in.
0.4 in.
0.3 in.
0.2 in.
ENERGY DISSIPATION PER CYCLE (in-lb)
TENSION (lb.)
0
0.5
1.0
1.5
2.0
2.5
3.0
0
500
1000
2000
3000
4000

FIGURE R-27

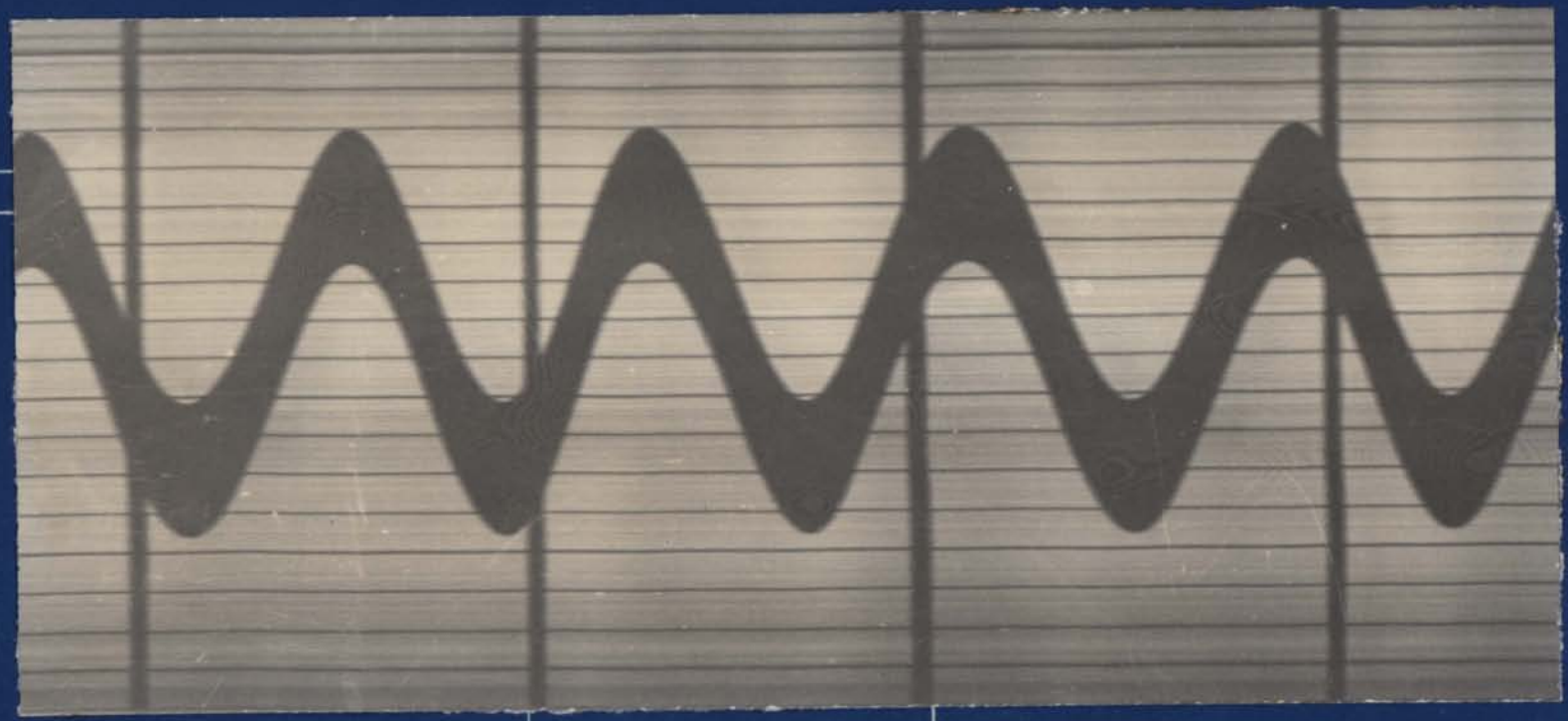

FIGURE R-28. STEADY SUSTAINED VIBRATIONS OF CABLE

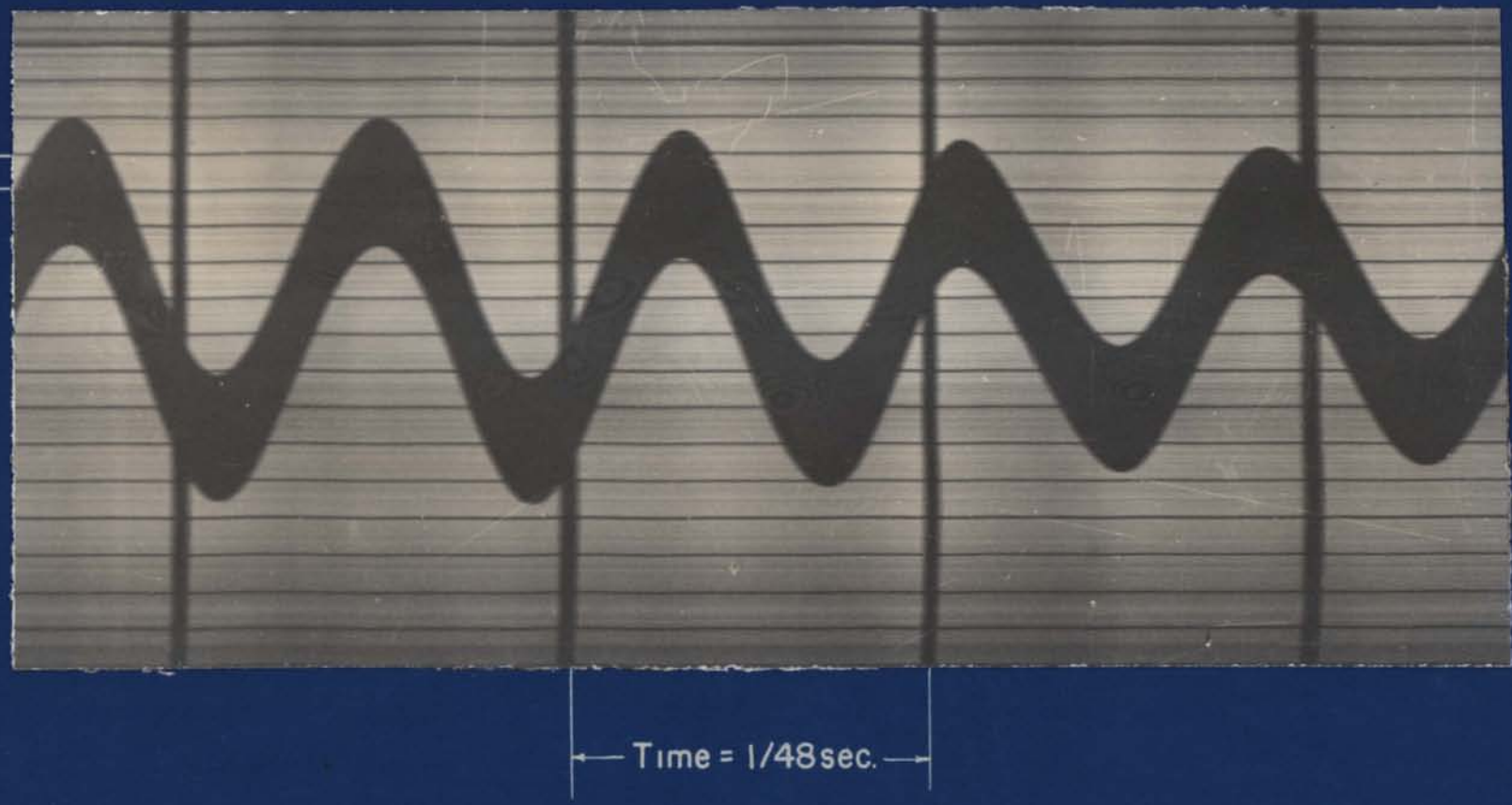

Specimen 771 — 3/8" 7-strand
38" Loop length — 1000 lb. tension.

FIGURE R-29 DAMPED VIBRATIONS OF CABLE

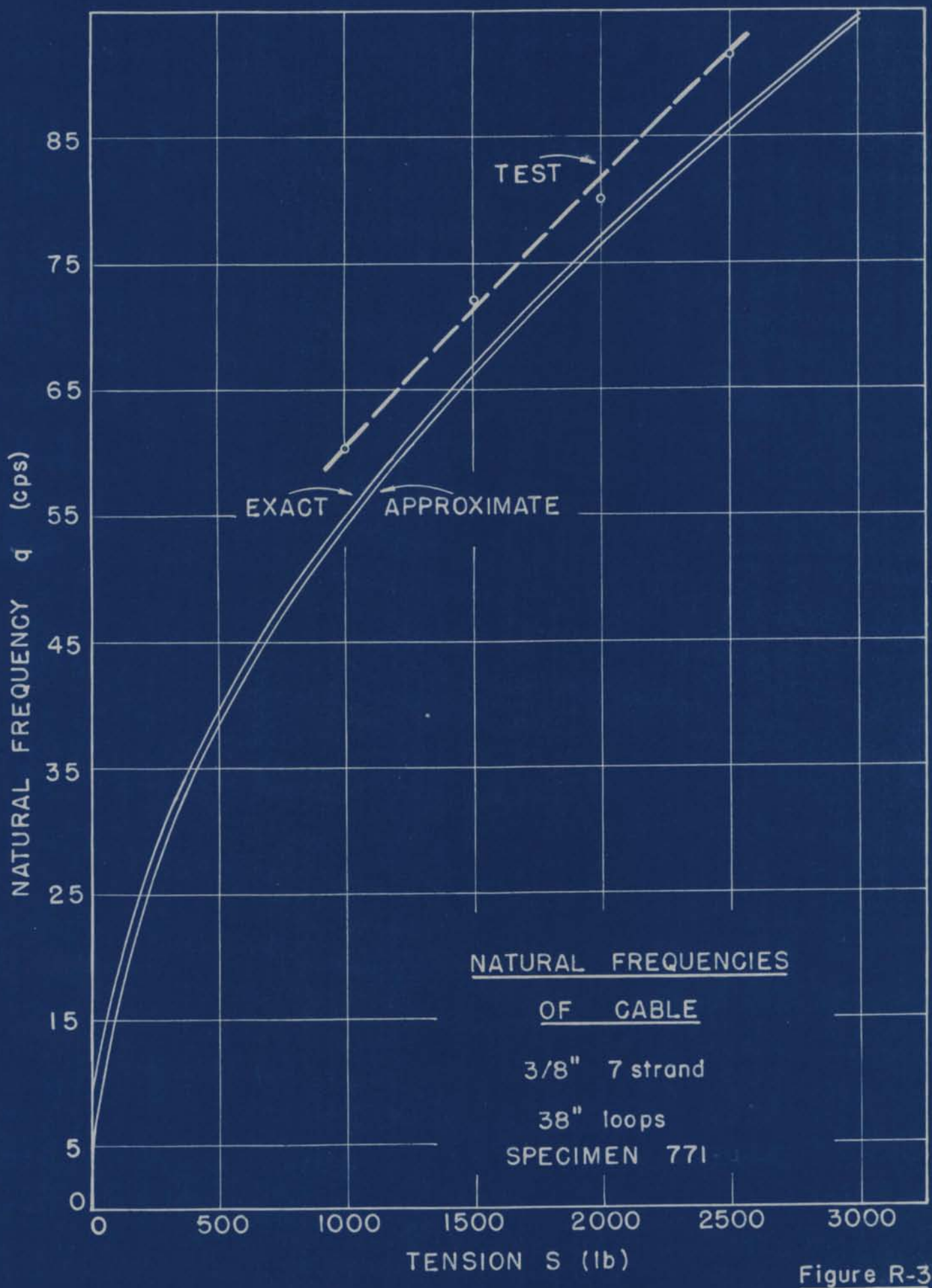
NATURAL FREQUENCY q (cps)
0
5
15
25
35
45
55
65
75
85
0
500
1000
1500
2000
2500
3000
TENSION S (lb)
TEST
EXACT
APPROXIMATE
NATURAL FREQUENCIES
OF CABLE
3/8" 7 strand
38" loops
SPECIMEN 771

Figure R-30

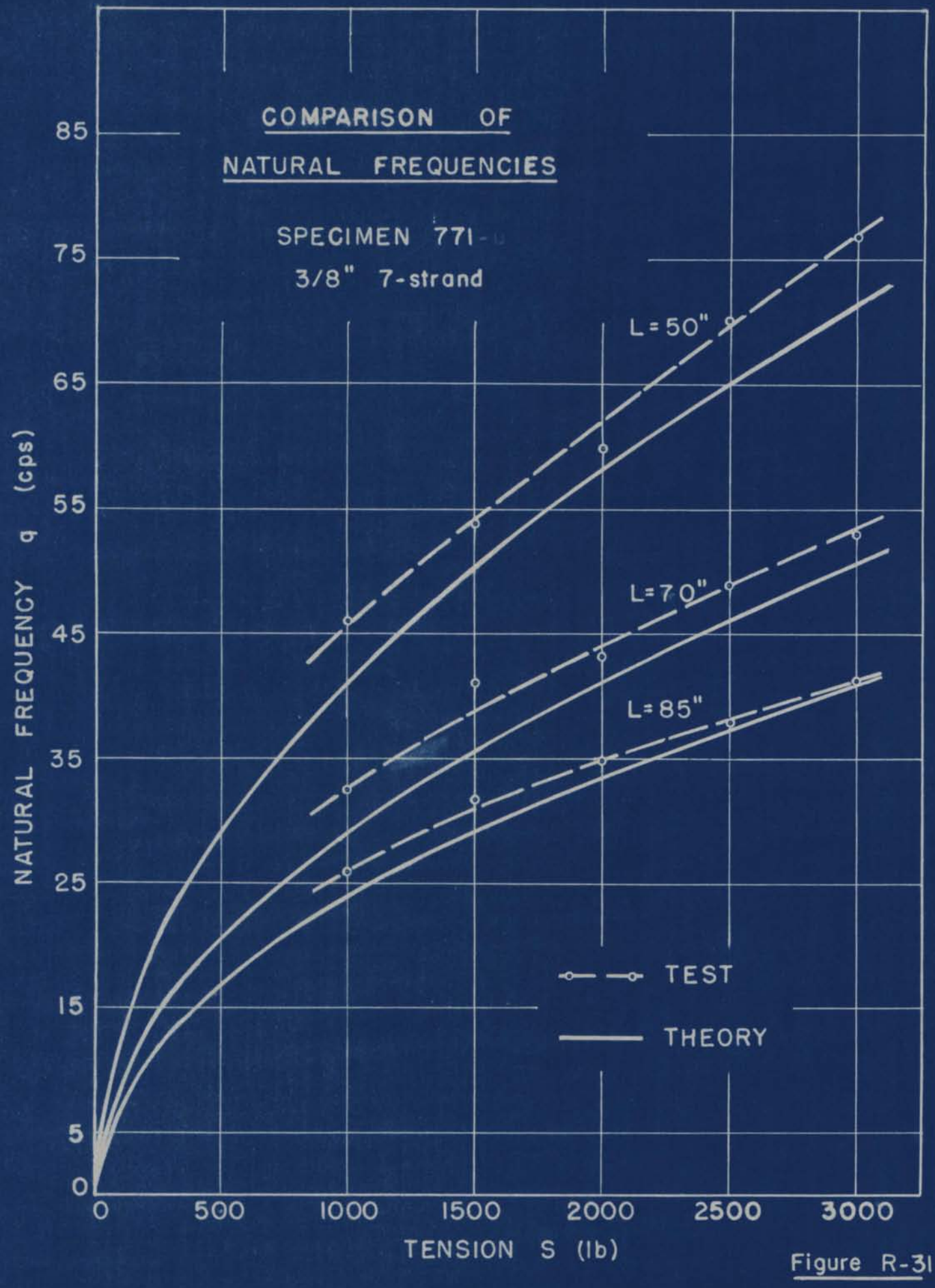
COMPARISON OF
NATURAL FREQUENCIES
SPECIMEN 771-
3/8" 7-strand
L=50"
L=70"
L=85"
TEST
THEORY
NATURAL FREQUENCY q (cps)
TENSION S (lb)
0
5
15
25
35
45
55
65
75
85
0
500
1000
1500
2000
2500
3000

Figure R-31

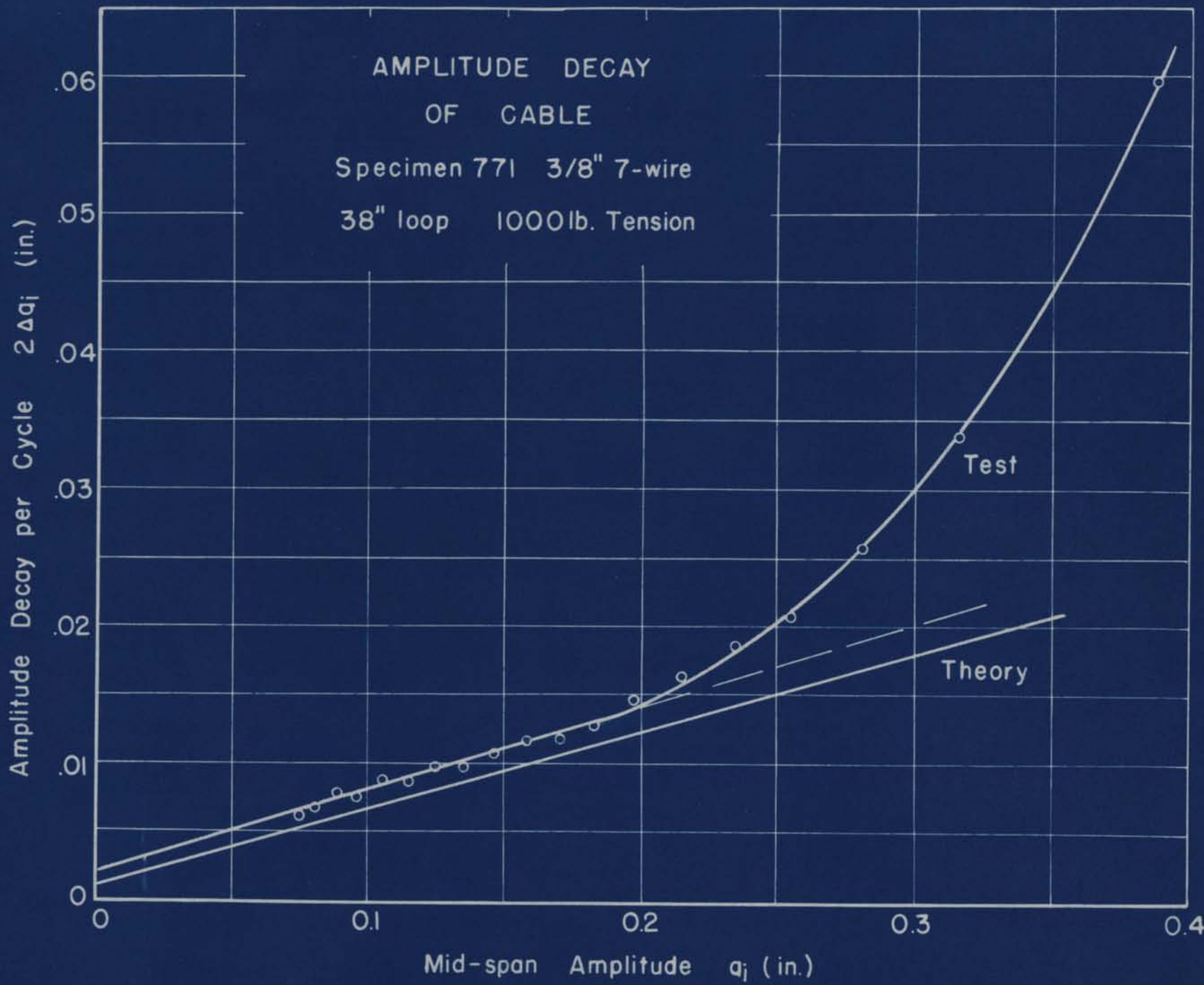
AMPLITUDE DECAY
OF CABLE
Specimen 771 3/8" 7-wire
38" loop 1000 lb. Tension
Test
Theory
Amplitude Decay per Cycle 2Δqj (in.)
Mid-span Amplitude qj (in.)
0
.01
.02
.03
.04
.05
.06
0
0.1
0.2
0.3
0.4

Figure R-32

VITA

The author, Ai-ting Yu, was born on January 6, 1921, in Chenghai, Chekiang, China. He is the youngest son of the late Hsin-ken Yu and Aichen Chow Yu, both of Chenghai, Chekiang, China.

He was graduated from National Central University, Chungking, China, with the degree of B.S. in Aeronautical Engineering, in July, 1943. From March, 1945 to February, 1946, he attended Massachusetts Institute of Technology where he received the degree of M.S. in Aeronautical Engineering.

From July, 1946 he began his work towards his Doctorate at Lehigh University and during the same period of time he has been a Research Fellow at Fritz Laboratory in charge of a Vibration Fatigue program sponsored by the Bethlehem Steel Company.

He was elected as an active member of the Lehigh Chapter of the Society of Sigma Xi, in May 1948. He has been a member of the American Mathematical Society for the past two years.

He has published the following technical papers:

"Shear Lag in Plywood Sheet-Stringer Combination Used as the Chord Member of a Box Beam" - National Advisory Committee for Aeronautics T. N. No. 1443, March 1948

"A Method for Vibration Fatigue Tests of Stranded Conductor" - Proc. Society for Experimental Stress Analysis, Vol. VI, No. 2, 1948, pp. 1-6.